AN AUTOMATED SYSTEM FOR INTERPRETING GRAVITATIONAL ANOMALIES (THE MINIMIZATION METHOD)

Ye. G. Bulakh

Translation of "Avtomatizirovannaya Sistema Interpretatsii Gravitatsionnykh Anomaliy," Kiev, "Naukova Dumka" Press, 1973, 111 pages.

NATIONAL AERONAUTICS AND SPACE ADMINISTRATION
WASHINGTON, D. C. 20546 JANUARY 1975

STANDARD TITLE PAGE

1. Report No.	2. Government Accession No.	3. Recipient's Catalog No.
NASA TT F-15750		

4. Title and Subtitle	5. Report Date
AN AUTOMATED SYSTEM FOR INTERPRETING GRAVITATIONAL ANOMALIES (THE MINIMIZATION METHOD)	January 1975
	6. Performing Organization Code
7. Author(s)	8. Performing Organization Report No.
Ye. G. Bulakh	10. Work Unit No.
9. Performing Organization Name and Address	11. Contract or Grant No.
Techtran Corporation P.O. Box 729, Glen Burnie, Md. 21061	NASW-2485
	13. Type of Report and Period Covered
12. Sponsoring Agency Name and Address	Translation
National Aeronautics and Space Administration Washington, D. C. 20546	14. Sponsoring Agency Code

15. Supplementary Notes

Translation of "Avtomatizirovannaya Sistema Interpretatsii Gravitatsionnykh Anomaliy," Kiev, "Naukova Dumka" Press, 1973, 111 pages.

16. Abstract

This monograph describes an automated system for interpreting gravitational anomalies based on the minimization method and consisting of separate components. It includes solving direct problems, calculating a background function, computing the density parameters of blocks which form the region under investigation, and determining the parameters which characterize the coordinates and dimensions of the geological feature. The use of all components of the system is illustrated by several practical examples in geological interpretation. The monograph is intended for geophysicists.

17. Key Words (Selected by Author(s))	18. Distribution Statement
	Unclassified - Unlimited

19. Security Classif. (of this report)	20. Security Classif. (of this page)	21. No. of Pages	22. Price
Unclassified	Unclassified	110	

TABLE OF CONTENTS

TABLE OF CONTENTS (Continued)

AN AUTOMATED SYSTEM FOR INTERPRETING GRAVITATIONAL ANOMALIES (THE MINIMIZATION METHOD)

Ye. G. Bulakh

Introduction

Geophysical survey methods are of primary importance in geological surveying. /3* A properly designed survey using geophysical methods makes it possible to direct future survey work efficiently and to decrease its cost significantly.

One of the most important components of any geophysical survey method is the geological interpretation of field material. In the end result this interpretation, together with correct methodology and field operational technology, determines the success of survey operations carried out using geophysical methods.

Computers have recently begun to be used to process and interpret geophysical materials. They have been used widely to interpret gravitational data.

While not setting ourselves the goal of reviewing the possibilities of applying computers to all areas of exploratory geophysics, we will examine several questions concerning the use of computers to interpret gravitational anomalies.

It is possible to distinguish four independent trends among questions concerning the possibility of using and applying computers to quantatively interpret gravitational anomalies.

To the first trend we assign work associated with transforming observed anomalies and with calculating various correction factors. This work is usually very unwieldy. The results of the conversions and transformations of the field observed can be used both for qualitative and for quantatitive interpretation.

The second trend includes the problem of directly interpreting anomalies with existing computers. This involves programming and machine solution of a number of tasks relating to calculation of parameters which determine perturbing masses. In this process the initial data are represented by the values of the anomalous function.

The third trend includes questions concerning use of computers to calculate various measuring grids, nomograms, tables, and other interpretative aids. These aids can increase the effectiveness of methods of interpretation already known, /4 and can aid in developing new methods which could not be introduced earlier because of the cumbersome calculations involved.

*Numbers in the margin indicate pagination in the foreign text.

The fourth trend comprises work toward creation of specialized problem-solving machines to interpret anomalies.

Let us examine each trend in somewhat more detail.

First trend. Computers make it possible to perform calculations relatively quickly even with the most complicated formulas. Hence it is natural that, from the very start, research on the use of computers to process and interpret geophysical observations was aimed at automating laborious calculations.

By the time computer technology was introduced into gravimetry, the calculations associated with field transformation were extremely cumbersome. Therefore, programs were written primarily on field transformation to perform gravimetric calculation problems.

In the USSR I. A. Balabushevich, B. V. Bondarenko, R. S. Volodarskiy, O. K. Litvinenko, V. N. Strakhov, and others became the first to use computers for the transformation of fields. The use of computers for the transformation of anomalies required the development of more sophisticated computer design (G. I. Karatayev, A. K. Malovichko, M. G. Serbulenko, V. N. Strakhov, M. LaPorte, and others). This trend includes work in computer calculation of correction factors for the influence of landscape relief in surveying with a gravimeter (V. I. Aronov, L. A. Koval', M. Bott, M. Kane, and others). A fairly circumstantial review of the research in this direction has been made in [36, 49, 85, 111, etc.].

The second trend, i.e., use of computers to interpret anomalies, was developed almost simultaneously with the first trend. Computers make it possible to carry out even the most difficult calculations in a relatively short time. However, the basic importance of these investigations for the interpretation of anomalies is the fact that, with the new capabilities of technology, qualitatively improved methods of interpretation can be created. Now there arises the task of developing more universal methods of interpretation which cannot be applied without using computers. It is impossible to create one universal machine method for interpreting gravitational anomalies; the interpretation methods differ under various physicogeological conditions. It is necessary to generate a small array of these methods and then carefully determine the areas in which they can be used. Works are already available on creating effective machine methods of interpretation.

The first stage of the second trend is development of effective methods of solving direct problems, a task which has great significance for automated computation in interpreting anomalies. No matter the methods by which anomalies /5
are interpreted, the diagram of the geological structure of a region will be built, as a result, on the basis of all the data (geological and geophysical). It is necessary to solve the direct problem of gravitational survey to confirm the correctness of this diagram's structure. In addition, many researchers are coming to the conclusion that when using field transformation it is impossible to single out an anomaly caused only by the geological feature in question. The so-called geological reduction method has been widely applied in the

practice of interpretation. Its basic characteristic is the fact that the fields are divided by subtracting from the observed gravitational field the effict of the feature, the position and dimensions of which are established according to geological data or during interpretation of the data of other geophysical methods. In this process it is necessary again to solve the direct geological structure problems formulated by the researcher.

When calculating anomalies for certain geological features, we encounter an abundance of perturbing masses. This causes great difficulties. However, the calculation process for solving this direct problem can be unified with an adequate degree of precision.

In fact, say that it has been established to be possible to consider a perturbing body as being two-dimensional. Let us further assume that the perturbing masses are concentrated in one or several areas. Each area can be well approximated by a segmented straight line boundary. Thus, the gravitational field created by any two-dimensional body is approximated by the sum of the gravitational fields of its projections. Each projection is determined by five parameters: x_1, h, x_2, H, which are the coordinates of the angular points, and σ which is the excess density.

Calculations for three-dimensional bodies can be unified in a similar way. For this purpose it is sufficient to represent the perturbing bodies as the sum of projections of limited extent or as the sum of parallelepipeds. In the latter case each geological feature is described by seven parameters. Six of them characterize the location of the boundaries, and the seventh characterizes the excess density. This approximation makes it possible to describe bodies of variable density.

The programs which have been written make it possible to calculate the observed field. From the interpretation stage, in which the hypothesis concerning the geological structure of the region was formulated, one proceeds to calculate the anomaly. It is necessary to feed into the computer information which reflects the determined geological configuration. This is a system of five-dimensional vectors (for a two-dimensional geological section) or seven-dimensional ones (for a three-dimensional section). In addition, it is necessary to have a clear idea of the coordinates of the initial point, the distance between the points on the profile, and the distance between the profiles, as well as the coordinates of the terminal point. The programs are written for an indeterminate number of vectors which reflect the geological structure. A maximum limit is imposed on this number, depending on the volume of the effective memory. Thus, it is necessary in each specific case to feed into the computer /6
a number equal to the number of vectors providing information which describes the geological configuration.

The effectiveness of these calculations has been verified by means of numerous examples in interpreting regions complex in the geological sense of the word.

O. K. Litvinenko, M. Bott, M. Tal'vani, and others have concerned themselves with the solution of similar problems.

The second stage is the development of automatic machine methods for interpreting anomalies. These methods have been given a theoretical basis by the research of A. N. Tikhonov, V. K. Ivanov, M. M. Lavrent'ev, and others. It is also possible to classify the methods of searching for singular points [59, 60, 74] under the works in this direction. Relatively stable algorithms have been obtained which make it possible to carry out the calculation processes by computer.

In the works of S. V. Shalayev [75-77], study is made of the problem of approximating an observed anomaly by a rational fraction. Such an approximation makes it possible to find the singular points of perturbing masses. A linear programming device is used for the actual calculations.

In [56a, 80] a summary is given of the methods of determining the position and dimensions of perturbing bodies and the excess mass (the grid method). A similar task situation is also presented in [89]. The half-space in which the perturbing masses are concentrated is divided into elementary bodies (prisms or parallelepipeds). By minimizing the difference between the observed and theoretical anomalies, one finds the values of the excess densities within each elementary body. S. V. Shalayev [77, 78] developed this method further in his works. He reduced the problem to linear programming.

A second variation of the grid method has been summarized in [31]. A number of works have since appeared, in which this variation has been put to practical use [37, 52, 53].

In a number of works the solution of the inverse problem is reduced to iteration processes [87, 91, 114, etc.]. In order to minimize the specially constructed functional, the least square method [90, 93, 96] is used.

In [100] the relaxation method is used to solve the inverse problem. The perturbing body is approximated by the sum of vertical prisms with their square bases. The gravitational effect is calculated at points of a square grid. The method can be used if one knows the depth of the interface at least one point and the excess density.

On the basis of the Poincaire theorem, D. Zidarov has worked out an original method for determining the configurations of perturbing geological features [117]. If the centers of the masses are known, then it is possible to construct a convergent iteration process for "sweeping out" the perturbing masses into the surrounding space. The computation cycles are repeated until homogenous geological features are obtained which have the assigned excess density. /7

Methods of special correlation analysis [33] have been developed for forecasting in geology. By taking a certain area as a standard, it is possible to predict geological structure on the basis of observations of geophysical fields in other similar regions.

I. Nedyalkov [102] has proposed a heuristic method for solving one class of inverse problems of the theory of potential. The parameters of the geological configuration are determined by using specially constructed self-learning [sic] algorithms.

One could continue this list of the works the theme of which adheres to this trend. They would include the fundamental monograph by F. M. Gol'tsman [20] and a large number of works by other researchers. The works cited in this review can serve only to illustrate the general content of the second trend in research.

As regards the third trend, as indicated earlier, it comprises works which make use of computers to calculate tables, nomograms, measuring grids, etc. The results of the calculations serve the purpose of practical application of a new method or a new means of processing and interpreting anomalies. At first glance the question of the means used to calculate these measuring grids or tables is not one of fundamental importance. This is true when the formulas are not too cumbersome and allow calculations using tables and an adding machine. However, one often encounters problems solution of which cannot be accomplished without using computer technology. The calculation of integral measuring grids [14] may serve as an example.

It is not possible to give a complete survey of works in the third trend of research. Many calculations have been carried out recently using computers, and by no means all authors concentrate their attention in this area [82-84].

A review of the works in the fourth trend has been given in [57]. Almost all of the specialized analog devices are based on the fact that the various physical fields have common properties. These devices make use of the mathematical analogy between gravitational fields and electrical, radioactive, electromagnetic, and light fields.

Researchers have come to the conclusion that analog computers can be used effectively to interpret an observed field only when the following conditions are satisfied:

1. The parameters of the perturbing body undergo slight variation;

2. Calculation of the field is done relatively quickly;

3. The results of the calculation are printed out in a form in which the calculated and observed anomalies can be quickly and easily compared;

4. The device must be simple, reliable, and convenient to use.

Despite their seeming simplicity, the models set up to interpret by the matching method have not been widely used. One of the basic reasons for this is the fact that by no means all of the analog computers meet the above-mentioned requirements. /8

The problems in the second area of research have been examined in this monograph. Research is cited which uses the minimization method to solve the inverse problem. This method makes it possible to create a closed automated system for quantitative calculations. This system of calculations includes the stages of the preliminary survey type (calculation of the direct problem), search for a background effect, and lastly automated search for a new variation of the geological configuration.

CHAPTER I

SOLVING INVERSE PRELIMINARY GRAVIMETER SURVEY PROBLEMS BY THE MINIMALIZATION METHOD

Section 1. Statement of the Problem /9

When we speak about using computers to process and interpret gravimetric data, we mean primarily the automation of calculation operations. Computers unquestionably make it possible to carry out even the most complicated calculations relatively quickly and accurately. The basic reason for using these machines in interpretation practice is nevertheless the fact that, on the basis of new technical capabilities, quantitatively new methods of processing and interpretation can be developed and used.

The entire cycle of calculation operations and logical operations can be reduced to a single automated system for processing and interpreting gravimetric data. Structurally this system consists of two independent parts. The first part consists of the processing of observations, the introduction of various correction factors and reductions, and the process of obtaining an anomalous gravitational field. If necessary, various transformations can be carried out here. The field can be converted to any other level, higher derivatives or field potentials can be computed, and other special functions can be constructed for the field under study, such as the Saksov function, the Nigard function, etc. The results of the processing are usually presented in the form of catalogs and graphs along fixed profiles and charts of the anamalous field and its transformations. After comprehensive processing of the observed data, it is possible to thoroughly analyze all the material obtained and compare it with the data of other geophysical methods and with information on the geological structure of the region. This is the total of the subject of qualitative interpretation.

Various reductions are introduced into the observed field; correction factors or observed data have been converted to other functions so that it will be possible to state with confidence that the anomaly obtained has been caused only by heterogeneities in the geological structure. On a plan or graphs places are pinpointed in which bodies with too little or too much mass are concentrated, the configurations of these masses are established in general form, their approximate epicenters are indicated, and several conclusions are drawn about the geometric form of the geological features.

The second step is represented by quantitative calculations. The numerical /10
values of the parameters of the geological features and the density characteristics of the rocks which make up these features must be established on the basis of the peculiarities of the anomalies. The choice of the methods of making the quantitative calculations depends on both the type of anomalous field and on the geological premises which the researcher has accepted as his basic working material.

The second part of the automated system, i.e., the system for interpreting the gravimetric data, is associated with the quantitative interpretation. The magnitudes which characterize the occurrence of the masses of interest to us can be estimated quantitatively by several methods. Each of these methods has both strong and weak aspects, and as a result of this each one can give satisfactory and unsatisfactory results in determining the indicated magnitudes. This depends on the geological conditions under which the anomaly being interpreted has been obtained. Where one of the means gives satisfactory results and can therefore be used successfully, another one is not used.

As a whole all of these methods should be considered to be of equal value, but each of them must be used while taking into account the geological structure of the region in which the anomaly being interpreted is located. If the region being studied is relatively complicated in the physico-geological sense, and if the researcher has somewhat limited information about the structure and makeup of the geological objects, then often the only effective means of interpreting under these conditions is the selection method. The researcher constructs his geological model on the basis of all information available about the region's geological structure, while taking into account the anomalous field. The direct problem is solved, and the gravitational effect is found from the appropriate geological model. By comparing the observed and theoretically calculated anomalies, the researcher should change the geological model constructed earlier in such a way that the newly calculated gravitational effect comes as close as possible to the actually observed field. In this process it is first necessary to know how to solve the direct problem quickly, and second to know how to construct the type of algorithm which would make it possible to answer the questions of how to use the geological model so that the observed anomaly coincides in the best way possible with one which has been calculated theoretically.

In the following section we will dwell on a description of this type of algorithm. Calculation of the direct problem is a component part of this algorithm. Thus, in order to solve the problem of determining the parameters of geological bodies, we have an observed anomaly, all variations in which are related to geological heterogeneities and the initial variation of the geological structure model. The observed field and the tentative model of the geological structure together form the initial data for the quantitative calculation. It is necessary to change some of the geological parameters so the observed and theoretically calculated fields may more closely coincide.

Now in the observed field let us fix end points with the coordinates (x_i and y_i). Let these be the most widely varied points at which the observed gravitational anomaly manifests itself in its most characteristic manner (extremums, points of inflection, etc.). In the future we will select a field only at the fixed point. /11

We will introduce one restriction. Let the geological model be constructed in such a way that its gravitational effect can be recorded in an analytic form.

If the geological bodies are approximated by putting together projections (gravitational steps) which are finite in space, then even the most complicated structural model can be assembled with relative ease from these elementary features.

Thus on the one hand we have the observed anomaly $V_{obse}(x_i, y_i)$, and on the other hand the theoretical anomaly $V_{theo}(p_1, p_2, \ldots p_m, x_i, y_i)$, i = 1, 2, ...,n. Here the function V can stand for any component of the gravitational field (Δg, V_{xz}, etc.). If the geological model has been described using m elementary bodies, and each body is characterized by s parameters, then the result of solving the direct problem will be the theoretical anomaly

$$V_{\text{theo}}(x, y) = \sum_{j=1}^{m} V(P_j, x, y). \tag{1.1}$$

By the symbol P_j we indicate the vector which characterizes the location and dimensions of the elementary bodies, $P_j = (p_{j1}, p_{j2}, \ldots p_{js})$. Let us illustrate this with an example. Let the geological structure of an area be approximated by a collection of direct projections which are limited in space. The location and dimensions of each projection are characterized by these parameters: σ is the excess density, h and H are the depths to the upper and lower limits, l_1 and l_2 are the parameters which characterize the projection's dimensions in space, and d is the location of the vertical boundary relative to the selected beginning of the coordinates. The value of these parameters is shown in Figure 1. Thus the totality of the vector $P_j = (\sigma_j, h_j, H_j, l_{1j}, l_{2j}, d_j)$ characterize the geological schematic of the region being investigated.

Now it is necessary to find the value of the parameters P_j at which the function V_{theo} best coincides with V_{obse}. The process of comparing these two curves can vary. Let us examine one of them.

In order to compare the functions $V_{obse}(x, y)$ and $V_{theo}(x, y)$, let us set up the functional /12

$$F = \sum_{i=1}^{n} [V_{\text{obse}}(x_i, y_i) - V_{\text{theo}}(x_i, y_i)]^2. \tag{1.2}$$

Since the points with the coordinate (x_i, y_i) have been fixed, then F depends only on the parameters P_j. Having numbered them sequentially, one can write

$$F = F(p_1, p_2, \ldots, p_N). \tag{1.3}$$

Expression (1.3) can be regarded as a function from one N-dimensional vector $P = (p_1, p_2, \ldots, p_N)$.

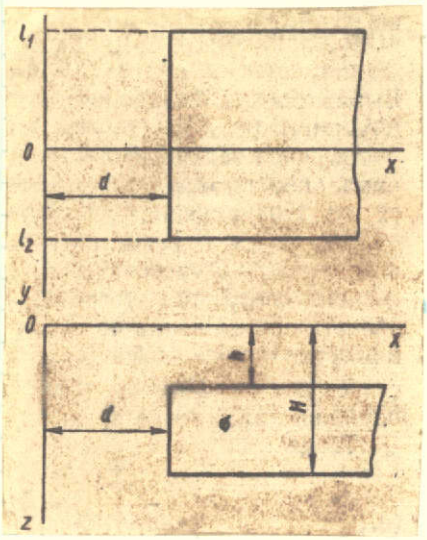

Figure 1. Values of Parameters Characterizing the Location and Dimensions of an Elementary Geological Body, i.e., the Direct Projection Limited in Space.

Let us select a vector P so that the functional (1.2) acquires minimum value. Thus the task of interpretation is reduced to the extreme problem of the function with many variables.

Let us turn our attention to some theorems about the extremums of several variables. The following theorem speaks of the condition necessary for the existence of an extremum. Let function (1.3) be such that in the area where it is being investigated there are partial derivatives of the first and second orders. Then if at point M_0 ($p_1^{(o)}$, $p_2^{(o)}$, 111, $p_N^{(o)}$) a local extremum exists, then all partial derivatives of the first order at this point are equal to 0.

Then

$$\left.\frac{\partial F}{\partial p_j}\right|_{M_0} = 0 \quad (j = 1, 2, \ldots, N) \tag{1.4}$$

is the necessary condition for the local extremum. System (1.4) makes it possible to find the points of the possible extremum (or a stationary point). It is possible to have cases where the function $F(p_1, p_2, \ldots, p_N)$ does not attain the extremum, and thus (1.4) turns out to be a necessary condition, but not a sufficient one.

In order to obtain an unambiguous answer to the question of extremums, it is necessary to use another theorem. In it another differential of function (1.3) is examined. This differential is the quadratic form from the differential dp_1, dp_2, ... dp_N and can be written in symbolic form as

$$d^2F = \left(\frac{\partial}{\partial p_1} dp_1 + \frac{\partial}{\partial p_2} dp_2 + \cdots + \frac{\partial}{\partial p_N} dp_N\right)^2 F \tag{1.5}$$

and in general form as

$$d^2F = \Phi = \sum_{i,j=1}^{N} a_{ij} h_i h_j; \quad a_{ij} = a_{ji}. \tag{1.5a}$$

Here the differential dp_k is designated by h_k. The quadratic form (1.5a) is called positively determined (negatively determined) if, for any values of the variables not equal to 0, at the same time this form has positive (negative) value. The positively and negatively determined forms are combined under a general designation, i.e., fixed forms. If the quadratic form (1.5a) acquires both positive and negative values, then it is called sign variable. If in (1.5a) the form has values of one sign, but at some point acquires 0 values, then this quadratic form is called quasi-fixed.

/13

Let us now turn to the theorem itself. Let the extremum of function $F = F(p_1, p_2, \ldots, p_N)$ be possible at point $M_o(p_1^{(o)}, p_2^{(o)}, \ldots, p_N^{(o)})$. Let us examine at this point the second differential d^2F/m_o. This differential can be written using expression (1.5). If (1.5) at point M_o has a local extremum. Meanwhile, if $d^2F < 0$, then the function at point M_o reaches a maximum, and if $d^2F > 0$, then it reaches a minimum. When the second differential is a sign-variable form, then at this point the function does not have an extremum. When the second differential has a quasi-fixed form, the function can either have or lack an extremum. Further research is required to clarify this question.

The criterion for determining the sign of a quadratic form was established by Sil'vestr and is named after him.

The quadratic form (1.5a) is characterized by the symmetrical matrix

$$A = \begin{bmatrix} a_{11}a_{12} & \ldots & a_{1N} \\ a_{21}a_{22} & \ldots & a_{2N} \\ \ldots & \ldots & \ldots \\ a_{N1}a_{N2} & \ldots & a_{NN} \end{bmatrix}. \tag{1.6}$$

The determinants are

$$A_1 = a_{11}, \quad A_2 = \begin{vmatrix} a_{11} & a_{12} \\ a_{21} & a_{22} \end{vmatrix}, \quad A_3 = \begin{vmatrix} a_{11} & a_{12} & a_{13} \\ a_{21} & a_{22} & a_{23} \\ a_{31} & a_{32} & a_{33} \end{vmatrix}, \ldots,$$

$$A_N = \begin{vmatrix} a_{11} & a_{21} & \ldots & a_{1N} \\ a_{12} & a_{22} & \ldots & a_{2N} \\ \ldots & \ldots & \ldots & \ldots \\ a_{N1} & a_{N2} & \ldots & a_{NN} \end{vmatrix}$$

and are called the principal minors of matrix A.

In order for the quadratic form (1.5a) to be positively determined, it is necessary and sufficient to fulfill the following inequality

$$A_1 > 0, \ A_2 > 0, \ A_3 > 0, \ \ldots, \ A_N > 0.$$

In order for the quadratic form to be negatively determined, it is necessary and sufficient that the signs of the principal minors $A_1, A_2, \ldots, A_N$ alternate while $A_1 < 0$.

This is the classic method. To implement it, it is necessary to find a solution for system (1.4). When solving gravimetric problems, this is a system of transcendental equations. This system is not solved in a general form. In every actual case it is solved by using approximate numerical methods. /14

It is possible to approach the minimization of functional (1.3) in another way. Some restrictions in the form of

$$\varphi_i(p_1, p_2, \ldots, p_N) \leqslant 0; \quad i = 1, 2, \ldots, n. \tag{1.7}$$

can be imposed on the parameters p_j. The area D is determined by the system of relationship (1.7). The problem consists of finding among the points of area D the point P* for which the following is attained

$$F(P^*) = \min F(P), \quad P \in D.$$

The problem formulated in this way relates to the class of problems in nonlinear programming. In its most general form this is a problem of functional programming. Depending on the type of function F and the area D which is determined by the inequalities (1.7), the problem can be simplified by reduction to problems for which solution methods are known. In particular if the function (1.2) is convex and smooth, and if the inequalities (1.7) determine the convex area D, then this problem is reduced to convex programming.

The concept that the function is convex is very important. For convex functions, theorems have been established regarding the criteria for the uniqueness of the inverse problem. Let us examine some formulas and theorems of convex function. Here they have been presented without proof. A more complete analysis of this question can be found in [13, 27].

Let two points $P^{(1)}$ and $P^{(2)}$ be assigned in N-dimensional space. The set of points $P = P^{(1)} + t(P^{(2)} - P^{(1)})$, where t is any number within the segment [0, 1] ($0 \leqslant t \leqslant 1$), is called section $P^{(1)}\ P^{(2)}$ connecting these points.

Set P is called convex if, together with any two of its points $P^{(1)}\ P^{(2)}$, all points in the section $P^{(1)}$, $P^{(2)}$ belong to this set.

Let the function F (P), $P = [p_1, p_2, \ldots, p_N]$ in N dimensional space. F (P) is a convex function in set P if for any two points $P^{(1)}$ and $P^{(2)}$ the following condition is satisfied

$$F(P^{(1)} + t(P^{(2)} - P^{(1)})) \leqslant F(P^{(1)}) + t[F(P^{(2)}) - F(P^{(1)})]. \tag{1.8}$$

If in (1.8) the inequality sign is strictly correct, then one speaks of a strict convexity.

The theorem which established the criterion of convexity is extremely important. Let the function F (P), which is assigned in the convex set P be differentiated twice. If at two points in this set the second differential d^2F is a positively determined form, then F (P) is a convex function in set P. /15
Thus on the basis of an investigation of the second differential, one concludes that the function is convex.

Why is it so important to establish the convexity of the minimized function? The reason is the uniqueness of the minimum. The following theorem confirms this.

The differentiated, strictly convex function F (P) which is assigned in the convex set P can have a local minimum only at one point in this set.

It is true that, in its most general form, functional (1.3) can be non-convex since the inverse problems fall within the class of incorrect problems and do not have a unique solution. However, by imposing restrictions on the form of the elementary body and by assigning some of its parameters, we can always ensure that the solution to the problem will not come from a particular class. This unique controlling factor ensures that the sole solution to the problem has been achieved.

Two basic tendencies are distinguishable among the methods for solving non-linear programming problems. One of them combines the methods of a systematic search for a solution. Various multi-step searches for a solution are constructed. The direction of the search is selected at each step, while the various local properties of the minimized function (for instance, the gradient of this function) are used. The second tendency uses the random search method. Each tendency has both strong and weak points.

The systematic method has complex algorithms. If the minimized function has local or boundary minimums, then similarity is, as a rule, not guaranteed between the results of the calculation and the global principal minimum. A sampling of the initial points of the search is required in a search for the global minimum.

In the random search method the algorithms are relatively simple, but they require that the entire function be calculated frequently.

When minimizing (1.2) or (1.3), their relative cumbersomeness should be kept in mind. Derivatives of the functions are computed almost without further expenditures of time, i.e., when computing the function itself. However, not all of these distinctive characteristics are germane to choosing a minimization method. One should take into account the fact that the choice of an initial approximation made by a qualified specialist who takes into account that which is already known about the geological peculiarities of the region under investigation makes it possible to obtain a solution to the problem in a previously selected class. This latter is the decisive factor in choosing a minimization method. In order to minimize (1.2) or (1.3), we use the gradient method of the fast descent. Let the vector $P = (p_1, p_2, \ldots, p_N)$ turn (1.2) or (1.3) into a minimum. Then at all other proximate points which are characterized by the vectors $p^{(k)}$, the functional

$$F(P^{(k)}) > F(P).$$

the search for the point P comprises the following: Let the initial approximation $p^{(o)} = (p_1^{(o)}, p_2^{(o)}, \ldots, p_N^{(o)})$ be known. Let us construct the vector grad $F(P^{(o)}) = (F_{p1}, \ldots, F_{pN})$. It is well known that the function F (P) will increase in the direction of the vector gradient, i.e., in the opposite direction /16

this function will decrease. Through point $P^{(o)}$ in the direction of the vector gradient, we will draw the straight line

$$P = P^{(0)} - \lambda \operatorname{grad} F(P^{(0)}). \tag{1.9}$$

By ascribing the various values to the coefficient λ, we will obtain various points on the straight line (Figure 2). If λ is greater than 0, then the point P will be located in the area where the function F (P) decreases. The value of the minimized function at any point on the given straight line can be written thus:

$$F = F(P^{(0)} - \lambda \operatorname{grad} F(P^{(0)})),$$

or

$$F = F(\lambda).$$

We will find the value $\lambda = \lambda_o$ at which $F(\lambda_o) = \min$. For this it is necessary to solve the equation

$$\frac{\partial F}{\partial \lambda} = 0. \tag{1.10}$$

Thus the point on straight line (1.9) has been determined

$$P^{(1)} = P^{(0)} - \lambda_0 \operatorname{grad} F(P^{(0)}),$$

at which $F(P^{(1)})$ assumes the least of its possible values. Now we take the point $P^{(1)}$ as the initial approximation and determine the new point $P^{(2)}$. All of the calculations are reduced to the following determination of the vector components. The calculations are carried out according to the formulas

$$\begin{aligned} p_1^{(k+1)} &= p_1^{(k)} - \lambda_k (F'_{p_1})_k, \\ p_2^{(k+1)} &= p_2^{(k)} - \lambda_k (F'_{p_2})_k, \\ &\cdots\cdots\cdots \\ p_N^{(k+1)} &= p_N^{(k)} - \lambda_k (F'_{p_N})_k. \end{aligned} \tag{1.11}$$

where k = 1, 2, ... - the iteration number. First it is necessary to calculate the coefficient λ_k. If difficulties arise when setting up and solving equation (1.10), then it is possible to make use of the approximated value λ_k as determined by the Newton method. In contrast to the exact value, the approximated value of the coefficient is designated by λ_{kN}.

$$\lambda_{kN} = \frac{F_k}{(F'_{p_1})^2 + (F'_{p_2})^2 + \cdots + (F'_{p_N})^2}. \tag{1.12}$$

Great interest is attributed to the value of the function $F = F_{fin}$ at which the minimization process can be concluded. We will assume that a mistake in calculating the function will be due only to a mistake in the observations, and that all calculations are carried out with considerable precision. In this case the error can be replaced by the differential of the function /17

$$\Delta F = 2 \sum_{i=1}^{n} [V_{obse}(x_i, y_i) - V_{theo}(x_i, y_i)] \Delta V_{obse}$$

Let us further assume that the difference between the observed and the calculated anomalies at the end of the computation will not exceed the observation error.

$$F_{\text{fin}} = \Delta F = 2\sum_{i=1}^{n} (\Delta V_{\text{obse}})^2,$$

or

$$F_{\text{fin}} = 2n\,(\Delta V_{\text{obse}})^2. \qquad (1.13)$$

It must be noted that all of this is correct if the perturbing geological masses can be described exactly using approximating bodies. In actuality the equality (1.1) does not approximate the observed function with absolute exactness, and the minimum of function (1.2) turns out to differ from 0. If the small value of the error in the field ΔV_{obse} is chosen, then $F_{\min} > \Delta F_{\text{fin}}$ can be obtained. In this case it is necessary to minimize function (1.2) to its smallest possible value. One should expect that, having obtained the smooth decresing sequence $(F^{(k)})$, we will not attain F_{fin} while $F^{(k)}$ will differ slightly from $F^{(k+1)}$. It is worthwhile to stipulate the termination of the calculation according to the criterion of the relative difference

$$\frac{|F^{(k)} - F^{(k+1)}|}{F^{(k+1)}} = \Delta. \qquad (1.14)$$

The value Δ can be determined from the model investigations, or it is established during the process of sampling the actual practical problems.

2. Other Variations of the Problem

There can be other approaches to comparing the observed and theoretically calculated functions. Let us examine several of them.

1. Let us set up the functional

$$F = \sum_{i=1}^{n} |V_{\text{obse}}(x_i, y_i) - V_{\text{theo}}(x_i, y_i)|. \qquad (1.15)$$

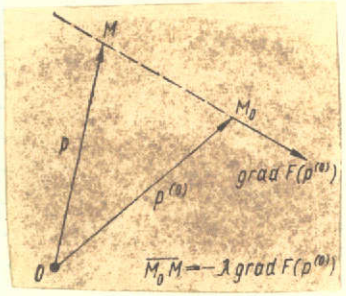

Figure 2. Search For a Point Along a Vector Gradient.

The latter expression can be written in a somewhat different manner. (1.15) includes N components, each of which is taken at its absolute value. We will divide these components into two groups. In the first group we will include those where $[V_{\text{obse}}(x_i, y_i) - V_{\text{theo}}(x_i, y_i)] \geqslant 0$, and the rest will be in the second group. We will designate by r the number of components which have turned up in the first group, and thus the number of components in the second group will be (n - r). Now (1.15) can be written /18

$$F = \sum_{i=1}^{r} [V_{\text{obse}}(x_i, y_i) - V_{\text{theo}}(x_i, y_i)] + \sum_{i=r+1}^{n} [V_{\text{theo}}(x_i, y_i) - V_{\text{obse}}(x_i, y_i)]. \qquad (1.15a)$$

Now a specific function (1.15a) will underlie minimization. Here the gradient method of the fastest incline can be used without any kind of restrictions.

2. When comparing the two functions $V_{obse}(x, y)$ and $V_{theo}(x, y)$, we select one of the fixed points (x_i, y_i). For it we will write equation

$$\Delta i = V_{obse}(x_i, y_i) - V_{theo}(x_i, y_i, P), \tag{1.16}$$

where, just as earlier, P is the vector which characterizes the location and dimensions of the geological bodies $P = [p_1, p_2, \ldots, p_N]$.

In the initial model of the geological structure, $P^{(o)} = p_1^{(o)}, p_2^{(o)}, \ldots, p_N^{(o)}$. One must find the values of P such that Δi is as small as possible. Let $P = P^{(o)} + \Delta P$, i.e.

$$\left.\begin{aligned} p_1 &= p_1^{(0)} + \Delta p_1, \\ p_2 &= p_2^{(0)} + \Delta p_2 \\ &\cdots\cdots\cdots \\ p_N &= p_N^{(0)} + \Delta p_N. \end{aligned}\right| \tag{1.17}$$

Now (1.16) will depend only on $(\Delta p_1, \Delta p_2, \ldots, \Delta p_N)$. As a rule the function $V_{theo}(s, y, P)$ is relatively complex, and the parameters p_j belong under the signs of transcendental function. We linearize the problem. Let us put $V_{theo}(P)$ (at a fixed point) $(x_i, y_i))$ into a Taylor series and let us restrict ourselves to only the linear part.

$$V_{theo}(P) \approx V_{theo}\left(P^{(0)}\right) + \left.\frac{\partial V}{\partial p_1}\right|_0 \Delta p_1 + \left.\frac{\partial V}{\partial p_2}\right|_0 \Delta p_2 + \cdots + \left.\frac{\partial V}{\partial p_N}\right|_0 \Delta p_N. \tag{1.18}$$

Expression (1.16) is rewritten thus:

$$\Delta i = V_{obse}(x_i, y_i) - V_{theo}(P^{(0)}, x_i, y_i) - \sum_{j=1}^{N} A_{ij}\Delta p_j. \tag{1.19}$$

Here

$$A_{ij} = A_{ij}(x_i, y_i, P^{(0)}) = \left.\frac{\partial V}{\partial p_j}\right|_0.$$

having accepted $\Delta_i \to 0$ (1.19) can be written in the form

$$\sum_{j=1}^{N} A_{ij}\Delta p_j = V_{obse}(x_i, y_i) - V_{theo}(x_i, y_i, P^{(0)}) = \delta_i. \tag{1.20}$$

Parameter i acquires values equal to 1, 2, ..., n, i.e., (1.20) is a system of linear equations with N unknowns. If n > N, then a redefined system has been obtained which can be written in matrix form as /19

$$A\Delta P = \delta$$

where

$$A = \begin{bmatrix} A_{11}A_{12} & \dots & A_{1N} \\ A_{21}A_{22} & \dots & A_{2N} \\ \dots & \dots & \dots \\ A_{n1}A_{n2} & \dots & A_{nN} \end{bmatrix}, \quad \Delta P = \begin{bmatrix} \Delta p_1 \\ \Delta p_2 \\ \vdots \\ \Delta p_N \end{bmatrix}, \quad \delta = \begin{bmatrix} \delta_1 \\ \delta_2 \\ \vdots \\ \delta_n \end{bmatrix}.$$

This system can be solved by using the least-squares method. The method itself will relieve us of the necessity of investigating the compatibility of the selected system [45].

Without citing any calculations, we will simply indicate that vector ΔP is found from solving the system

$$A'A\Delta P = A'\delta, \tag{1.21}$$

where A' is the transformed matrix A. As is well known, this relationship always leads to a fully defined system of exactly the same number of equations as we have unknowns [45].

3. It is possible to introduce additional limitations into the function which should be minimized. These limitations will play the role of regulating parameters (according to A. N. Tikhonov). We will require that during minimization the desired parameters do not differ so sharply from their initial values. For this purpose we introduce into the functional (1.2) another member

$\sum_{i=1}^{N} \lambda_i (p_i - p_i^{(0)})^2$, where λ_j is the constant coefficient which plays the role of a weighting function. Wherever the version of the parameters, according to the geological data, should be small, the coefficient λ_j will be selected by the researcher to be large. If the variation of any parameter is not restricted by the geological data, λ_j can be selected to be sufficiently small or equal to 0.

The basis of the final minimization is the functional

$$F = \sum_{i=1}^{n} [V_{\text{obse}}(x_i, y_i) - V_{\text{theo}}(x_i, y_i)]^2 + \sum_{j=1}^{N} \lambda_j (p_j - p_j^{(0)})^2. \tag{1.22}$$

This functional depends not only on the geological parameters p_j, but also on the regularization parameters λ_j.

The minimization method can be used to interpret various anomalies by postulating differing forms for perturbing masses. Relatively simple relationships for computers calculation can be obtained in cases where the perturbing bodies are approximated by a group of spheres, right-angled prisms, etc. Through

identifying the area of the perturbing body by the total of its projections, it is possible to obtain a solution to the problem for an arbitrary contour with an arbitrary distribution of masses.

3. Solving the Inverse Problem for a Group of Cylinders by the Anomaly V_{xz} /20

We will illustrate with an example the interpretation of gravitational anomalies using the minimization method. Let an anomaly V_{xz} be assigned and let there be established the possibility of approximating the perturbing bodies with cylinders. The position and geometric dimensions of each cylinder can be characterized by the following parameters: d is the abscissa of the epicenter, h is the depth at which the axis occurs, and σ is the excess density (Figure 3). Here it should be noted that the derivatives have very small values according to their mass. Therefore, changes in this parameter are small in comparison to the others. This kind of inequality in changing the parameters leads to a very slow convergence of the calculations' iteration processes. We will express the mass by means of a linear parameter.

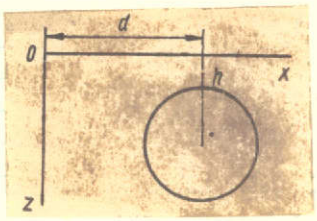

Figure 3. Values of the Parameters Characterizing the Location of a Cylindrical Body.

The mass of a unit of the cylinder length is determined by the relationship $M = \eta R^2\sigma$. As is well known, it is not possible to determine σ and R separately. We will designate $\sigma_j R_j^2 = t_j^2$ and we will determine parameter t in the future. In order to be able to take into account the sign of the excess density, we accept

$$\sigma_j R_j^2 = \operatorname{sign}(\sigma_j) t_j^2.$$

Here

$$\operatorname{sign}(\sigma_j) = \begin{cases} 1, & \text{if } \sigma_j \geqslant 0, \\ -1, & \text{if } \sigma_j < 0. \end{cases}$$

Thus the position and dimensions of each cylinder determine the following four parameters [t, h, d, sign (σ)]. We will set up the function

$$F = \sum_{i=1}^{n} \left\{ V_{xz\,\text{obse}}(x_i) - 4\pi k \sum_{j=1}^{m} \left[- \frac{\operatorname{sign}(\sigma_j)\, t_j^2 h_j (x_i - d_j)}{[(x_i - d_j)^2 + h_j^2]^2} \right] \right\}^2. \qquad (1.23)$$

We will consider the parameters of sign (σ_j) to be constant, and then m three-dimensional vectors will be unknown:

$$P_j = [t_j, h_j, d_j].$$

We find the components of these vectors, of which function (1.23) will become the smallest possible.

We will assign the initial approximation: $P_j^{(0)} = [t_j^{(0)}, h_j^{(0)}, d_j^{(0)}, \text{sign}(\sigma_j)]$. We will determine the following approximations by the formulas

$$\begin{aligned} t_j^{(k+1)} &= t_j^{(k)} - \lambda_k (F'_{t_j})_k, \\ h_j^{(k+1)} &= h_j^{(k)} - \lambda_k (F'_{h_j})_k, \\ d_j^{(k+1)} &= d_j^{(k)} - \lambda_k (F'_{d_j})_k \qquad (j = 1, 2, \ldots, m). \end{aligned} \tag{1.24}$$

The derivatives will be expressed thus: /21

$$F'_{t_j} = 16 \operatorname{sign}(\sigma_j)\, \pi k \sum_{i=1}^{n} \delta_i \frac{t_j h_j (x_i - d_j)}{[(x_i - d_j)^2 + h_j^2]^2},$$

$$F'_{h_j} = 8 \operatorname{sign}(\sigma_j)\, \pi k \sum_{i=1}^{n} \delta_i \frac{t_j^2 (x_i - d_j)[(x_i - d_j)^2 - 3h_j^2]}{[(x_i - d_j)^2 + h_j^2]^3},$$

$$F'_{d_j} = -8 \operatorname{sign}(\sigma_j)\, \pi k \sum_{i=1}^{n} \delta_i \frac{t_j^2 h_j [h_j^2 - 3(x_i - d_j)^2]}{[(x_i - d_j)^2 + h_j^2]^3},$$

where

$$\delta_i = V_{xz\,\text{obse}}(x_i) - V_{xz\,\text{theo}}(x_i).$$

In the last relationships

$$V_{xz\,\text{theo}}(x) = 4\pi k \sum_{j=1}^{m} \operatorname{sign}(\sigma_j) \left\{ -\frac{t_j^2 h_j (x - d_j)}{[(x - d_j)^2 + h_j^2]^2} \right\}.$$

We will calculate the coefficient λ by the Newtonian method of Newton (1.12).

4. An Example of Solving the Problem

We will examine the use of the method in the following examples. Let an anomaly of the horizontal gradient of the force of gravity (Figure 4) be given, and let it be established that the perturbing geological bodies can be related to two-dimensional bodies, for instance according to the method of A. A. Yun'kov [81]. Even a cursory analysis shows that the perturbing masses are scattered along the profile. It is possible to distinguish three anomalously shaped objects. Let us assume that the problem has been posed of evaluating individually each geological body, i.e., determining its mass and center of gravity. It is possible to approximate each geological body as a cylinder in order to solve the problem. The parameters of three cylinders (9 magnitudes in all) form the basis of the determination. Let us fix the most characteristic points of the observed anomaly along axis Ox. In all, 13 points are distinguished, which have been reduced to tabular form (Table 1). Taking into account the dimensions of the anomaly, meters have been adopted as linear units. Using the most general /22 premises as a basis, we will select the model of the first approximation, the parameters of which have been cited in Table 2. (Some remarks of a methodological nature on the calculation of these parameters will be given in the second chapter).

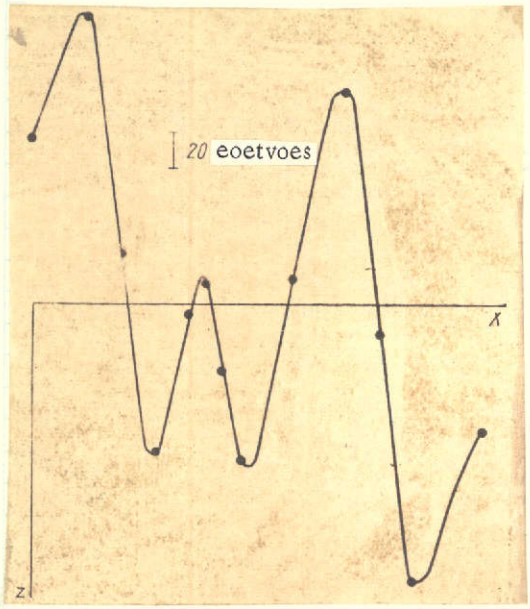

Figure 4. Anomaly V_{xz}, as Caused by Three Perturbing Bodies.

The data in Tables 1 and 2 are the initial data for solving the problem. The results of the solution are given in Table 3. Here all the intermediate results of the calculations from iteration to iteration (some iterations have been omitted) are shown.

The function at the initial values of the parameter was found to be equal to 18768 eoetvoes^2. The function F in the following iterations acquires these values: 12449, 7369, 4376, 2780, ...

We will determine the value of F at /23 which it would be necessary to conclude the computation. Let us turn to formula (1.13). In our case n = 13. If we accept that the error in the observation is 3 eoetvoes, then F_{fin} = 234 eoetvoes^2. In the 26th approximation F_{26} = 153 eoetvoes^2, and the value of the unknown vectors is P_1 = (147, 199, 302), P_2 = (82, 137, 600), and P_3 = (148, 198, 1049). After the 37th approximation, we obtain F_{37} = 31 eoetvoes^2 and P_1 = (149, 200, 301), P_2 = (86, 144, 600), and P_3 = (149, 198, 1050).

Let us assume that the cylinders have excess densities $\sigma_1 = 1$, $\sigma_2 = 0.8$, and $\sigma_3 = 1$. In this case it is easy to calculate the radii $R_i = \frac{t_i}{\sqrt{\sigma_i}}$. We obtain R_1 = 301, R_2 = 97, and R_3 = 149.

The cited anomaly was calculated for three cylinders which had the following parameters: P_1 = (150; 200; 300), P_2 = (89.4; 150; 600); and P_3 = (150; 200; 1050).

TABLE 1.

No. of the point	1	2	3	4	5	6	7	8	9	10	11	12	13
x	0	200	300	400	500	550	600	650	800	950	1050	1150	1350
V_{xz}	74	168	32	—88	—5	13	38	83	159	123	—17	—162	—72

TABLE 2.

No. of the perturbing body	t	h	d
1	120	200	320
2	60	100	570
3	130	220	1040

TABLE 3.

Parameter of the Perturbing Body	No. of Approximation																					Exact value
	0	1	2	3	4	5	6	7	8		10	11	12	13	14	15	16	17	18	26	37	
t_1	120	123	129	132	136	137	139	138	139	141	141	142	143	142	143	146	144	145	146	147	149	150
h_1	200	198	194	192	190	190	189	193	192	192	194	194	194	195	195	195	195	197	197	199	200	200
d_1	320	319	316	313	309	306	306	305	306	306	305	305	305	304	304	305	304	303	304	302	301	300
t_2	60	54	53	57	58	65	62	71	68	66	73	72	70	75	73	72	74	79	78	82	86	89,4
h_2	100	104	105	104	105	106	109	111	113	115	117	119	121	122	123	127	126	129	130	137	144	150
d_2	570	573	578	583	588	594	594	596	596	596	597	597	597	598	598	598	598	599	599	600	600	600
t_3	130	134	141	146	149	149	149	148	148	148	148	148	148	148	148	149	148	147	147	148	149	150
h_3	220	218	213	209	206	205	205	203	203	201	201	201	201	201	200	200	200	199	199	198	198	200
d_3	1040	1040	1042	1043	1045	1047	1048	1049	1049	1049	1049	1049	1049	1049	1049	1049	1049	1049	1049	1049	1050	1050
F	18768	12499	7369	4376	2780	2378	1899	2559	1628	1302	1709	1092	909	1098	737	823	578	603	396	153	31	—

5. Nature of the Convergence of the Fast Descent Method When Solving Inverse Problems For a Group of Cylinders

Let us examine Table 3 in which the results of the computations are cited. At first the function decreases. In the seventh iteration a disturbance is observed in the function's smooth progression. Meanwhile, the gradient of the function's change in the following step acquires its largest value. After the 10th iteration, one again observes an increase in the value of F which must be minimized. Sudden changes in the values of the function become relatively frequent from this point on. /24

What is the cause of the sudden changes?

As was noted earlier, a vector gradient is sought by the fast descent method. The greatest change in the function occurs in the vicinity of the selected approximation along this vector. At the very beginning the change is sharply reduced, and then, reaching a minimum at some certain point, it begins to increase. The problem is to determine the point at which the function attains the

minimum. The coefficient λ_k also determines this point. However, this is quite difficult to calculate. The approximated value of λ_k, as determined by the Newtonian method, does not always provide the necessary precision.

Let us again turn to the example cited in the previous paragraph.

In each iteration we carry out several computations of the function F along the vector gradient. For this we will assume that $\lambda_k = S\lambda_{kN}$. We will give parameter s the values 1/4, 1/2, 3/4, 1, 5/4, and 3/2. Of the six values of the function we will select $F = F_{min}$ and the λ_k (values) which correspond to this function. We will use this coefficient in future calculations of the parameters of the cylindrical bodies. The calculations made in this manner are shown in Table 4. /25

TABLE 4.

Parameters of the Perturbing Body	Nos. of the Approximations																						Exact value
	0	1	3	5	7	9	11	13	15	17	19	20	21	22	23	24	25	30	35	37	39	40	
t_1	120	127	135	137	140	140,9	142,4	143,5	144,5	145,7	146,3	146,5	147,1	142,2	145	147,3	146,2	147,9	148,8	149	149,2	149,4	150
h_1	200	195	190	190	190	192	193,6	195,1	195,4	197	197,2	197,5	197,5	198,6	197	196,4	197,6	198,1	199,6	195,6	199,8	199,7	200
d_1	320	317	310	308	305	305	305	304,4	304,2	303,4	302,8	302,8	302,7	303,4	303,6	302,6	302,1	301,8	300,9	300	300,6	300,6	300
t_2	60	47	57	61	66	68	70,6	73,5	74,4	77,1	78,4	80	79,6	82,6	79,7	81,6	81,5	83,4	86,6	86,9	87,6	87,5	89,4
h_2	100	107	106	107	113	116,5	120,4	124,1	126,4	131,3	133,5	134,1	135,2	134,1	136,1	136,6	138,1	140,8	145	145,7	146,7	146,9	150
d_2	570	576	586	590	597	599	597	597,8	598,1	596,4	598,7	599	599,2	599	598,9	599,1	599,6	599,7	600,1	600,1	600,2	600,1	600
t_3	130	137	149	149	148	148	148,1	147,8	147,7	149,1	148	147,4	147,7	147,5	147,4	147,3	147,9	147,7	148,3	148,5	148,7	148,8	150
h_3	220	216	207	206	203,5	202,4	201,3	200,3	199,9	198	198,6	198,9	198,6	198,6	198,4	198,2	197,9	198	198,2	198,4	198,6	198,6	200
d_3	1040	1044	1044	1046	1049	1048,8	1048,8	1048,9	1049	1049	1049,1	1049,2	1049,3	1049,3	1049,4	1049,4	1049,3	1049,5	1049,8	1049,8	1049,8	1049,8	1050
λ	—	0,02102	0,0247	0,01157	0,0810	0,07954	0,07634	0,1064	0,0580	0,0304	0,2098	0,2152	0,1278	0,1043	0,01165	0,1560	0,1237	0,1060	0,3996	0,3450	0,4060	—	—
Values of the Function F																							
0,25	—	14897	3820	2235	1471	1164	896	672	551	451	276	244	219	955	737	192	298	84	31	19	13,9	11	—
0,5	—	12449	3365	2269	1697	1316	1044	822	579	436	291	288	264	3437	558	187	169	100	28	23	13,7	9,7	—
0,75	—	11137	3319	2686	2386	1901	1396	1201	716	492	370	407	374	7673	418	219	195	141	30	333	16	10	—
1	—	10728	3627	3431	3568	2865	2030	1838	965	623	515	603	547	13690	318	288	261	208	36	48	21	12	—
1,25	—	11032	4242	4457	5272	4260	3018	2733	1332	831	724	877	781	21537	256	396	357	299	47	70	29	15	—
1,5	—	11398	5121	5724	7529	6119	4285	3872	1821	1119	1000	1230	1071	31283	232	543	481	416	—	—	—	—	—
F_{min}	18768	10728	3319	2235	1471	1164	896	672	551	436	276	244	219	955	232	187	160	84	28	19	13,7	9,7	—

Commas indicate decimal points.

Figure 5 shows graphs of the function change along the vector gradient. In the first iterations the minimum of the function corresponds to the value $\lambda_k = \lambda_{kN}(s = 1)$. However, right after the second approximation the function F acquires its minimum value at $\lambda_k = s\lambda_{kN}$, where at first the parameter s = 3/4, then s = 1/2, and s = 1/4. It is evident from curve 7 that the calculated value of the function F at s = 1 will be larger than in the previous approxi-

mation. Solving the problem with the fixed value s = 1, we also obtained sudden jumps in the changes in function F (Figure 5, b).

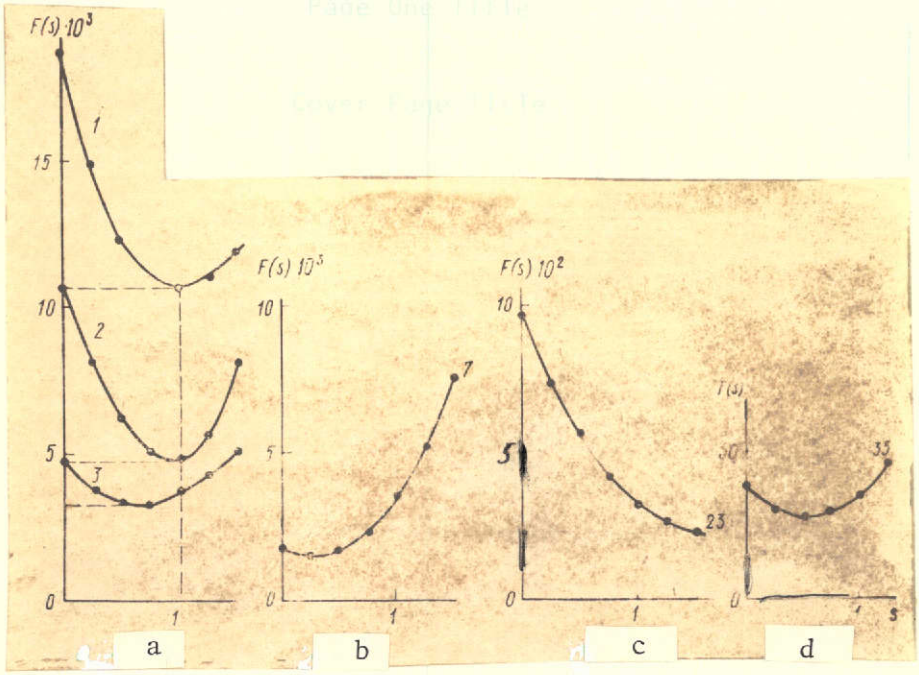

Figure 5. Change in Function F Along the Vector Gradient (Various Iterations).

One must also consider one other peculiarity. After the sharp jumps in the value of the function the next iteration, as a rule, is accompanied by a large value for the coefficient s. Thus it is evident from Table 4 that, after the 21st approximation, a malfunction occurred in the machine (the calculations were not being re-checked), the smooth decrease in the function was disturbed, and the 22nd approximation became worse than the previous one. During calculation of the 23rd approximation the value of the coefficient was s = 3/2. /26
This means that the vector had raised considerably. The change in the function along the vector is illustrated in Figure 5c. In following iterations, when the value of the function is small, its change along the vector gradient becomes less sharp (Figure 5d).

The example cited indicates that it is necessary to determine the coefficient s during the calculation. Henceforth, all computer programs have been set up with allowance made for the calculated value of s.

6. Increasing Convergence of the Fast Descent Method While Solving the Inverse Problems of Gravitational Survey

The nature of the function change along the vector gradient was established in the previous section. In this vector, the function F which must be minimized is dependent upon one parameter, which is the magnitude of s. The problem lies

in finding the value of parameter s at which the function F along the vector gradient acquires its maximum value. It is possible to come to a conclusion about the nature of this function by using the fast descent geometric interpretation method. Let us assume that the function F changes according to the parabolic law

$$F = as^2 + bs + c. \tag{1.25}$$

This approximation agrees completely with the computed results shown in Figure 5.

We will find the s at which $F(s) = F_{min}$. For this purpose it is sufficient /27 to find the root of the equation $\frac{\partial F}{\partial s} = 0$. By differentiating (1.25), we find

$$2as + b = 0$$

From this

$$s = -\frac{b}{2a}.$$

In order to compute the unknown parameter s, it is necessary to find coefficients a and b in the equality (1.25).

We know the value of the function $F(0) = F_o$. At $s = 0$ the function acquires the value of the preceding computation. In order to find coefficients a and b, we compute the function F (s) at the two values $s = s_1$ and $s = s_2$. Let $F(s_1) = F_1$ and let $F(s_2) = F_2$. Inserting these values into (1.25), we obtain

$$F_o = c,$$

$$F_1 = as_1^2 + bs_1 + F_0,$$
$$F_2 = as_2^2 + bs_2 + F_0.$$

From the last two equations we find a and b, and after this it is easy to determine parameter s.

$$s = \frac{s_2^2(F_1 - F_0) - s_1^2(F_2 - F_0)}{2[s_2(F_1 - F_0) - s_1(F_2 - F_0)]}. \tag{1.26}$$

Thus the following calculation method is recommended. We will designate the previously determined value of the function by F_o. We compute function F (s) at $s = s_1$ and $s = s_2$. We obtain $F(s_1) = F_1$ and $F(s_2) = F_2$. We compute coefficient s according to formula (1.26), and then compute the value of function F (s).

There is a question about the choice of the values s_1 and s_2. Let $s_1 < s_2$. The best result in searching for the minimum of the function F (s) should be expected when $s_1 < s_{min} < s_2$. In choosing values s_1 and s_2, it is

recommended that one use the value $s = s_{pr}$, as calculated in the preceding iteration, and accept $s_1 = 1/2 s_{pr}$, and $s_2 = 3/2$ of s_{pr}. In calculations of the first iteration, one can assume that $s_1 = 1$, and that $s_2 = 2$.

7. Another Algorithm For the Minimization of the Function of Many Variables

We have established that, when solving the inverse problem, the minimization is based on the function

$$F = F(p_1, p_2, \ldots, p_N). \tag{1.27}$$

The algorithm described here is based on the fast descent gradient method [10, 22]. Let us establish some initial value $(p_1^{(0)}, p_2^{(0)}, \ldots, p_N^{(0)})$ by which a certain point is fixed in N-dimensional space. Now we choose one direction in such a way that it coincides with the vector gradient, but such that its direction is the opposite of the vector gradient. If a function increases as much as possible along the vector gradient, then in the other direction it will decrease. The chosen line is described by the directing cosines

/28

$$\cos \alpha_j = \frac{-F'_{p_j}}{\sqrt{\sum_{i=1}^{N} (F'_{p_j})^2}}.$$

Function (1.27) along the vector gradient can be written like the function of one variable l. For this purpose it is necessary to introduce into (1.27) the parameters

$$\bar{p}_j = p_j^{(0)} + l \cos \alpha_j \qquad (j = 1, 2, \ldots, N). \tag{1.28}$$

Thus along the selected axis $F = F(l)$.

Now let us pose the problem of finding the value $l = l^*$ for which $F(l^*) = \min$. For this purpose it is necessary to solve the equation

$$F'(l) = \varphi(l) = 0. \tag{1.29}$$

The new designation of the function $\varphi(l)$ has been introduced for the sake of convenience in future work. It is necessary to find the root of the transcendental equation (1.29).

We use the reduction method of solving transcendental equations to solve differential equations [58].

Thus, the equation is given

$$\varphi(l) = 0 \tag{1.30}$$

Let us examine the function

$$t = \varphi(l). \tag{1.31}$$

The value $l = l^*$ which converts this function to 0, is the root of equation (1.29). If function (1.31) has the reverse form

$$l = L(t), \tag{1.32}$$

then the task of finding the root of equation (1.29) is reduced to computing function (1.32) at t = 0 because

$$l^* = L(t^*) = L(0). \tag{1.33}$$

The derivative of function (1.32) is like the reverse (1.31)

$$\frac{dL}{dt} = \frac{1}{\varphi'(l)}. \tag{1.34}$$

Thus we have the differential equation of function (1.32). Having selected the arbitrary value $l = l_0$ and having inserted it into (1.31), we obtain the initial conditions for solving differential equation (1.34) at $t = t_0 = \varphi(l_0)$, $l = l_0$.

Only one value of function (1.32) $l = L(0)$ is of interest to us. /29
The integration interval is determined by

$$\Delta t = t_{\text{fin}} - t_{\text{ini}} = 0 - t_0 = -\varphi(l_0).$$

It is completely natural to select the initial value $l_0 = 0$, and then

$$\Delta t = -\varphi(0).$$

If we use the Runge-Kutta method to calculate l^*, having accepted a computation step equal to Δt, then it is necessary to compute

$$k_1 = \frac{-\varphi(0)}{\varphi'(0)}, \quad k_2 = \frac{-\varphi(0)}{\varphi'\left(\frac{1}{2}k_1\right)}, \quad k_3 = \frac{-\varphi(0)}{\varphi'\left(\frac{1}{2}k_2\right)}, \quad k_4 = \frac{-\varphi(0)}{\varphi'(k_3)}.$$

Then

$$l^* = \frac{1}{6}(k_1 + 2k_2 + 2k_3 + k_4).$$

Now new values for the unknown magnitudes are determined according to (1.28), by

$$p_j = p_j^{(0)} + l^* \cos\alpha_j. \tag{1.35}$$

If, at the computed values of the parameters, the function is sufficiently small, then the computation is complete. The formulas (1.35) give the final

results of the solution. If not, the iteration cycle is repeated. This point, the coordinates of which are calculated according to formulas (1.35), is accepted as the initial point.

8. Program For Solving the Inverse Problems by Using the Minimization Method (Fast Descent)

In its general form, the entire program is written in algorithmic language (ALGOL-60). It consists of individual blocks and constructions. The magnitudes encountered in the program are described at the start of the program. We will subsequently discuss these magnitudes in somewhat more detail.

In order to solve the inverse problem, numerical information has to be fed into the computer. This information consists of several groups. The first group is the information which describes the observed gravitational field and contains the coordinates of the points and the value of the field at given points XT [1:n], YT [1:n], and GNABL [1:n]. The second group contains the parameter values of the bodies which approximate the geological model: PP1 [1:m], PP2 [1:m], ... PPT [1:m] and P1 [1:m], P2 [1:m], ... PK [1:m]. In massifs PP1, PP2, ... PPT [1:m] the parameters to be determined (the variable parameters) are unified. They belong to functions (1.2) and (1.3).

Massifs P1, P2, ... PK [1:m] determine the geological model but, when the problem is solved, they are confirmed and take on the role of constant parameters.

Since the dimensions of the first and second group can vary when solving the various problems, it is necessary to put into the computer memory the values of the magnitudes n, i.e., the number of points which are used in solving problems m, i.e., the number of perturbing bodies through the use of which the geological model is approximated. With regards to the magnitudes (T + K), i.e., the general number of parameters in an elementary geological body, this is constant for every actual problem. For instance, if a geological body is a made up of cylindrical bodies, then T + K = 4, T = 3 (these are parameters t, h, d) and parameter K = 1 is sign σ. If the geological model is described as a group of straight projections finite in space (Figure 1), then most often T = 1 (this parameter is d, the position of the projection's boundaries). The magnitude K = 5 (σ, h, H, ζ_1, ζ_2), these are all considered constant and are not subject to change during the minimization process (1.2). /30

In addition, values F_{fin} and Δ_{fin} must be placed in the machine's memory. These magnitudes determine the end of the computation cycle according to criteria (1.13) and (1.14).

Value F_{fin} can be computed, but magnitude Δ_{fin} is assigned. This magnitude must be determined during the process of sampling the actual practical problem, or it must be established from research with models. Most often this magnitude varies within the limits of 0.05 - 0.02. Thus, the massif of the initial value is determined within the operational memory device in order to solve the problem. We will designate this M_1. The dimensions of this massif depend on magnitudes n and m.

Data fed into the computer is printed. This is necessary because one might want to check the initial data. After all, even an error in the numerical data fed in which at first appears insignificant can distort the intent of the interpreter, and the problem will not be solved.

Now we again turn to a description of the variable magnitudes in the program. The variable indices are designated by the symbols i and j: i changes from 0 to n, and j changes from 0 to m. Magnitudes SKL, TKL, P35, and P7 are determined within the program itself. The first two magnitudes are needed to transmit directions to switches KLM2: = A0, A1, A2, A3; switch KL37: = T6, T14, D. Near the switch designation, marks are indicated by means of which several instructions in the program are designated. The magnitude SKL, during the process of solving the problem, can acquire a value from 1 to 4. Depending on the value of this magnitude, switch KLM2 sends directions to one of the operators with mark A0, A1, A2, or A3. Magnitude TKL can acquire values from 1 to 3 during the calculation process. The entire numbers P35 and P7 are also used to transmit directions.

The massifs of the operative numbers are then described. First come the coordinates of the points and the values of the field at the given points, and then come the parameters of the geological model. In order to record the intermediate data, two groups of massifs, M_2 and M_3, are distinguished. Within group M_2, massifs PP1 and 2, PP2 and 2, ... PPTM2 [1:m] are distinguished in order to record the results of the calculations in the regular iteration of the geological model's parameters. In each cycle of the calculation process, after changes have been made in the geological model, the gravitational field V_{theo} /31
(x_i, y_i) is computed at n points. In the program this massif is designated as GTM2 [1:n]. The calculated values of the geological parameters and the calculated gravitational field (massifs PP1 and 3, PP2M3, ... PPTM2 [1:n] and GTM3 [1:n]) are re-written into massif M3. Symbols FPR1, FPR2, ... FPRT [1:m] designate the massif of the values derived from function (1.2) according to the desired parameters.

Then follows a description of the operative number. S has already been indicated, F_{fin} and Δ_{fin} are introduced at the same time as initial data. They are described by the identifiers FKON and DELT. We will discuss the value of the other numbers later.

Now let us go to a description of the program itself. The values corresponding to 1.0 and 2.0 assume magnitudes s_1 and s_2. The whole number P7 receives the value 0. Then follows the component operator, described by the sign M. The values of the variable parameters in massif M_2 are rewritten within the cycle. Variable P35, SKL, and TKL acquire the value 1, and directions are given to the operator assigned the symbol A.

At the very end of the program are located four groups of operators, next to which are the symbols A, B, C, and K. They are closely interrelated and are essentially specialized sub-programs.

The symbol A designates the block in which the values are computing

$$V_{\text{theo}}(x_i, y_i) = \sum_{j=1}^{m} V_{j\,\text{theo}}(x_i, y_i).$$

Under the symbol B is written the block for computing the function

$$F = \sum_{i=1} [V_{\text{obse}}(x_i, y_i) - V_{\text{theo}}(x_i, y_i)]^2.$$

The block operates four times in one computer cycle. Switch KLM2 (switch KLM2: = A0, A1, A2, A3;) is located here. The function F is written in turn into four different memory cells.

The next block (symbol C) is activated only if the number P35 is not equal to 0. Here the derivatives of the function F are computed according to the desired parameters. In each cycle these magnitudes are calculated only once. This means that every time, when switching to A (and this means to block B as well which follows it), the values of number P35 must always be noted.

Using operator K, an output is made from the unique sub-program into the necessary position in the basic program.

It is worth noting that operators A and C cannot be actually described in the general program. In each case its function will be $V_{j\ \text{theo}}(x_i, y_i)$, and this means that they will be various values of the derivatives of function F. When examining the actual problems, it is necessary to describe these blocks.

One moves from the sub-program with the symbol A - B - C - K to operator T6 at (TKL = 1). The computed value of function F, the massif $V_{\text{theo}}(x_i, y_i)$, and the values of the variable parameters are rewritten into massif M_t. /32

Directions are then given to operator T9. The decision is then made to print the direct problem. Thus, there is the possibility of comparing $V_{\text{obse}}(x_i, y_i)$ with $V_{\text{theo}}(x_i, y_i)$ computed for the model of the first approximation. Here the entire computation process can be stopped, and a corrective factor can be introduced into the model of the first approximation of geological structure if the interpreter decides that the correction was not constructed satisfactorily earlier. By means of operator P7: = 1, access to operator T9 is closed in the future.

In block T10 the coefficient λ_{kN} is calculated. Then (operator T11) one determines the values of the desired parameters for $s = s_1$ and $s = s_2$, while each time reference is made to the sub-program (blocks A - K). Before moving to block A, parameters P35 and TKL are given values corresponding to 0 and 2.

This is necessary in order to avoid computing the derivatives (block C), and to return to operator T14. Here $F = F_{min}$ is searched for, and the values of the parameters in the geological model, as well as the massif $V_{theo}(x_i, y_i)$ which correspond to them, are rewritten into massif M_3.

The coefficient s is then computed according to formula (1.26), and the values of the geological parameters are again computed (during this process instructions are again transmitted to sub-programs A - K). Symbol D designates the operators which minimalize the calculated function F. Some relationships are then checked. If F_{fin} (which has identifier FM3) is equal to F_o, then this is evidence of the fact that the function has not decreased in the given cycle. We have reached the possible F_{min} for concrete geological data. The computation should be finished.

The end of the computation occurs when F_{min} is less than or equal to F_{fin} or when the character of the function's monotonic progression is sufficiently small. Meanwhile the results of the minimization are printed out: the values of parameters, the collected function, and the function F itself. (symbol D1).

If none of the described criteria have been fulfilled, then it prepares to move on to a new iteration and directions are transmitted to blocks N.

Minimization Program for Functionals

```
Begin
        integer n, m, i, j, P7, P35, SKL, TKL, T;
        real array XT, YT, GNABL [1:n],
                   PP1, PP2, ... PPT [1:m],
                   P1, P2, ... PK [1:m],
                   PP1M2, PP2M2, ... PPTM2 [1:m],
                   GTM2 [1:n],
                   PP1M3, PP2M3, ... PPTM3 [1:m],
                   GTM3 [1:n],
                   FPR1, FPR2, ... FPRT [1:m];
        real       FKON, DELT, FM2, FO, F1, F2, FF,
                   FM3, LAM, S1, S2, SW;
        switch     KLM2:=AO, A1, A2, A3;
        switch     KL37:=T6, T14, D;
Input   Begin integer n, m; real FKON, DELT;
        real array XT, YT, GNABL [1:n],
                   PP1, PP2, ... PPT [1:m],
                   P1, P2, ... PK [1:m] end
Printout Begin real array XT, YT, GNABL [1:n],
                   PP1, PP2, ... PPT [1:m],
                   P1, P2, ... PK [1:m] end
        Begin      S1:=1.0; S2:=2.0; P7:=0 end
   N:   Begin      for j:=1 step 1 until m do
        Begin PP1M2[j]:=PP1[j]; PP2M2[j]:=PP2[j]; ...
                   PPTM2[j]:=PPT [j] end
                   P35:=SKL:=TKL:=1; go to A end
   T6:  for j : = 1 step 1 until m do
        Begin PP1M3[j]:= PP1M2[j]; PP2M3[j]:=PP2M2[j];
                   ...PPTM3[j]:=PPTM2[j] end
                   FM3:=FM2;
                   for i:=1 step 1 until n do
                   GTM3[i]:=GTM2[i];
                   if P7 = 0 then go to T9 else go to T10;
```

/33

```
T9: Begin P7:=1;
      Printout real FO; array GTM2 [1:n]} end
T10: Begin real sum, KW;
            sum:=0.0
      for j:=1 step 1 until m do
      Begin KW:=FPR1[i]↑2 + FPR2[j]↑2 ... + FPRT[j] ↑ 2;
            sum:=sum+KW end
            LAM:=FM2/sum end
T11: for SW:=S1, S2 do
      Begin for j:=1 step 1 until m do
      Begin PP1M2 [j]:=PP1 [j] — SW × LAM × FPR1[j];
            . . . . . .
            PPTM2[j]:=PPT[j] — SW × LAM × FPRT[j] end
            P35:=0; TKL:=2; go to A;
T14: of FM3 > FM2 then
      Begin FM3:=FM2;
      for j:=1 step 1 until m do
      Begin PP1M3 [j]:=PP1M2 [j];
            . . . . . .
            PPTM3 [j]:=PPTM2 [j] end
      for i:=1 step 1 until n do
            GTM3 [i]:=GTM2 [i] end end
            SW:=(S2 × S2 × (F1 — F0) — S1 × S1 × (F2 — F0))/
            (2.0 × (S2 × (F1 — F0) — S1 × (F2—F0)));
      for j:=1 step 1 until m do
      Begin PP1M2[j]:=PP1[j] — SW × LAM × FPR1[j];
            . . . . . .
            PPTM2[j] = PPT[j] — SW × LAM × FPRT[j] end
            TKL:=3; go to A;
D: if FM3 > FM2 then
      Begin FM3:=FM2;
      for i:=1 ster 1 until n do
            GTM3[i]:=GTM2[i];
      for j:=1 step 1 until m do
      Begin PP1M3[j]:=PP1M2[j];
            . . . . . .
            PPTM3[j]:=PPTM2[j] end
            if (FM3 = FO) V (FM3 ≤ FKON) V (abs (((FM3 — FO)/FM3)
            <DELT)) then go to D1;
Begin Printout FM3; on key transmit directions to printout array GTM3 [1:n],
      PP1M3, ... PPTM3[1:m]} end
      for j:=1 step 1 until m do
      Begin PP1[j]:=PP1M3[j];
            . . . . . .
            PPT[j]:=PPTM3[j] end
            S1:=0.5 × SW; S2:=1.5 × SW; go to N;
D1: Printout (FM3; array GTM3 [1:n],
      PP1M3 [1:m]
      . . . . . .
      PPTM3 [1:m];} Stop!
 A: Begin real array DGT [1:m], description Vi;
      for 1:=1 step 1 until n do
      Begin GTM2 [i]:=0.0
      for j:=1 step 1 until m do
      Begin DGT[j]:=Vi (PP1M2, ... PPTM2, PI, ..., PK, XT, YT);
            GTM2[i]: = GTM2 [i] + DGT[j] end end
 B:   Begin real F, RAZN, RAZN2;
            F: = 0.0;
      for 1:=1 step 1 until n do
      Begin RAZN:=GNABL[i] — GTM2 [i];
            RAZN2:=RAZN × RAZN;
            F:=F + RAZN2 end
            FM2:=F; go to KLM2 [SKL];
            A0: F0:=F; go to L1;
            A1: F1:=F; go to L1;
            A2: F2:=F; go to L1;
            A3: FF:=F;
            L1: SKL:= SKL + 1;
            if P35 = 0 then go to K end
```

/34

```
C:  Begin real array description f1, ..., fT; FPR1 ... FPRT;
    for j:=1 step 1 until m do
    Begin FPR1[j]:=... FPRT[j]:=0.0;
    for i:=1 step 1 until n do
    Begin f1[i]:=f1
                .
                .
          fT[i]:=fT
          FPR1[j]:=FPR1[j] + f1[i]
                .
                .
          FPRT[j]:=FPRT[j] + fT[i] end end end
K:go to KL37[TKL] end end
```

CHAPTER II

ESTIMATING THE SIZE OF PERTURBING BODIES' EXCESS MASSES AND CENTERS OF GRAVITY

1. Solution of the Inverse Problem of an Anomaly in Gravitational Force for a Group of Spherical Perturbing Bodies

Let an anomaly in the force of gravity be given. Let us assume that the perturbing masses are isolated bodies. Some of them can be located relatively close to one another, thus creating a general, complicated picture of a gravity field upon the surface. In order to estimate approximately the location and dimensions of the perturbing masses, we will identify their form as spheres. The position of each sphere can be characterized by these parameters: x_o, y_o are the coordinates of the epicenter, h is the depth to the center, and M is their excess mass.

In an observed field it is almost always possible to establish a number of perturbing objects. We will designate by M the number of spheres by which the perturbing bodies are identified. Now the observed gravitational field on plane x0y can be approximated using the following formula:

$$\Delta g(x, y) = k \sum_{j=1}^{m} \frac{M_j h_j}{[(x - x_{oj})^2 + (y - y_{oj})^2 + h^2]^{3/2}}. \tag{2.1}$$

Is is most convenient to express linear values in kilometers. We will consider the excess mass in units of 10^9m. For instance, if the excess mass is $12 \cdot 10^{10}$m, then the formula should be written as M = 120 units. When selecting units of measurement in this way, the coefficient k in formula (2.1) must be accepted as equal to 6.67, and the gravitational force anomaly will then be expressed in milligals.

Each sphere is designated by four parameters. Four M parameters go to make up expression (2.1).

In the observed field we will fix N points with coordinates (x_i, y_i). We will include in the number of these points the most descriptive points of the gravitational anomaly. We will establish the function

$$F = \sum_{i=1}^{n} [\Delta g_{\text{obse}}(x_i, y_i) - \Delta g_{\text{theo}}(x_i, y_i)]^2. \tag{2.2}$$

The function Δg_{theo} (s, y) is determined by formula (2.1). Relationship (2.2) contains four M parameters $(x_{oj}, y_{oj}, h_j, M_j)$, j = 1, 2, ..., m.

Of the total sum of the proximate values of these parameters, we will choose those which can convert function (2.2) into a minimum. We will minimize function (2.2) by using the fast descent method. All computations are reduced to a sequential determination of parameters according to the formulas /36

$$\begin{aligned} x_{0j}^{(k+1)} &= x_{0j}^{(k)} - \lambda_k (F_{x_{0j}})_k, \\ y_{0j}^{(k+1)} &= y_{0j}^{(k)} - \lambda_k (F_{y_{0j}})_k, \\ h_j^{(k+1)} &= h_j^{(k)} - \lambda_k (F_{h_j})_k, \\ M_j^{(k+1)} &= M_j^{(k)} - \lambda_k (F_{M_j})_k, \end{aligned} \tag{2.3}$$

where k is the iteration number.

The computation model was described in sufficient detail in the previous chapter. Now we may cite only values for derivatives of functions (2.2) according to the desired parameters:

$$\begin{aligned} F_{x_{0j}} &= -6kM_j h_j \sum_{i=1}^{n} \frac{\delta_i (x_i - x_{0j})}{[(x_i - x_{0j})^2 + (y_i - y_{0j})^2 + h_j^2]^{5/2}}, \\ F_{y_{0j}} &= -6kM_j h_j \sum_{i=1}^{n} \frac{\delta_i (y_i - y_{0j})}{[(x_i - x_{0j})^2 + (y_i - y_{0j})^2 + h_j^2]^{5/2}}, \\ F_{h_j} &= -2kM_j \sum_{i=1}^{n} \frac{\delta_i [(x_i - x_{0j})^2 + (y_i - y_{0j})^2 - 2h_j^2]}{[(x_i - x_{0j})^2 + (y_i - y_{0j})^2 + h_j^2]^{5/2}}, \\ F_{M_j} &= -2kh_j \sum_{i=1}^{n} \frac{\delta_i}{[(x_i - x_{0j})^2 + (y_i - y_{0j})^2 + h_j^2]^{5/2}}, \end{aligned} \tag{2.4}$$

where $\delta_i = \Delta g_{obse}(x_i, y_i) - \Delta g_{theo}(x_i, y_i)$.

It should be noted that the inverse problem for a group of spherical bodies leads us to convex programming. This follows from the theorem of V. P. Zidarov [116]. Let the distribution of the anomalous field of gravitational for ce be known on plane x0y (V = 0), and let it be established that the anomalous geological objects can be approximated by N spherical bodies, each of which has excess mass M_k.

Let us assume that the centers of these masses are concentrated at points Q_k (ξ_k, η_k, ζ_k). We examine the integral

$$U = \int\int_S \left[\Delta g(P) - \sum_{k=1}^{N} \frac{m_k \zeta_k}{R_k^3} \right]^2 ds.$$

where $\sum_{k=1}^{N} \frac{m_k \zeta_k}{R_k^3}$ is the value of the gravitational force from the spherical /37 perturbing bodies at point P (x, y, 0) of plane S, and $R_k = \sqrt{(x - \xi_k)^2 + (y - \eta_k)^2 + \zeta_k^2}$ is the distance between points P and Q_k.

It is proven that there exists only one position of points K_q at which U has its minimum.

2. An Example of Solving the Inverse Problem

Figure 6 shows a gravitational force anomaly. Here four perturbing bodies are quite clearly distinguished. The position and size of the excess mass can be characterized by 16 parameters. Let us establish the beginning of the coordinates at some certain point in the field. We will superimpose coordinate axes 0x and 0y on the plane where the anomaly has been determined.

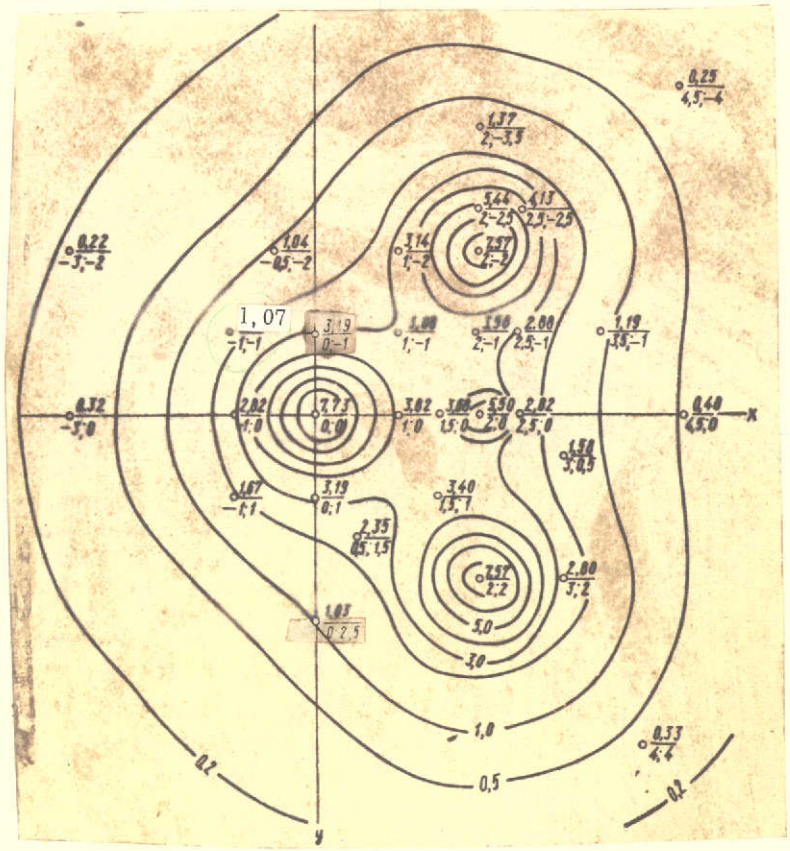

Figure 6. A Gravitational Force Field Caused by Several Isometric Masses.

We will confirm N points which would best describe the observed field. We include in the number of these points the field's extreme points, and some points in the area where the field changes monotonically. These points are noted by circles. Numbers have been placed next to them, indicating the observed value of the anomaly and the coordinates of the point. We will record the coordinates of these points and their corresponding gravitational force anomalies (Table 5). In all 31 points (n = 31) have been fixed. /38

TABLE 5.

Number of point	Coordinates x	Coordinates y	Δg_{obse}	Number of points	Coordinates x	Coordinates y	Δg_{obse}	Number of point	Coordinates x	Coordinates y	Δg_{obse}
1	0	0	7,73	12	—1,0	—1,0	1,67	22	2,5	—1,0	2,88
2	1,5	0	3,68	13	—0,5	—2,0	1,04	23	2,0	0	5,50
3	2,5	0	2,82	14	—1,0	1,0	1,67	24	—1,0	0	2,82
4	4,5	0	0,48	15	0	2,5	1,03	25	2,5	—2,5	4,13
5	0	—1,0	3,19	16	0,5	1,5	2,35	26	2,0	—2,5	5,41
6	1,0	—1,0	3,08	17	1,5	1,0	3,40	27	3,0	2,0	2,80
7	3,5	—1,0	1,19	18	2,0	2,0	7,57	28	2,0	3,0	2,73
8	1,0	—2,0	3,14	19	3,0	0,5	1,58	29	0	1,0	3,19
9	2,0	—2,0	7,57	20	4,0	4,0	0,33	30	1	0	3,82
10	2,0	—3,5	1,37	21	2,0	—1,0	3,56	31	4,5	—4,0	0,25
11	—3,0	0	0,32								

Commas indicate decimal points.

In the observed field we will determine the initial values of the perturbing bodies' parameters. We will establish the coordinates of the perturbing bodies' epicenters on the basis of the field's strongest points. Then we will examine the anomaly from each point individually. We will construct a graph of the field, according to its most descriptive profile. We will determine the depth to the center of the masses according to the well-known relationship $h = 1.334\ x_{1/2}$, where $x_{1/2}$ is the distance from the point of the field's maximum to the point where $\Delta g = 1/2\ \Delta g_{max}$. It is possible to determine the size of the excess mass according to the relationship $M = 150\ h^2\ \Delta g_{max}$. Here the anomaly is expressed in milligals, the depth is expressed in kilometers, and the excess mass is expressed in millions of tons. In our example the initial approximations were deliberately made worse than those obtained through computation. We will reduce the geological premises into a single table (Table 6). We will not compute the value of the function F at which the computation should be ended. We will make use of formula (1.13). We will assume the observation error to be equal to 0.25 milligals. In this case

$$F_{fin} = 2 \cdot 31 \cdot 0.0625 = 3.88\ mgl^2.$$

TABLE 6.

No. of the perturbing body	X_o	Y_o	h	M in units of 10^9 m
1	0	0	0,9	0,9
2	2,0	2,0	0,9	0,85
3	2,0	—2,0	0,9	0,85
4	1,5	0	0,25	0,3

Commas indicate decimal points.

In Table 7 we have shown the change of the minimized function from iteration to iteration. The computations continued until the seventh approximation where $F_7 = 2.99\ mgl^2$. This corresponds to an average deviation of the calculated field from the observed field of 0.23 mgl. /39

TABLE 7.

Number of Approximation	0	1	2	3	4	5	6	7
F	925,1	147,2	15,6	12,7	9,33	6,84	4,55	2,99

Commas indicate decimal points.

In Table 8 the results of the calculations are shown. Since a theoretical example was examined, it is possible to compare the observed parameters with those which were assigned when computing the anomaly. The latter are given in Table 9. /40

TABLE 8.

Parameter	Number of the Perturbing Body			
	1	2	3	4
x	—0,02	2,01	1,99	1,99
y	0,00	2,0	—2,01	0,00
h	0,99	0,98	0,98	0,58
M	$1,05 \cdot 10^9$	$1,02 \cdot 10^9$	$1,04 \cdot 10^9$	$0,179 \cdot 10^9$

Commas indicate decimal points.

TABLE 9.

Parameter	Number of the Perturbing Body			
	1	2	3	4
x	0	2,0	2,0	2,0
y	0	2,0	—2,0	0
h	1,0	1,0	1,0	0,5
M	$1,07 \cdot 10^9$	$1,07 \cdot 10^9$	$1,07 \cdot 10^9$	$0,135 \cdot 10^9$

Commas indicate decimal points.

In Table 10, the gravitational force field selected at the 31st point is compared with the observed values. Here are also given the values of an anomalous field from bodies of the first approximation.

TABLE 10.

No. of the Point	Coordinates		Value of Δg			No. of the point	Coordinates		Value of Δg		
	x	y	In the Initial Approx.	After the 7th Approx.	Observed		x	y	In the Initial Approx.	After the 7th Approx.	Observed
1	0	0	7,94	7,74	7,73	17	1,5	1,0	3,00	3,32	3,40
2	1,5	0	3,39	3,86	3,68	18	2,0	2,0	7,33	7,59	7,57
3	2,5	0	1,64	2,98	2,82	19	3,0	0,5	1,14	1,60	1,58
4	4,5	0	0,30	0,47	0,48	20	4,0	4,0	0,25	0,32	0,33
5	0	—1,0	2,76	3,13	3,19	21	2,0	—1,0	2,98	3,55	3,56
6	1,0	—1,0	2,70	3,03	3,08	22	2,5	—1,0	2,29	2,85	2,88
7	3,5	—1,0	0,89	1,15	1,19	23	2,0	0	4,34	5,41	5,50
8	1,0	—2,0	2,66	3,12	3,14	24	—1,0	0	2,45	2,85	2,82
9	2,0	—2,0	7,33	7,58	7,57	25	2,5	—2,5	3,59	4,08	4,13
10	2,0	—3,5	1,07	1,35	1,37	26	2,0	—2,5	4,90	5,44	5,41
11	—3,0	0	0,24	0,31	0,32	27	3,0	2,0	2,30	2,74	2,80
12	—1,0	—1,0	1,37	1,66	1,67	28	2,0	3,0	2,26	2,71	2,73
13	—0,5	—2,0	0,81	1,02	1,04	29	0	1,0	2,76	3,15	3,19
14	—1,0	1,0	1,38	1,67	1,67	30	1,0	0	5,81	3,79	3,82
15	0	2,5	0,80	0,99	1,03	31	4,5	—4,0	0,18	0,24	0,25
16	0,5	1,5	1,91	2,27	2,35						

Commas indicate decimal points.

3. A Practical Example in Evaluating the Depth of Location and Mass of a Group of Perturbing Bodies

In one of the areas, gravitational and magnetic survey sketches were made. After excluding the regional component, a sufficiently clear gravitational maximum (Figure 7 a) was distinguished.

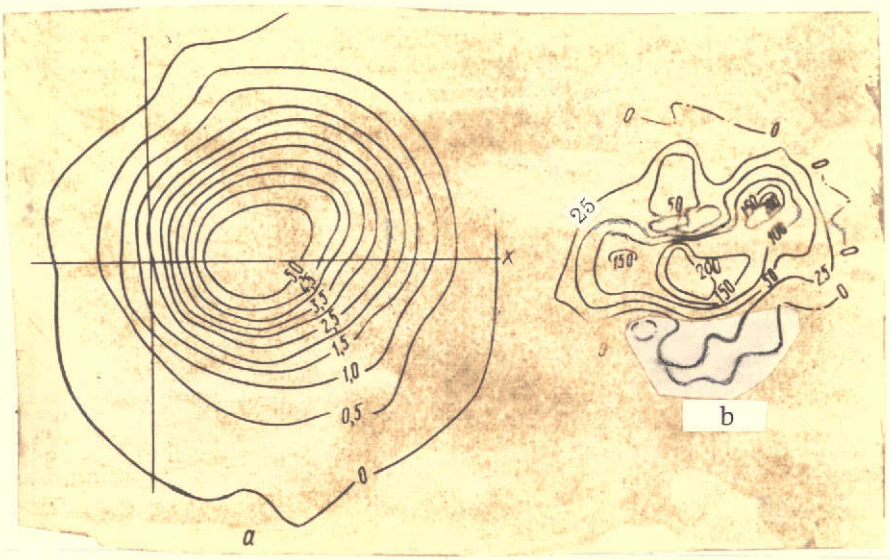

Figure 7. The Gravitational Force Field and Magnetic Field in One Area of the Investigation.

In this same area three local objects (Figure 7 b) were distinguished in the magnetic field. One can make various conjectures about which perturbing objects caused these anomalies. It is possible that the bodies which cause magnetic and gravitational anomalies cannot be compared to one another. In a given region rocks can exist which create both magnetic and gravitational anomalies. There can be any number of intermediate variations in which dense rocks are distinguished from magnetic rocks, or there can be rocks which are characterized by excess density and by higher values of magnetic properties.

The researcher who is thoroughly familiar with the geological structure /41
of the region in which he is operating and with the physical properties of the rocks can choose one hypothesis or another.

The following problem was posed to us. On the basis of the geological premises in a given region, it is possible to propose the existence of four perturbing objects with excess masses. It is necessary to find four centers of mass and to determine the excess mass of each body.

In order to solve this question we approximate the perturbing masses in the very first approximation by using four spheres. We will fix 22 points

(n = 22), choosing them in such a way that they describe the field being interpreted as completely as possible. Table 11 shows a listing of these points where the coordinates and values are given for the gravitational force anomaly. We calculate F_{fin} according to formula (1.13). We set $\delta\Delta g = 0.2$ mgl, and then $F_{fin} = 1.76\ \text{mgl}^2$.

TABLE 11.

No. of the point	Coordinates x	Coordinates y	Value of Δg: In the Initial Approx.	Value of Δg: After solution	Value of Δg: Observed	No. of the Point	Coordinates x	Coordinates y	Value of Δg: In the Initial Approx.	Value of Δg: After solution	Value of Δg: Observed
1	0,3	0	16,4	4,4	4,2	11	1,75	0,75	3,0	1,9	2,2
2	0,75	0,55	13,0	4,6	4,2	12	1,75	0	2,7	2,3	2,3
3	0,85	—0,15	22,0	5,6	5,2	13	1,25	—0,50	2,4	2,7	3,0
4	1,50	0,40	14,0	4,3	4,0	14	0,50	—0,50	3,8	2,7	3,0
5	0,55	—0,10	12,0	5,2	5,3	15	0	0	6,0	2,1	2,0
6	1,25	0,125	6,5	4,8	5,0	16	0,75	0,15	10,4	5,4	5,5
7	1,125	0,55	7,1	4,4	4,5	17	—0,35	0,50	1,0	0,7	0,5
8	0,55	0,35	9,3	4,4	4,7	18	0,60	1,25	1,4	1,0	1,0
9	0,25	0,75	2,8	1,7	1,7	19	2,35	0,25	0,7	0,7	0,5
10	1,25	1,00	2,3	1,9	2,3	20	2,00	—0,35	0,8	1,0	1,0
						21	0,75	—1,25	0,5	0,6	0,5
						22	—0,25	—0,75	0,7	0,6	0,4

Commas indicate decimal points.

Table 12 shows the parameters of the four spheres by which we approximated the perturbing bodies in the first approximation. The results of solving the problem are shown in the same table: in Table 12 are the parameters of the selected bodies, and in Table 11 the observed and selected values of the anomaly have been compared. As is evident, the selection was made with sufficient precision. The maximum deviation is observed at 3 points and is 0.4 MGL. /42

TABLE 12.

Parameter	No. of Perturbing Body 1	2	3	4
Initial Approximation				
x	0,3	0,75	0,85	1,5
y	0	0,55	—0,15	0,4
h	0,3	0,35	0,25	0,3
In Units of $M \cdot 10^9$ m	0,19	0,20	0,18	0,17
Solution				
x	0,38	0,79	0,93	1,44
y	—0,02	0,62	—0,20	0,37
h	0,44	0,55	0,57	0,56
In Units of $M \cdot 10^9$ m	0,078	0,124	0,18	0,139

Commas indicate decimal points.

4. Solving the Inverse Problem for Anomaly V_{xz} for a Group of Cylindrical Perturbing Bodies

The solution to this problem has essentially been given in the first chapter. Here we will simply explain what concerns the immediate problem and we will make some remarks on methodology in selection of the initial approximation.

The function which must be minimized is written by relationship (1.23). Formulas (1.24) are used to write the recurrent relationship to determine the desired parameters $\{t_j, h_j, d_j\}$, $j = 1, 2, \ldots, m$, where m is the number of cylindrical bodies.

Now let us examine the question of selecting component values for the first approximation: $\{t_j^{(o)}, h_j^{(o)}, d_j^{(o)}, \text{sign } \sigma_j\}$ (all information about the geological structure must be taken into account here, or hypotheses about the distribution of the perturbing masses must be introduced). The parametric values of the cylindrical masses for the first approximation can be computed.

At the very start it is convenient to determine components $d_j^{(o)}$. $d_m^{(o)}$ can be accepted as equal to the values of the abscissas of the point where $V_{xz} = 0$, or the points relative to which the function is symmetrical in a narrow region. Each local anomaly can be examined individually. By fixing the beginning of the coordinates at points $x_i = d_j^{(o)}$ each time, we computed the initial approximations of depth according to the relationship $h_i = x_e\sqrt{3}$ (x_e is the abscissa of the extreme point). The initial values of the parameters can be computed according to the known relationships for the mass of a cylinder

/43

$$\lambda_j^{(0)} = \frac{4\sqrt{3}\,|h_j^{(0)}|^2}{9k}(V_{xz})_{\max},$$

or

$$\lambda_j^{(0)} = 0.01\,|h_j^2(V_{xz})_{\max}.$$

If the magnitudes h are expressed in meters, and if V_{xz} is expressed in Eoetvoes then λ_j will have the dimensionality m/m. Now it is easy to calculate the parameter $t_j^{(o)} = \sqrt{\lambda_{i/\rho}}$.

In conclusion, let us examine a practical example. In one of the ultrabasic massifs, an anomaly was obtained for the horizontal gradient of the force of gravity (Figure 8). By their nature the perturbing masses can be identified with two-dimensional bodies. A detailed examination makes it

possible to distinguish five perturbing masses. One body has a very deep location, and its anomaly has determined the general nature of the field. The four other bodies are small masses, and their location is not deep. They cause anomalies in the background of the basic field. We will identify each perturbing body as a cylinder. Since the position and dimensions of the cylinder are characterized by three parameters, 15 magnitudes form the basis of the determination. By taking into account the nature of the fields, we will fix 17 points equidistant from one another. Table 13 shows the numerical values of the abscissas of the points and the anomalies which correspond to them.

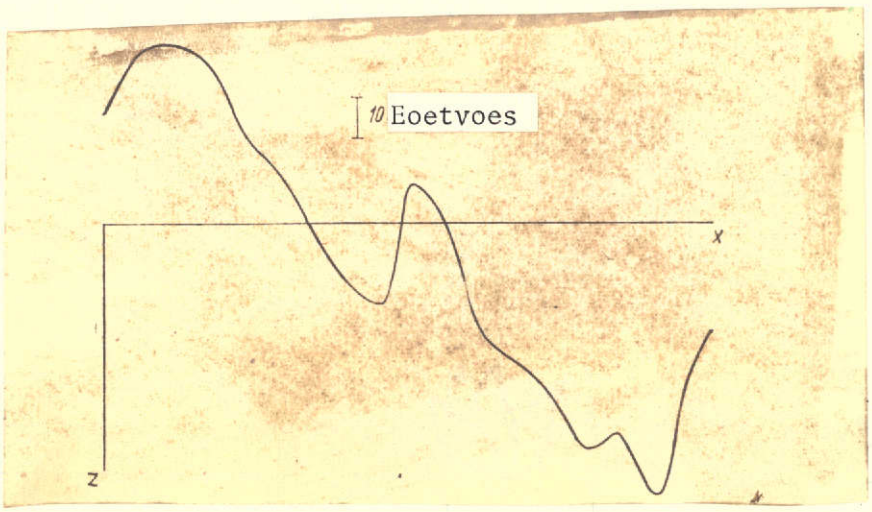

Figure 8. Anomaly V_{xz} in One Area of the Investigation.

TABLE 13.

No. of the point	x, m	U_{xz} Selected	U_{xz} obse	No. of the point	x, m	U_{xz} Selected	U_{xz} obse
1	0	36	26	10	360	5	9
2	40	41	40	11	400	6	0
3	80	44	42	12	440	—25	—26
4	120	43	39	13	480	—29	—33
5	160	33	22	14	520	—35	—40
6	200	15	13	15	560	—51	—54
7	240	—2	0	16	600	—43	—51
8	280	—9	—13	17	640	—65	—65
9	320	—6	—19				

On the basis of the observed field, we calculate the initial approximations of the unknown parameters. These are shown in Table 14. We will determine F_{fin} according to formula (1.13). We will accept δV_{xz} = 5 Eoetvoes, and then F_{fin} = 850 Eoetvoes^2. Tables 13 and 14 show the results of the solution. The initial value of the minimized function F is 4399 Eoetvoes^2, and the final value of F_{fin} is 622 Eoetvoes^2. This corresponds to an average deviation of the observed and selected fields of within 4.2 Eoetvoes. As is /44

evident, the selection has been made with sufficient precision. In Table 13 the observed and selected anomalies have been compared. The maximum deviation between them is 13 Eoetvoes.

TABLE 14.

Parameter	No. of the Perturbing Body				
	1	2	3	4	5
Initial Approximation					
t	150	40	25	25	10
h	500	140	80	85	35
d	360	240	400	530	620
Solution					
t	141	47	23	23	3.9
h	505	162	75	85	12.2
d	317	196	425	526	633
λ. m/μ	$62{,}8 \cdot 10^3$	$6{,}9 \cdot 10^3$	$1.7 \cdot 10^3$	$1{,}7 \cdot 10^3$	$0{,}05 \cdot 10^3$

Commas indicate decimal points.

CHAPTER III

DETERMINING THE CONTOURS OF TWO-DIMENSIONAL GEOLOGICAL BODIES ON THE BASIS OF GRAVITATIONAL ANOMALIES

In this chapter an examination is made of the questions of solving inverse problems of gravitational force and horizontal gradient anomalies. The unknown controu of the perturbing body is approximated by segmented straight lines with right angles. /45

The methods of solving the problem are illustrated by theoretical and practical examples.

1. Solving the Inverse Problem For Two-Dimensional Perturbing Bodies Bounded by Segmented Straight-Line Contours

On the basis of the observed gravitational anomaly, it is necessary to determine the contours within which the excess masses are located. We approximate the unknown controu by using a segmented straight line. In this case it is possible to consider the gravitational anomaly as the sum of the effects from oblique or straight steps. We will accept that within each step the excess density is a constant and known value. By changing the individual density from step to step, it is possible to describe the configuration of a geological body with a variable density.

In order to simplify the solution somewhat, we will give the segmented straight-line contours right angles. If there are m steps, then the anomaly can be approximated in the following manner:

For the gravitational force anomaly

$$\Delta g(x) = k\sum_{j=1}^{m}\sigma_j\left|\pi(H_j-h_j)+2H_j\operatorname{arctg}\frac{x-d_j}{H_j}-\right.$$
$$\left.-2h_j\operatorname{arctg}\frac{x-d_j}{h_j}+(x-d_j)\ln\frac{H_j^2+(x-d_j)^2}{h_j^2+(x-d_j)^2}\right|, \tag{3.1}$$

and for the horizontal gradient anomaly of the force of gravity

$$V_{xz} = k\sum_{j=1}^{m}\sigma_j\ln\frac{H_j^2+(x-d_j)^2}{h_j^2+(x-d_j)^2}. \tag{3.1a}$$

Each projection is characterized by four parameters: h_j and H_j which are the depths to the upper and lower boundaries of the projections, d_j which is /46

the abscissa which determines the location of the vertical boundary relative to the beginning of the coordinates, and σ_j which is the excess density of the masses. The value of these parameters was shown in Figure 1. In this case a two-dimensional problem is being examined where $l_1 \to -\infty$ and $l_2 \to +\infty$.

We will fix in the observed field n points with abscissa x_i. We include those points which are most descriptive of the gravitational anomaly. We will construct a function like (1.2) which will now be expressed in the following manner:

For the gravitational force anomaly

$$F = \sum_{i=1}^{n} [\Delta g_{\text{obse}}(x_i) - \Delta g_{\text{theo}}(x_i)]^2, \tag{3.2}$$

For the anomaly of the horizontal gradient of the force of gravity

$$F = \sum_{i=1}^{n} [V_{xz\,\text{obse}}(x_i) - V_{xz\,\text{theo}}(x_i)]^2. \tag{3.2a}$$

The values of Δg_{theo} (x) and $V_{xz\ \text{theo}}$ (x) are determined according to formula (3.1) and (3.1a).

Thus the function F will contain four m parameters: σ_j, h_j, H_j, and d_j (j = 1, 2, ..., m). We will assign the values of parameters h_j, H_j and σ_j. d_j remains the variable parameter. Of all the possible values for these parameters, we will choose those which may change function (3.2) into a minimum.

We will carry out the calculations according to the formulas

$$d_j^{(k+1)} = d_j^{(k)} - \lambda_k (F' d_j)_k,$$

where k is the number of the approximation (iteration). In these expressions F'_{dj} acquires the values:

For the gravitational force anomaly

$$F'_{d_j} = 2k\sigma_j \sum_{i=1}^{n} \delta_i \ln \frac{H_j^2 + (x_i - d_j)^2}{h_j^2 + (x_i + d_j)^2}, \qquad \delta_i = \Delta g_{\text{obse}}(x_i) - \Delta g_{\text{theo}}(x_i), \tag{3.3}$$

And for the anomaly of the horizontal gradient of gravitational force

$$F'_{d_j} = -4k\sigma_j \sum_{i=1}^{n} \delta_i \frac{(x_i - d_j)(H_j^2 - h_j^2)}{[H_j^2 + (x_i - d_j)^2][h_j^2 + (x_i - d_j)^2]}, \qquad \delta_i = V_{xz\,\text{obse}}(x_i) - V_{xz\,\text{theo}}(x_i). \tag{3.3a}$$

In these formulas k is the gravitational constant. It is most convenient to express linear units in kilometers. In order to express the gravitational force anomaly in milligals, it is necessary to accept the coefficient k as equal to 6.67 in formulas (3.1) and (3.3). When calculating the anomaly of the horizontal gradient of gravitational force, it is necessary in the formulas (3.1a) and (3.3a) to accept k = 66.7, whatever the dimensionality of the linear values. In this case the anomaly is expressed in eoetvoes. /47

2. Method of Selecting the Contours of a Perturbing Body

We will assume that a gravitational anomaly is given and that it is established that the perturbing body is two-dimensional. Let us examine how the interpretation is done by the selection method, using the measuring grids of Barton. All half-space $z > 0$ is divided up by straight lines $z = h_j$ into a number of elementary strips. In each of these strips, right-angle areas are distinguished by straight lines $x = d_t$ ($t = 1, 2, \ldots$). It is assumed that the perturbing masses are concentrated within these areas.

The problem consists of finding a series of numbers $d_1, d_2, \ldots, d_n$ in all the strips such that the anomaly calculated from the selected body coincides sufficiently well with the observed anomaly.

Let us assume that we know some value $z = h_0$, beginning from which the areas with excess density can be found in half-space $z > 0$. We will fix a certain sequence $\{h_j\}$ with a finite number of digits.

The magnitudes h_j can be determined according to the following relationship:

$$h_j = h_{j-1} + \delta (h_{j-1} - h_{j-2}), \tag{3.4}$$

as has been accepted in the Barton measuring grid. In this case it is necessary to assign (in addition to h_0) the values h_1 and δ. The relationship (3.4) determines the thickness of the strip of some geometric progression with the denominator δ. In general it is not necessary to compute the sequence $\{h_j\}$, but rather it can be assigned either completely arbitrarily or by using the geological model.

Thus the finite sequence $\{h_j\}$ is given which forms m strips. In each j strip, the group of numbers $\{d_{1j}, d_{2j}, \ldots, d_{fj}\}_j$ are determined. The number of digits of each group can vary. These numbers describe the location of right-angle regions with excess masses. At an arbitrary point on axis Ox these masses create an anomaly which is determined by the equality (3.1) or 3.1a). Now it remains to fix n points and to establish function (3.2) or (3.2a).

The magnitude F is a function of the parameters: $F = F(d_1, d_2, \ldots, d_p)$.

We will illustrate the solution of the problem by the following example. Let a gravitational force (anomaly (Figure 9) be given. We will further assume that the possibility of classifying the perturbing bodies as two-dimensional has been established. We will choose the system of coordinates in the following way. We will direct the axis Ox along the observation profile. We will fix the beginning of the coordinates at some point in the profile. We will direct the axis Oz vertically downward.

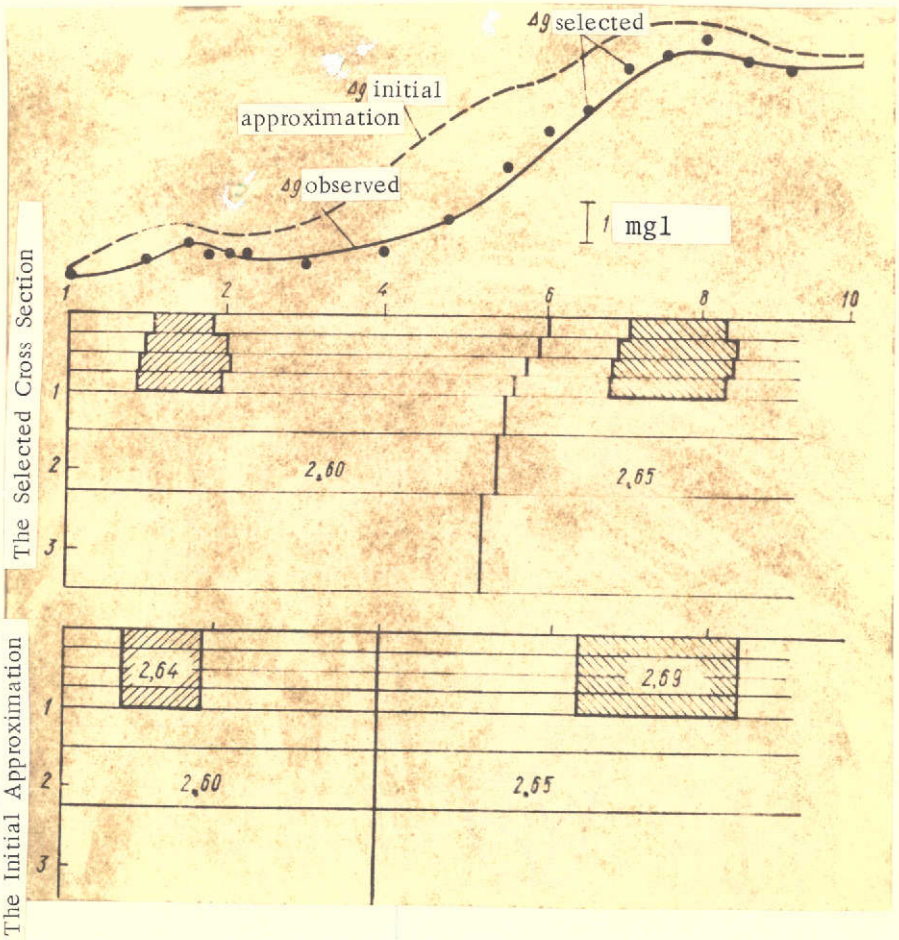

Figure 9. Example of the Selection of a Geological Cross-Section (Two-Dimensional Case) For a Gravitational Force Anomaly.

On the basis of general information about the geological structure of the region and taking into account the anomalous field, a geological cross-section, i.e., the first approximation, has been constructed. The surface layer is a homogeneous rock mass throughout its thickness. The thickness of the rock begins to vary at a depth of 10 meters. We will make a column graph like a Barton measuring grid, while taking into account the constructed geological model. The first line $z = h_0 = 0.01$ kilometers identifies the boundary between /48

the surface layer and the bedrock. Up to a depth of 1 kilometer, four more horizontal strips have been made, each of which is 250 meters thick. The thicknesses of the following 5th, 6th, and 7th strips have been accepted as equal to 500, 750, and 1250 meters, respectively. This makes it possible to describe in considerable detail the configurations of the geological bodies by using segmented straight-line contours with vertical boundaries. In this problem 23 projections have been distinguished. Their location is described by the selection of four-dimensional vectors $\{\sigma_j, h_j, H_j, d_j\}$. The values of these parameters are shown in Table 15.

TABLE 15.

Parameters of the perturbing body	No. of the body							
	1	2	3	4	5	6	7	8
σ	+0,04	+0,04	+0,04	+0,04	−0,04	−0,04	−0,04	−0,04
h	0,01	0,25	0,5	0,75	0,01	0,25	0,5	0,75
H	0,25	0,5	0,75	1,0	0,25	0,5	0,75	1,0
d	0,75	0,75	0,75	0,75	1,75	1,75	1,75	1,75

Parameters of the perturbing body	No. of the body							
	9	10	11	12	13	14	15	16
σ	+0,05	+0,05	+0,05	+0,05	+0,05	+0,05	+0,05	+0,04
h	0,01	0,25	0,5	0,75	1,0	1,5	2,25	0,01
H	0,25	0,5	0,75	1,0	1,5	2,25	3,5	0,25
d	4,0	4,0	4,0	4,0	4,0	4,0	4,0	6,5

Parameters of the perturbing body	No. of the body						
	17	18	19	20	21	22	23
σ	+0,04	+0,04	+0,04	−0,04	−0,04	−0,04	−0,04
h	0,25	0,5	0,75	0,01	0,25	0,5	0,75
H	0,5	0,75	1,0	0,25	0,5	0,75	1,0
d	6,5	6,5	6,5	8,5	8,5	8,5	8,5

Commas indicate decimal points.

Let us now turn to the anomalous field of gravitational force. On curve /49
Δg we will distinguish the points by which it would be possible to fully establish an anomaly, according to which the geological cross-section will be selected. A list of these points is shown in Table 16. Tables 15 and 16 present the initial data for solving the problem. We will also establish the value F of which it is possible to conclude the computation. We will make use of formula (1.13). We will assume that the selection error should be 0.25 MGL, and then $F_{fin} = 2.43\ MGL^2$.

Figure 9 shows the results of the solution in graphic form. As was said /50
earlier, the solution of the direct problem can serve as the criterion for the correctness of the model of the first approximation. The gravitational effect

from the geological model hypothesis is obtained as an intermediate step in the computation. This effect is constantly cited when solving any problem. These results can be of considerable help in analyzing the final solution.

TABLE 16.

Coordination of the anomaly	No. of the point							
	1	2	3	4	5	6	7	8
x	0	1,0	1,5	1,75	2,0	2,25	3,0	4,0
Δg_{obse}	0,81	1,30	1,69	1,64	1,45	1,30	1,43	1,89
Coordination of the anomaly	9	10	11	12	13	14	15	16	17	18
x	4,75	5,5	6,0	6,5	7,0	7,5	8,0	8,5	9,0	10,0
Δg_{obse}	2,46	3,37	4,43	5,37	6,05	6,78	6,92	6,66	6,47	6,56

Commas indicate decimal points.

Now let us turn to solving the problem concerning the anomaly V_{xz}. Figure 10 shows a graph of an anomalous field. In the observed field V_{xz} between the 1.5 kilometer and 3.0 kilometer peaks, a geological object is distinguished, /51
the rocks of which possess greater density than the enclosing medium. The nature of the anomalous curve in the area of the 2.0 - 2.5 kilometer peaks is evidence of the heterogeneity of this object. In addition, in the right part of the profile, contact between rocks of various densities is clearly distinguished. The location of the contact is approximately described by the maximum of the anomaly V_{xz}.

Taking into account data on the geological structure of the region and the physical properties of the rocks, and subjecting the observed anomaly to stringent analysis, we create a schematic hypothesis of the distribution of the geological object. Following this schematic, we assume that the upper covering over the entire area is homogeneous to a depth of 250 meters. The lower boundary of the rocks, the density of which is 3.4 g/cm^3, is located at a depth of 1.5 kilometers. Within this rock mass, rocks are distinguished with a density of 2.9 g/cm^3. Their lower limit reaches 850 meters.

Beginning from the peak at 4.75 kilometers, a second rock massif is distinguished with a density of 2.9 g/cm^3. On the basis of the nature of the field, it is possible to propose that it is relatively homogeneous. The lower boundary of the contact, on the basis of geological data, has been accepted as equal to 3.0 kilometers. The enclosing rocks over the entire expanse are homogeneous, and we accept their density as equal to 2.6 g/cm^3. However, between the two massifs described, the enclosing rocks have undergone changes, and their density should be accepted as equal to 2.5 g/cm^3. Having made all the constructions,

we divide the lower half-space ($z > 0$) into several strips as is done in the Barton measuring grid. The first line should be drawn at a depth of 0.25 kilometers. It will divide the upper covering from the heterogeneous rock mass located below. Further, four horizontal strips are distinguished by the line $z = 0.5$, $z = 0.85$, $z = 1.5$, and $z = 3.0$ kilometers. Now it is easy to code the geological schematic since we have already written up the location and dimensions of the 14 contacts (Table 17).

TABLE 17.

Parameters of the perturbing body	No of the perturbing body													
	1	2	3	4	5	6	7	8	9	10	11	12	13	14
a	0,8	0,8	0,8	—0,9	—0,9	—0,9	—0,5	—0,5	+0,5	+0,5	0,4	0,4	0,4	0,4
h	0,25	0,5	0,85	0,25	0,5	0,85	0,25	0,5	0,25	0,5	0,25	0,5	0,85	1,5
H	0,5	0,85	1,5	0,5	0,85	1,5	0,5	0,85	0,5	0,85	0,5	0,85	1,5	3,0
d	1,5	1,5	1,5	3.0	3,0	3,0	2,1	2,1	2,6	2,6	4,75	4,75	4,75	4,75

Commas indicate decimal points.

In curve V_{xz} we will fix the most descriptive points. As in the previous example, they are not selected uniformly. Wherever the anomaly is monotonic and has a uniform gradient, the points are selected more rarely. The points were selected more thickly at the most salient points of the curve. In all, 20 points were fixed. A list of those is shown in Table 18. In order to calculate F_{fin}, we will consider that the selection error should not exceed 5 eoetvoes. In this case F_{fin} = 1000 eoetvoes^2.

TABLE 18.

No of the points	1	2	3	4	5	6	7	8	9	10
x	0	0,75	1,0	1,25	1,5	1,75	2,0	2,25	2,5	2,75
V_{xz}	17	38	54	82	121	107	40	3	—5	—24

No. of the points	11	12	13	14	15	16	17	18	19	20
x	3,0	3,25	3,5	4,0	4,75	5,0	5.25	6,0	7,0	8,0
V_{xz}	—80	—86	—35	33	103	101	75	36	18	11

Commas indicate decimal points.

The results of solving the problem are shown in Figure 10. Here the anomaly V_{xz} is cited which has been stipulated by the geological model hypothesis (first approximation). /52

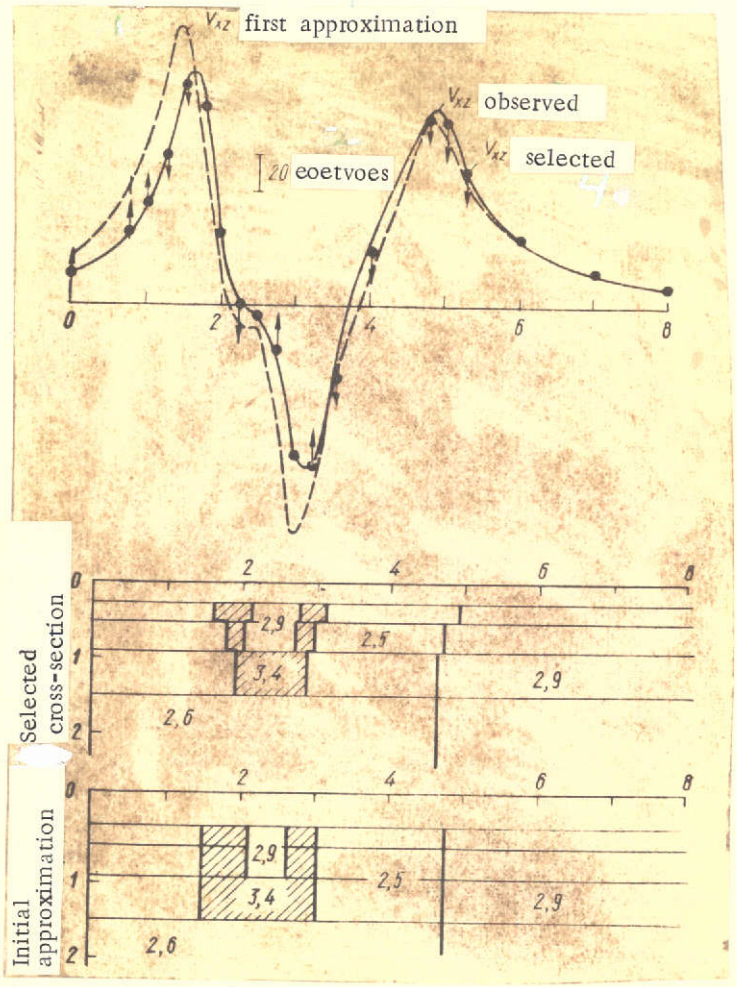

Figure 10. An Example of the Selection of a Geological Cross-Section (The Two-Dimensional Case) According to an Anomaly in the Horizontal Gradient of Gravitational Force.

We will illustrate the solution of the problem by one more selection of a fairly complex geological object. Figure 11a shows the density cross-section which has been constructed on the basis of available hypotheses about the geological structure of the region.

We will fix the start of the coordinates on the line of observation. We will direct the axis Ox along the line of observations, and we will direct the axis Oz vertically downward. The area where the perturbing masses are concentrated is divided into 11 horizontal strips by the straight-line $z = h_j$. In each strip the limits of the perturbing masses are indicated by the straight-

lines $x = d_j$. The density values of the rocks are written inside. The boundaries of the masses are enumerated (in the figure this numeration has been omitted). In the first and second strips, the boundaries are grouped together by nines (No. 1 - 9 and No. 10 - 18), in the third strip they are grouped together by 13 borders, etc. In all, 77 contact boundaries have been fixed. 66 points have been fixed for selection. One notes at once the rather large difference between the observed anomaly and the results of solving the direct problem from the initial model (especially in the area of 50 - 55 kilometers). This is evidence of the fact that rather significant errors were allowed during the construction of the initial variation of the geological model.

Figure 11b shows the selected cross-section. The theoretical and observed anomalies coincided quite well. Their lack of agreement in small areas can be explained by heterogeneities in the upper portion of the cross-section which were not taken into account. This example is a good illustration of the change in the geological model of the first approximation and its transformation into another model. Completely satisfactory agreement was attained between the observed and theoretically calculated anomalies by this process.

/53

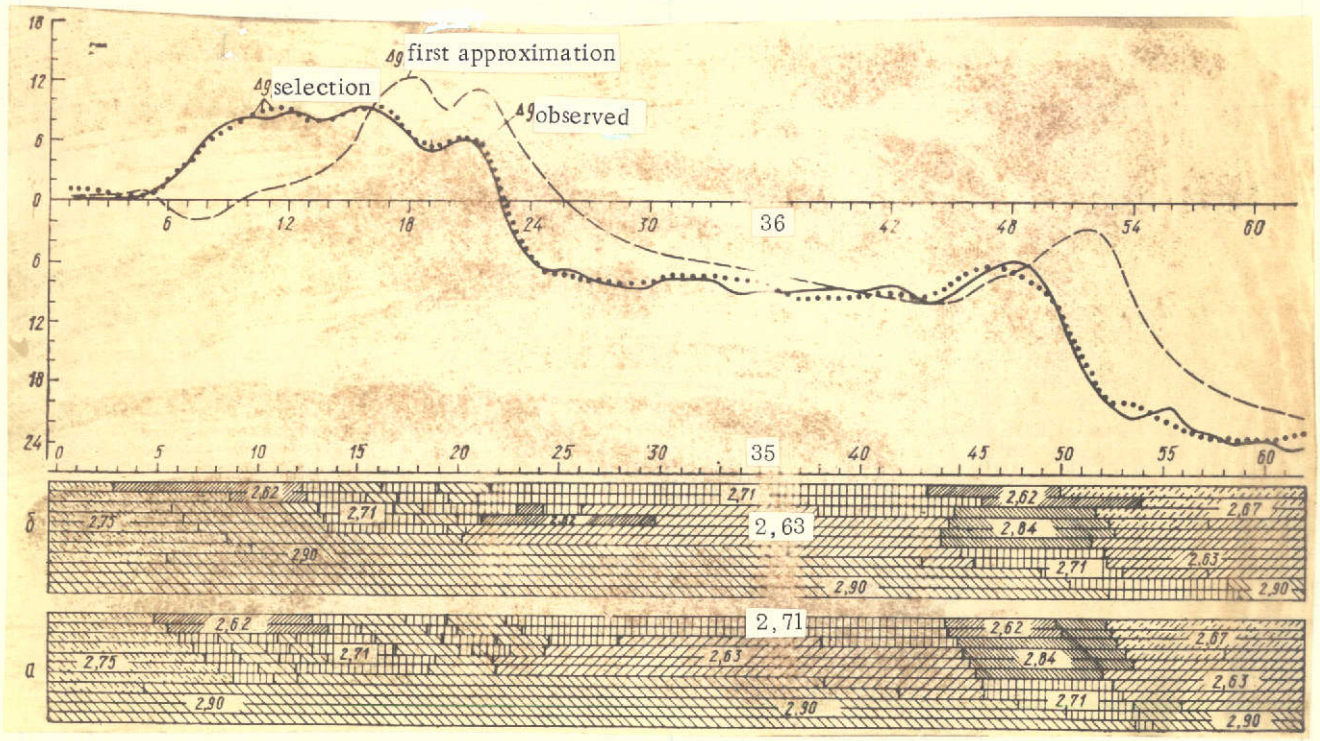

Figure 11. An Example of the Selection of a Geological Cross-Section According to the Gravitational Force Anomaly: a) Initial Approximation, b) Solution.

3. Determining the Contours of a Perturbing Body With Partially Known Parameters

/54

Additional requirements for searching for the contours of perturbing bodies often arise when solving practical problems.

Some parts of the cross-section are determined quite exactly on the basis of geological data or the data of other geophysical methods. These parts of the cross-section should not be changed during the process of selecting the contours. This means that among m steps by which the geological model is described, there are those in which the parameter g_j does not change during the computation process. We will divide all of the parameters of the geological model (steps) into two groups. We will include in the first of these groups the projections belong to this group. The second group will comprise the remaining projections, all the parameters of which are constant. Now formulas (3.1) and (3.1a), by which the observed anomalies are approximated, should be presented in this form:

$$\Delta g(x) = k\sum_{j=1}^{m_1} f(\sigma_j, h_j, H_j, d_j, x) + k\sum_{j=m_1+1}^{m} f(\sigma_j, h_j, H_j, d_j, x), \tag{3.6}$$

$$V_{xz}(x) = k\sum_{j=1}^{m_1} \varphi(\sigma_j, h_j, H_j, d_j, x) + k\sum_{j=m_1+1}^{m} \varphi(\sigma_j, h_j, H_j, d_j, x). \tag{3.6a}$$

Functions f and φ are determined by relationships (3.1) and (3.1a). In equality (3.6) and (3.6a), the second part is only the function of the coordinates.

We will now turn to (3.2). The function can be written as

$$F = \sum_{i=1}^{n}\left[\Delta g_{\text{obse}}(x_i) - k\sum_{j=1}^{m_1} f - k\sum_{j=m_1+1}^{m} f\right]^2 = \sum_{i=1}^{n}\left[\left\{\Delta g_{\text{obse}}(x_i) - k\sum_{j=m_1+1}^{m} f\right\} - k\sum_{j=1}^{m_1} f\right]^2,$$

or

/55

$$F = \sum_{i=1}^{n}[\Delta g^{*}_{\text{obse}}(x_i) - \Delta g_{\text{theo}}(x_i)]^2, \tag{3.7}$$

where now Δg_{theo} (x) is determined by equality (3.1) and is a function of only those projections in which the parameter d_j is a variable quantity. The function $\Delta g^{*}_{\text{obse}}$ (x) is determined by the relationship

$$\Delta g^{*}_{\text{obse}}(x) = \Delta g_{\text{obse}}(x) - k\sum_{j=m_1+1}^{m} f(\sigma_j, h_j, H_j, d_j, x) \tag{3.8}$$

and, is essentially a residual anomaly. The gravitational effect of the geological projections, the parameters of which are known and cannot change, are excluded from the observed anomaly. /56

Small additions to the previously described program make it possible to fully automate the calculation. The parameters of the geological model should be fed in by using two massifs. One includes the vectors among the components of which there are variable parameters, and the other includes the vectors in which the components are constant.

The second massif of initial data makes it possible to compute the second term of equality (3.8) and then function $\Delta g^*_{obse}(x)$. In the future this function will be used as $\Delta g_{obse}(x)$. Everything mentioned relates fully to function (3.2a) where the anomaly in the horizontal gradient is examined. We will illustrate this presentation with an example. Let there be in the geological model which was examined in section 2 (Figure 10) a well-known position for the line along which rocks with a density of 2.9 make contact with their enclosing medium. Thus, during the selection there is no basis for changing the position of the line. We will fix the parameters which describe this contact, and we will solve the problem by selecting the contours again. In this case, Table 17 should be replaced by Table 19. Here the projections, the position of which should be changed, are clearly indicated. The parameters which describe the location of the contact line are written up in a separate group. These quantities should not be changed during the selection process. /57

TABLE 19.

Parameter of perturbing body	No. of perturbing body													
	1	2	3	4	5	6	7	8	9	10	11	12	13	14
	Variable										Fixed			
σ	+0,8	+0,8	+0,8	−0,9	−0,9	−0,9	−0,5	−0,5	+0,5	+0,5	+0,4	+0,4	+0,4	+0,4
h	0,25	0,5	0,85	0,25	0,5	0,85	0,25	0,5	0,25	0,5	0,25	0,5	0,85	1,5
H	0,5	0,85	1,5	0,5	0,85	1,5	0,5	0,85	0,5	0,85	0,5	0,85	1,5	3,0
d	1,0	1,0	1,0	3,25	3,25	3,25	1,5	1,5	2,75	2,75	4,9	4,75	4,6	4,5

Commas indicate decimal points.

In order to solve the problem, 20 points have been chosen on the anomalous curve, as was done in the previous problem. This means that the data of Table 18 are included in the initial data, in addition to the data of Table 19. The results of the solution are shown in Figure 12. Figure 13 shows the solution of this same problem for the gravitational force anomaly. The position of the contact on the right in the geological cross-section has been confirmed. In the model of the first approximation, a group of rocks, the contours of which are to be found, has been given in a more tentative manner than in the previous problems.

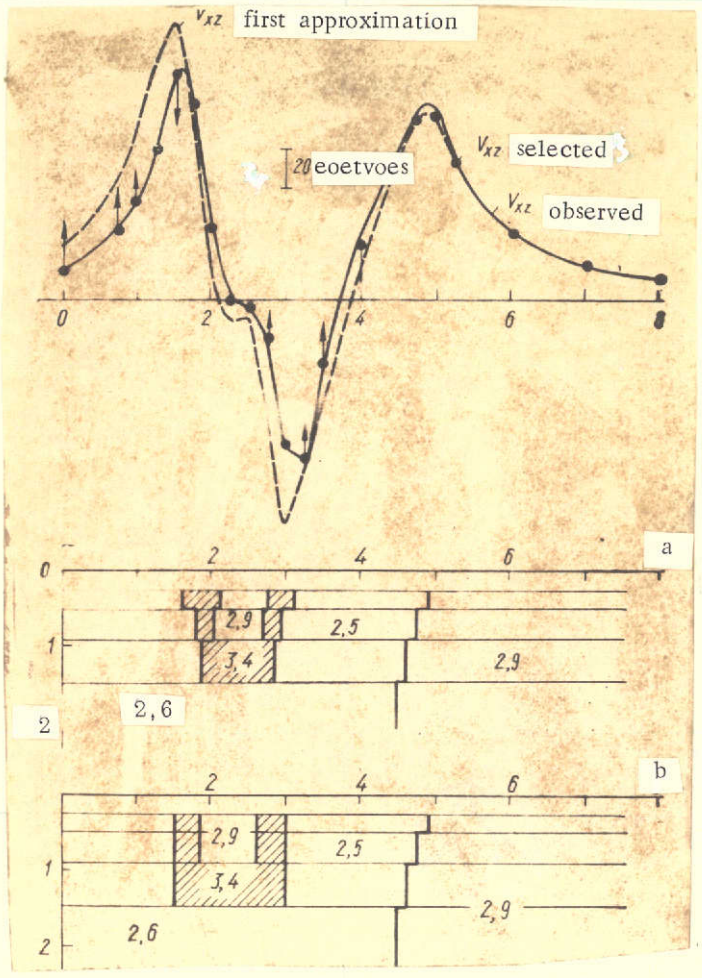

Figure 12. An Example of Selecting a Geological Cross-Section on the Basis of an Anomaly of the Horizontal Gradient of Gravitational Force.

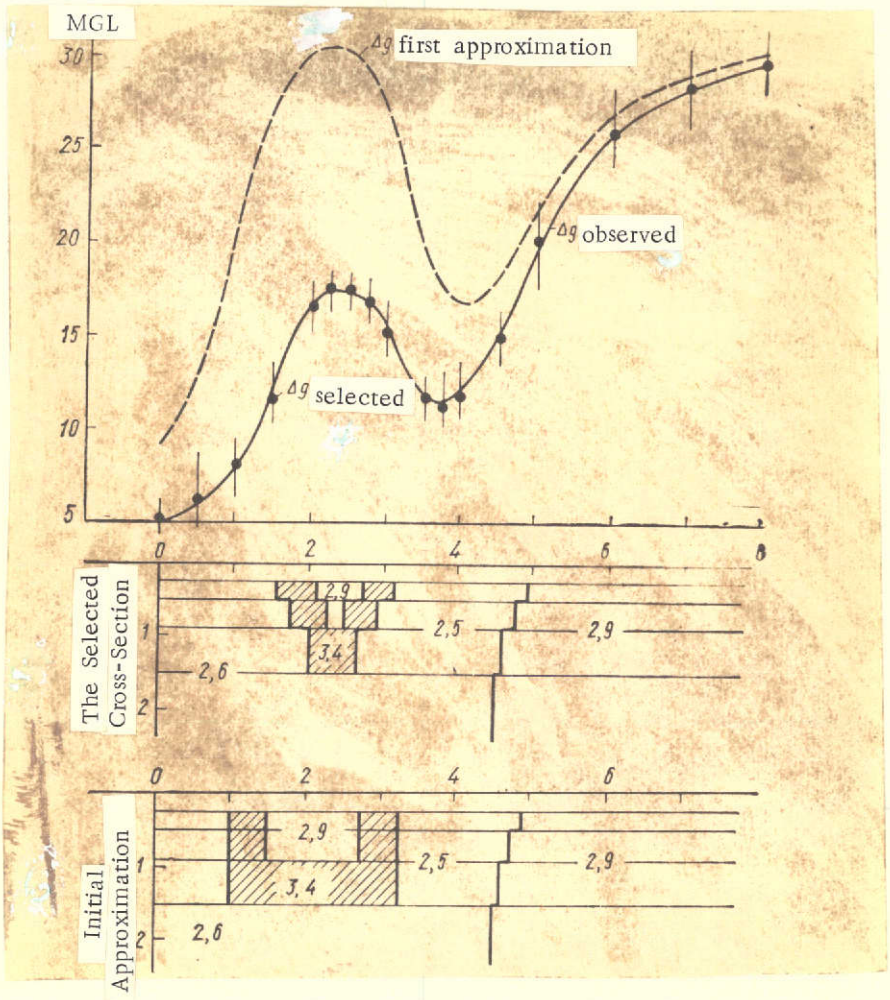

Figure 13. An Example of the Selection of a Geological Cross-Section For a Gravitational Force Anomaly.

CHAPTER IV

/58

DETERMINING THE CONTOURS OF THREE-DIMENSIONAL PERTURBING MASSES BY USING GRAVITATIONAL ANOMALIES

1. Formulas for the Computation

For an observed gravitational field, it is necessary to determine the spatial distribution of a perturbing object which is finite in space.

Everything which has been stated earlier about determining the contours of a two-dimensional body can be generalized to the three-dimensional case. We will look for the form of the perturbing bodies as a selection of straight steps which are finite in space. Each of these steps is described by 6 parameters (σ, h, H, l_1, l_2, d) The values of these parameters have been shown in Figure 1.

We will consider that the excess density is a constant quantity within each of these steps. By changing the density value from step to step in each case, it is possible to describe the configuration of a sufficiently complex geological body of variable density.

The gravitational effect of the masses included in such a step can be obtained by solution of the direct problem for a parallelepiped. It is sufficient to presume that parameter $x_2 \to \infty$.

If there are m steps, then the observed anomaly can be approximated in the following way:

For the gravitational force anomaly

$$\Delta g(x, y) = -k \sum_{i=1}^{m} \sigma_i \left\{ -(d_i - x) \ln \frac{[(l_{2i} - y) + A_i^{22}][(l_{1i} - y) + A_i^{11}]}{[(l_{1i} - y) + A_i^{12}][(l_{2i} - y) + A_i^{21}]} + \right. \tag{4.1}$$

$$+ (l_{2i} - y) \ln \frac{(d_i - x) + A_i^{21}}{(d_i - x) + A_i^{22}} - (l_{1i} - y) \ln \frac{(d_i - x) + A_i^{11}}{(d_i - x) + A_i^{12}} +$$

$$+ H_i \left[\operatorname{arctg} \frac{H_i}{l_{2i} - y} - \operatorname{arctg} \frac{H_i A_i^{22}}{(d_i - x)(l_{2i} - y)} - \right.$$

$$\left. - \operatorname{arctg} \frac{H_i}{l_{1i} - y} + \operatorname{arctg} \frac{H_i A_i^{12}}{(d_i - x)(l_{1i} - y)} \right] -$$

/59

$$\left. - h_i \left[\operatorname{arctg} \frac{h_i}{l_{2i} - y} - \operatorname{arctg} \frac{h_i A_i^{21}}{(d_i - x)(l_{2i} - y)} - \right. \right.$$

$$\left. \left. - \operatorname{arctg} \frac{h_i}{l_{1i} - y} + \operatorname{arctg} \frac{h_i A_i^{11}}{(d_i - x)(l_{1i} - y)} \right] \right\},$$

For the anomaly of the horizontal gradient:

$$V_{xx}(x) = k\sum_{j=1}^{m}\sigma_j \ln\frac{[l_{1j}+A_j^{12}][l_{2j}+A_j^{21}]}{[l_{2j}+A_j^{22}][l_{1j}+A_j^{11}]}, \tag{4.2}$$

where

$$A_j^{11} = \sqrt{(d_j-x)^2+(l_{1j}-y)^2+h_j^2},$$

$$A_j^{12} = \sqrt{(d_j-x)^2+(l_{1j}-y)^2+H_j^2},$$

$$A_j^{21} = \sqrt{(d_j-x)^2+(l_{2j}-y)^2+h_j^2},$$

$$A_j^{22} = \sqrt{(d_j-x)^2+(l_{2j}-y)^2+H_j^2}.$$

In the observed field we will fix n points with coordinates x_i and y_i. We will structure the same function as (1.2). In order to determine the parameter d_j, we will write the values of the derivatives:

For the anomaly of the force of gravity

$$F'_{dj} = 2k\sigma_j\sum_{i=1}^{n}[\Delta g_{\text{obse}}(x_i,y_i)-\Delta g_{\text{theo}}(x_i,y_i)]\times$$

$$\times\left\{-\ln\frac{[(l_{2j}-y_i)+A_j^{22}][(l_{1j}-y_i)+A_j^{11}]}{[(l_{1j}-y_i)+A_j^{12}][(l_{2j}-y_i)+A_j^{21}]}-\right.$$

$$+\left[\frac{(d_j-x_i)^2}{[(l_{2j}-y_i)+A_j^{22}]A_j^{22}}-\frac{(d_j-x_i)^2}{[(l_{1j}-y_i)+A_j^{12}]A_j^{12}}+\right.$$

$$\left.+\frac{(d_j-x_i)^2}{[(l_{1j}-y_i)+A_j^{11}]A_j^{11}}-\frac{(d_j-x_i)^2}{[(l_{2j}-y_i)+A_j^{21}]A_j^{21}}\right]+$$

$$+(l_{2j}-y_i)\left[\frac{1}{A_j^{21}}-\frac{1}{A_j^{22}}\right]-(l_{1j}-y_i)\left[\frac{1}{A_j^{11}}-\frac{1}{A_j^{12}}\right]+ \tag{4.3}$$

$$+\frac{H_j^2(l_{2j}-y_i)[(l_{2j}-y_i)^2+H_j^2]}{\{(d_j-x_i)^2(l_{2j}-y_i)^2+H_j^2(A_j^{22})^2\}A_j^{22}}-$$

$$-\frac{H_j^2(l_{1j}-y_i)[(l_{1j}-y_i)^2+H_j^2]}{\{(d_j-x_i)^2(l_{1j}-y_i)^2+H_j^2(A_j^{12})^2\}A_j^{12}}-$$

$$-\frac{h_j^2(l_{2j}-y_i)[(l_{2j}-y_i)^2+h_j^2]}{\{(d_j-x_i)^2(l_{2j}-y_i)^2+h_j^2(A_j^{21})^2\}A_j^{21}}+$$

$$\left.+\frac{h_j^2(l_{1j}-y_i)[(l_{1j}-y_i)^2+h_j^2]}{\{(d_j-x_i)^2(l_{1j}-y_i)^2+h_j^2(A_j^{11})^2\}A_j^{11}}\right\},$$

/60

For the anomaly of the horizontal gradient

$$F_{dj} = 2k\sigma_j \sum_{i=1}^{n} [V_{xz\,\text{obse}}(x_i) - V_{xz\,\text{theo}}(x_i)] \times$$
$$\times (x_i - d_j)\left\{\frac{1}{(l_{1j} + A_j^{12})\,A_j^{12}} - \frac{1}{(l_{2j} + A_j^{22})\,A_j^{22}} - \right.$$
$$\left. - \frac{1}{(l_{1j} + A_j^{11})\,A_j^{11}} + \frac{1}{(l_{2j} + A_j^{21})\,A_j^{21}}\right\}. \qquad (4.4)$$

2. Selection Methods

The methods of selecting three-dimensional bodies do not differ basically from those described for two-dimensional bodies. The first variation of the problem provides for a search for the contours of the perturbing body in the coordinate plane x0z while taking into account its dimensions in space. If some of the objects are not intersected by the coordinate plane, then a projection of the contours is sought.

We will use examples to illustrate all our methodological means.

The Gravitational Force Anomaly

Let a gravitational force anomaly (Figure 14) be given. As is evident, the perturbing object is nearly isometric, making it impossible to use the two-dimensional problem. We will fix the beginning of the coordinates in the center of the anomaly. We select the axis 0x across the course being noted. Then it is natural that the axis 0y should be directed along the course, and the axis 0z should be directed vertically downward. Figures 15 and 16 show the curve of the gravitational force anomaly. We will draw columns like the Barton measuring grids in planes x0z and y0z. Let it be established that the initial depth can be accepted as equal to h_0 = 0.25 kilometers, and the final depth is H = 4.0 /61
kilometers. We will divide this whole region into 6 strips by using the planes h_j = 0.25; 0.5; 0.875; 1, 375; 2.0; 2.75; 4.0 kilometers. We will solve the problem sequentially. At first we will make approximation in the plane x0z, then in y0z, etc.

For the zero approximation we will select the bar (parallelepiped) which /62
is bounded by the planes x_1 = -1.75 kilometers, x_2 = 2.0 kilometers, y_1 = 3.0 kilometers, and y_2 = +3.0 kilometers.

In the given case, in planes x0z and y0z the number of unknown parameters (d_j) will be the same (12 unknowns in each case).

Let us examine curve Δg (x). We will fix the most descriptive points on this curve. The coordinates and values of the anomaly are given in a table

(Table 20). Table 21 shows the geological model. Of every six parameters, the first five are constant, and the sixth d is variable. Tables 20 and 21 show the results of the solution. The calculated field agrees fully satisfactorily with the observed.

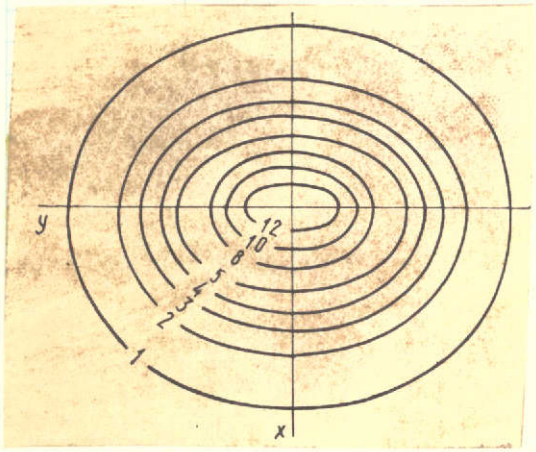

Figure 14. The Field of Gravitational Force.

Now we will move to selecting the contour along axis 0y (Figure 16). The parameters which describe the space have been taken from the previous solution (along axis 0x). Tables 22 and 23 show the coordinates of the points, the values of the anomaly, and the parameters of the geological model. The results of the solution are also shown. The first cycle of calculations is concluded with these calculations.

Analyzing the results of the calculations, one can state that the computation was done with considerable exactness. The selected and observed anomalies agree completely satisfactorily with one another. However, the contours in plane x0z have been selected with extremely approximate values for the dimensions of the masses which are anomalous in space. As one can see from Table 21, the uppermost block was computed under the condition that its space ranges from -3.0 to +3.0 kilometers. The values of these parameters have been computed according to the profile along axis 0y and are -1.83 and +1.13 kilometers. In order to clarify how this is reflected /64
in the results of the solution of the problem, it is necessary to repeat the computation, making a unique second cycle. Thus, in Table 21 parameters l_1 and l_2 have been taken from the results of the computations of the first cycle along axis 0y (Table 23).

The values of the parameters computed in the second cycle 0x are shown in Table 21.

Now the parameters in plane y0z can also be defined more exactly. After changing parameters l_1 and l_2, we will carry out a second cycle of computation along axis 0y. The results of these computations are shown in Table 23. When analyzing these data, it has been established that now the discrepancies in the desired parameters are small (they are less than 200 meters).

A third cycle was also carried out. Its results differ little from the second and are not shown in tables.

The results of the calculations are shown in Figures 15 and 16.

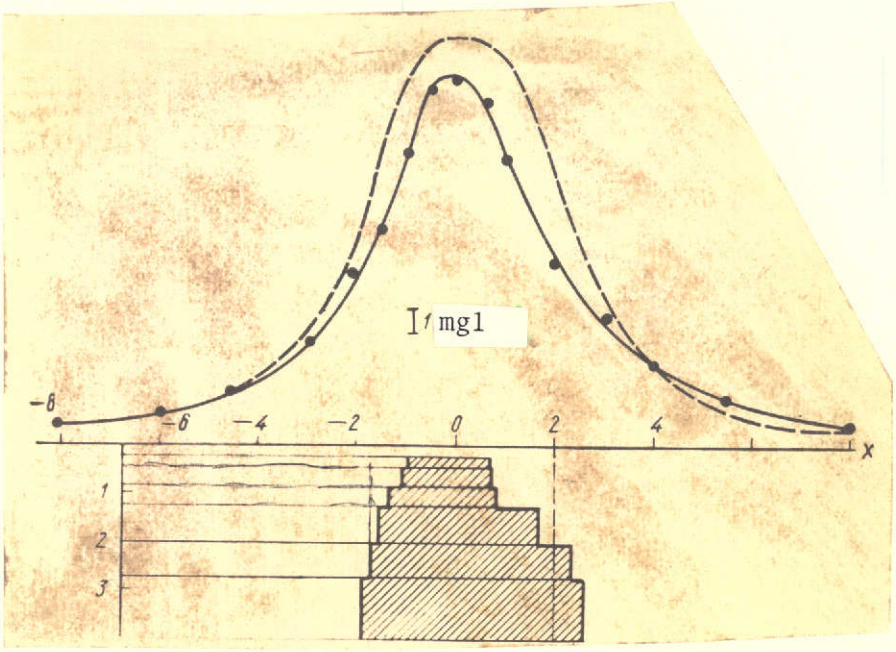

Figure 15. Selection of the Profile Along Axis 0x.

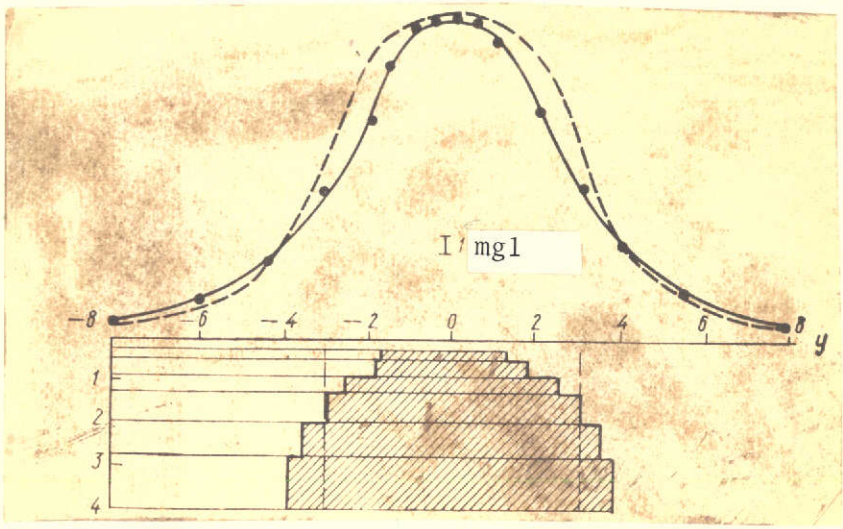

Figure 16. Selection of the Profile Along Axis 0y.

TABLE 22.

Coordinates		Value of Δg			
y	x	Observed	In the initial approximation (1 cycle)	Selected in the first cycle	Selected in the 2nd cycle
—8,0	0	0,82	0,62	0,76	0,78
—6,0	0	1,85	1,40	1,73	1,76
—4,5	0	3,61	3,06	3,46	3,53
—3,0	0	6,92	8,75	6,88	6,96
—2,0	0	10,52	13,26	10,49	10,45
—1,5	0	12,90	14,27	12,72	12,88
—1,0	0	14,27	14,87	14,26	14,33
—0,5	0	14,79	15,20	15,10	14,89
0	0	14,94	15,30	15,35	15,04
0,5	0	14,79	15,20	15,14	14,87
1,0	0	14,27	14,87	14,15	14,19
2,0	0	10,52	13,26	10,38	10,47
3,0	0	6,92	8,75	7,00	7,05
4,0	0	4,50	4,16	4,37	4,43
5,5	0	2,30	1,79	2,12	2,15
8,0	0	0,82	0,62	0,74	0,75

Commas indicate decimal points.

TABLE 23.

Parameters of the geological scheme	1	2	3	4	5	6
σ	0,25	—0,25	0,25	—0,25	0,25	—0,25
h	0,25	0,25	0,5	0,5	0,875	0,875
H	0,5	0,5	0,875	0,875	1,375	1,375
l_1	—0,93	—0,93	—1,05	—1,05	—1,32	—1,32
l_2	0,65	0,65	0,44	0,44	0,68	0,68
d_{assig}	—3,0	3,0	—3,0	3,0	—3,0	3,0
d_{calcul}						
I cycle	—1,83	1,13	—1,79	1,66	—2,37	2,48
II cycle	—1,69	1,32	—1,64	1,81	—2,45	2,53

Parameters of the geological scheme	7	8	9	10	11	12
σ	0,25	—0,25	0,25	—0,25	0,25	—0,25
h	1,375	1,375	2,0	2,0	2,75	2,75
H	2,0	2,0	2,75	2,75	4,0	4,0
l_1	—1,54	—1,54	—1,7	—1,7	—1,87	—1,87
l_2	1,70	1,70	2,28	2,28	2,65	2,65
d_{assig}	—3,0	3,0	—3,0	3,0	—3,0	3,0
d_{calcul}						
I cycle	—2,83	2,99	—3,44	3,42	—3,82	3,64
II cycle	—2,91	3,06	—3,52	3,50	—3,93	3,76

Commas indicate decimal points.

Figure 17 shows anomalies of the horizontal gradient of the force of gravity for the same geological object. The selection method remains the same as before.

In Tables 24 - 27 data are cited for the computation of the inverse problems for anomalies V_{xz} and V_{yz}. The parallelpiped, the boundaries of which converge with the extreme points has been accepted as the initial approximation. At the very beginning, using the approximated data about the dimensions of the body, along axis 0y, we determine its contour in the section x0z (Table 24 and 25). Then we move to the anomaly along axis 0y. The overall dimensions of the body have already been defined more exactly by the previous computation, and the results are shown in Tables 25 and 27. The first cycle of computation is concluded at this point.

TABLE 24.

Number of the Point	x	Value of the anomaly v_{xz} Observed	In the Initial Approximation (1st cycle)	Selected in the 1st cycle	Selected in the 2nd cycle	Number of the Point	x	Value of the anomaly v_{xz} Observed	In the Initial Approximation (1st cycle)	Selected in the 1st cycle	Selected in the 2nd cycle
1	—4,0	45	18	33	40	9	0,5	—160	—114	—149	—158
2	—3,0	79	38	67	75	10	1,0	—176	—242	—164	—172
3	—2.5	107	57	96	104	11	1.5	—160	—153	—152	—158
4	-2,0	146	90	137	143	12	2,0	—134	—90	—136	—134
5	-1.5	202	153	189	195	13	2,5	—109	—57	—106	—111
6	-1,0	255	242	237	250	14	3,0	—88	—38	—77	—87
7	-0,5	124	114	96	112	15	4,0	—55	—18	—39	—49
8	0	—22	0	—11	—14	16	5,0	—34	—10	—20	—27

Commas indicate decimal points.

TABLE 25.

Parameters of the Geological Model	1	2	3	4	5	6	7	8	9	10	11	12
σ	1	—1	1	—1	1	—1	1	—1	1	—1	1	—
h	0,25	0,25	0,5	0,5	0,875	0,875	1,375	1,375	2,0	2,0	2,75	2,
H	0,5	0,5	0,875	0,875	1,375	1,375	2,0	2,0	2,75	2,75	4,0	4,
l_1	—1,75	—1,75	—1,75	—1,75	—1,75	—1,75	—1,75	—1,75	—1,75	—1,75	—1,75	—1,
l_2	1,75	1,75	1,75	1,75	1,75	1,75	1,75	1,75	1,75	1,75	1,75	1,
d_{assig}	—1,0	1,0	—1,0	1,0	—1,0	1,0	—1,0	1,0	—1,0	1,0	—1,0	1,
d_{calcul} I cycle	—1,0	0,54	—1,10	0,98	—1,51	1,77	—1,69	1,96	—1,68	1,90	—1,67	1,
d_{calcul} II cycle	—0,93	0,47	—1,08	0,96	—1,37	1,36	—1,63	2,13	—1,73	2,13	—1,78	2,

Commas indicate decimal points.

The second cycle again begins by selecting the contours in plane x0z. By using the results of the computations along axis 0y, we define more precisely the body in space. The results of the computations in the second cycle are shown in the same tables.

TABLE 26.

/66

Number of the Point	y	Value of the anomaly v_{yz}				Number of the Point	y	Value of the anomaly v_{yz}			
		Observed	In the Initial Approximation (1st cycle)	Selected in the 1st cycle	Selected in the 2nd cyle			Observed	In the Initial Approximation (1st cycle)	Selected in the 1st cycle	Selected in the 2nd cycle
1	—5,0	51	19	26	48	12	0	0	0	—2	0
2	—4,0	78	37	77	86	13	0,5	—25	—47	—39	—27
3	—3,0	115	80	112	118	14	1,0	—67	—109	—86	—70
4	—2,5	140	127	139	148	15	1,25	—104	—153	—117	—111
5	—2,0	179	219	177	177	16	1,5	—173	—213	—151	—174
6	—1,75	200	260	176	207	17	1,75	—200	—260	—178	—204
7	—1,5	173	213	150	172	18	2,0	—179	—219	—179	—172
8	—1,25	104	153	114	109	19	2,5	—140	—127	—140	—144
9	—1,0	67	109	83	69	20	3,0	—115	—80	—116	—119
10	—0,75	40	75	57	44	21	5,0	—52	—19	—25	—48
11	—0,5	25	47	35	26						

Commas indicate decimal points.

TABLE 27.

Parameters of the Geological Model	1	2	3	4	5	6	7	8	9	10	11	12
σ	1	—1	1	—1	1	—1	1	—1	1	—1	1	—1
h	0,25	0,25	0,5	0,5	0,875	0,875	1,375	1,375	2,0	2,0	2,75	2,75
H	0,5	0,5	0,875	0,875	1,375	1,375	2,0	2,0	2,75	2,75	4,0	4,0
l_1	—1	—1	—1,1	—1,1	—1,5	—1,5	—1,7	—1,7	—1,68	—1,68	—1,67	—1,67
l_2	0,54	0,54	1,0	1,0	1,77	1,77	1,96	1,96	1,90	1,90	1,92	1,92
d_{calcul}	—1,75	1,75	—1,75	1,75	—1,75	1,75	—1,75	1,75	—1,75	1,75	—1,75	1,75
d_{assig}												
I cycle	—1,60	1,50	—1,77	1,79	—2,00	2,00	—2,17	2,09	—2,08	1,97	—2,00	1,90
II cycle	—1,67	1,66	—1,74	1,72	—2,82	2,96	—2,71	2,69	—3,42	3,39	—3,20	3,15

Commas indicate decimal points.

The computed anomalous function coincides sufficiently well with the observed function, and there is no need to repeat the iteration process. /68

The results of the selection are shown in Figure 17. Here two graphs are combined, and therefore the values of the anomalies in the first approximation are now shown in the tables. The figure shows the contours of the theoretical model for which all the computations were carried out.

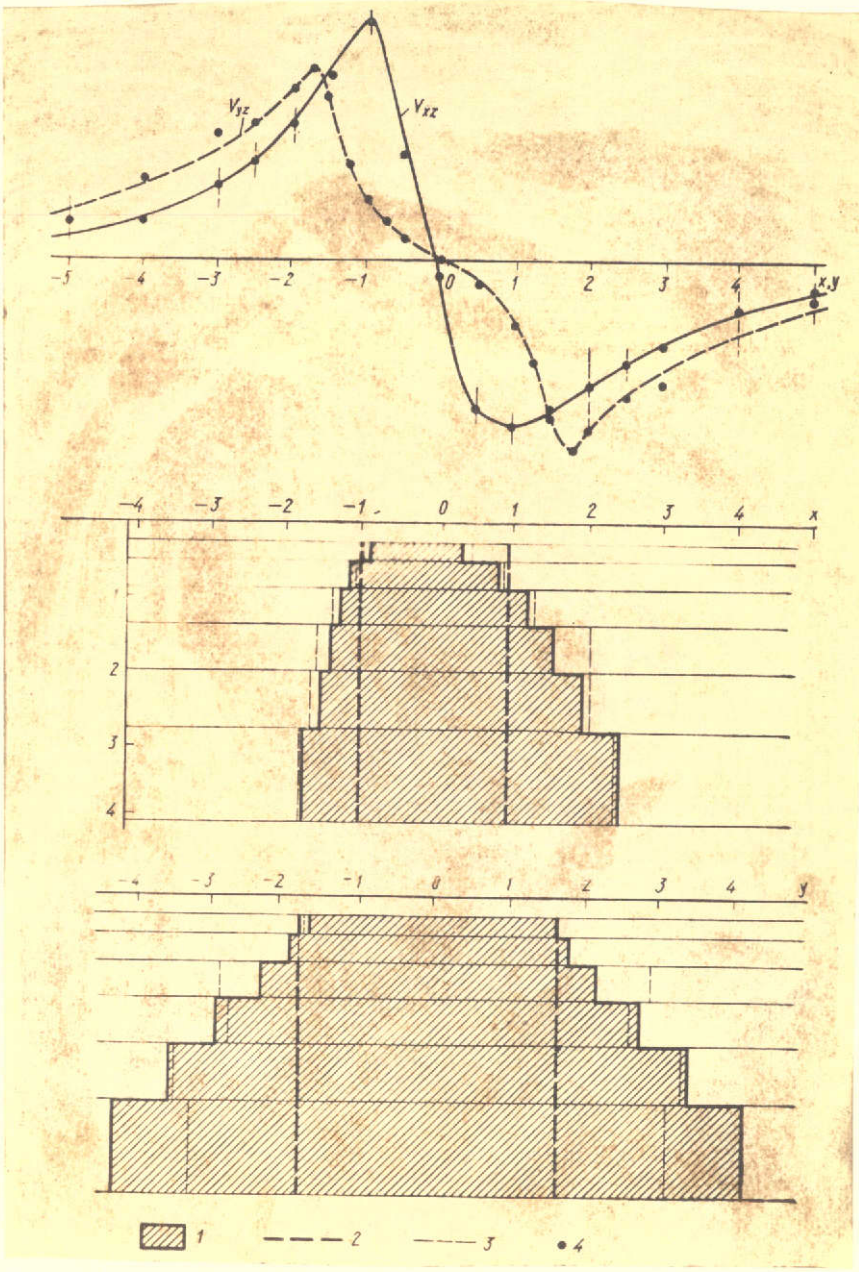

Figure 17. Selection for an Anomaly of the Horizontal Gradient of Gravitational Force: 1) Assigned Contour; 2) Contour of the First Approximation; 3) Selected Contour; 4) Selected Anomaly.

CHAPTER V

/69

INTERPRETING ANOMALIES COMPLICATED BY LOCAL BACKGROUND CONDITIONS

1. Posing the Problem

It is very important to know the level of a normal field when interpreting gravitational anomalies. For a variety of reasons, we very often have no absolute general knowledge about a gravitational force anomaly. These reasons can be inexact knowledge of the normal distribution of gravitational force and extremely approximated knowledge of the density parameters of the rocks which make up the intermediate layer. As a result of this the Buge correction factors and many other things can be very inexact.

When solving a direct problem for certain geological conditions, various investigators can obtain different readings for the field level. This can be illustrated by a very simple example.

Let there be in the cross-section a limitless plane-parallel layer in which contact is clearly distinguished between two types of rock which differ in density. Examining this cross-section from the side of the less dense rock, we obtain a general positive anomaly for the force of gravity. If the investigation of the region is carried out from the side of the dense rocks and if the normal field is selected at that point, then the anomalous effect of the contact will be located in the range of negative values for the force of gravity. The first and second anomalies differ from one another only by their constant components. Many similar examples can be cited.

We will now turn to questions of interpretation. The machine method of selection examined by us consists of comparing the observed field and the results of solving the direct problem. It is evidently clear that in a number of cases these fields can differ not only in details, but can have an absolutely different level reading. No attention is paid to this during manual selection. A simple parallel transfer (often completely automatic) solves the entire question. The situation is different with the machine selection method. Imaginary perturbing bodies will appear when the calculated body is combined with the observed body.

We will turn again to an example. Figures 18 and 19 show the results of selecting the contours of geological bodies for a gravitational force anomaly. The entire process was carried out using the computer method described in Chapter III. In the lower parts of the figures the geological model is shown /72
which was constructed by the investigator as the initial variation (the first kilometer of the cross-section has been excluded from the investigation). The direct problem for this geological structure on the level of the field differs by 15 mgl from the observed field.

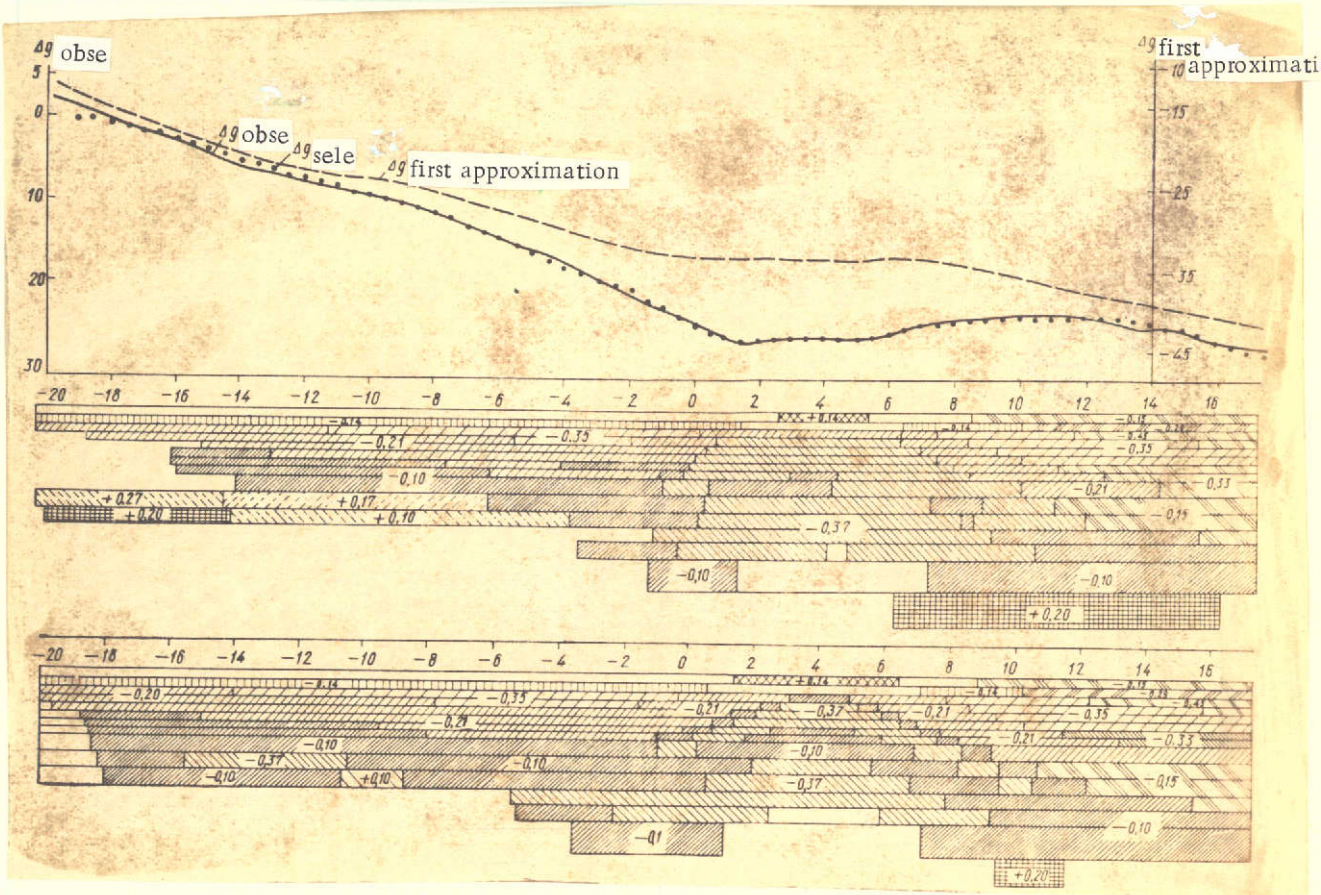

Figure 18. An Example of Automatic Selection Without Taking Into Account a Difference in the Levels of the Observed and Calculated Field.

Figure 18 (the upper cross-section) shows the results of the selection. In order to compensate for the 15 mgl, horizontal intermediate layers with excess densities of +0.27 and +0.17 have been inserted into the geological cross-section. These masses have been formed by the movement of heavy masses to the left. The horizontal dimensions of the masses which had a density of +0.1 and +0.2 have been sharply increased. Although the observed and selected anomalies coincided quite well, it is obviously difficult to evaluate positively the results of the selection.

A completely different picture was obtained after introducing into the observed anomaly correction factors for the field level (Figure 19). The observed anomaly and the results of solving the direct problem, it is true, differ considerably, but they coincide in their asymptotic parts. Now the result of the selection differs from the initial approximation only in a few details (although these details are very significant).

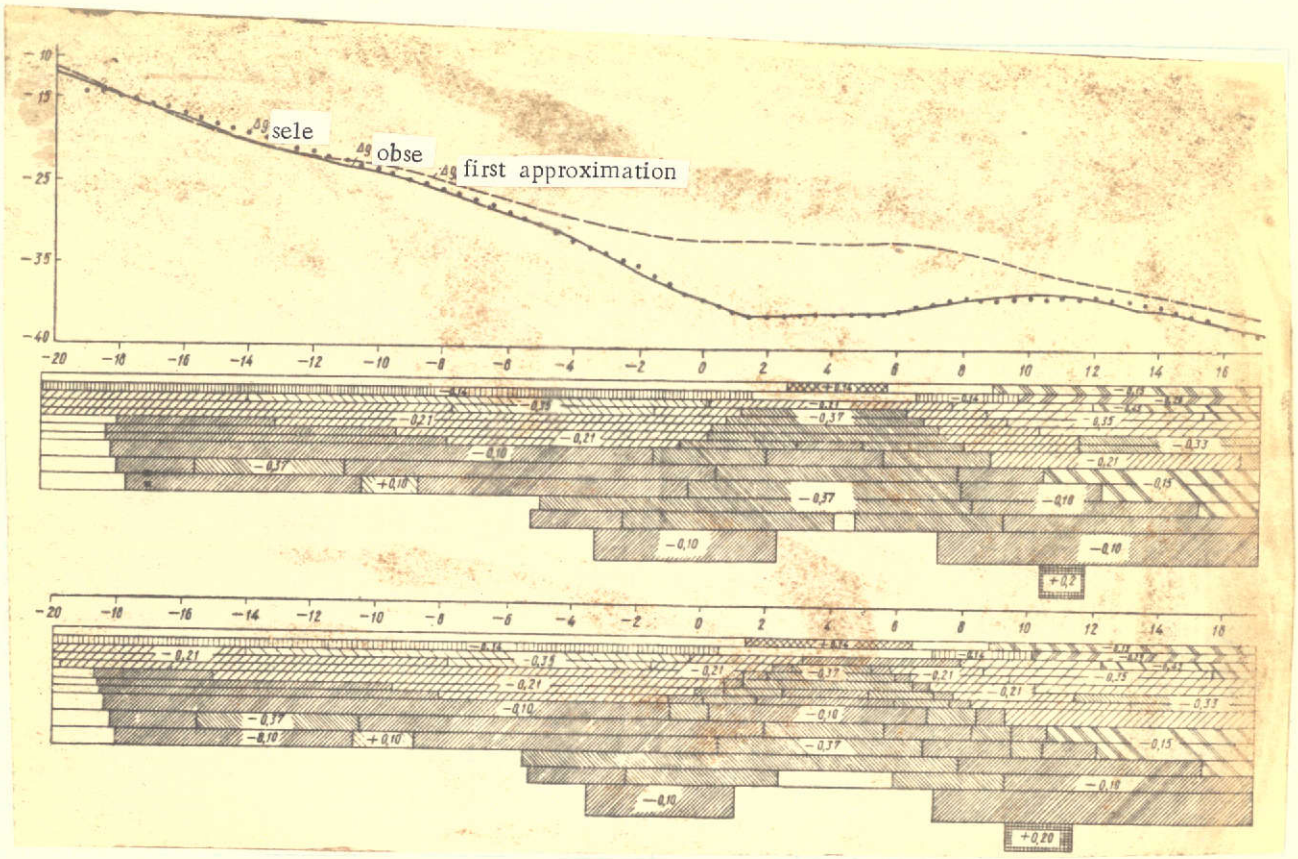

Figure 19. An Example of Automatic Selection Taking Into Account a Difference in the Levels of the Observed and Calculated Field.

Thus arises the task in the observed field of distinguishing two components, one of which can describe the geological heterogeneities, and the other the general local background. In its mathematical formulation, the task will consist of the following. Let an anomalous field V_{obse} (x, y) be assigned. (This can be any gravitational or magnetic anomaly). We will fix in this field n points with coordinates x_i and y_i. On the basis of all information about the geological structure, taking into account the field being interpreted, we construct a geological model in such a way that the anomalous effect from it can be computed. Let this effect be V_{theo} (x, y). Using the function f (x, y), we approximate the regional component of the fields as V_{reg} = f (x, y). Now we will compare the two groups of the function V_{obse} (x, y) and V_{theo} (s, y) + f (x, y). We will construct this expression:

$$F = \sum_{i=1}^{n} [V_{obse}(x_i, y_i) - V_{theo}(x_i, y_i) - f(x_i, y_i)]^2. \qquad (5.1)$$

For a certain geological cross-section and at the assigned coordinates of the points, the variable parameters will be contained here only in the function $V_{reg} = f(x, y)$. Expression (5.1) can be rewritten thus:

$$F = \sum_{i=1}^{n} [\Delta(x_i, y_i) - f(x_i, y_i)]^2, \tag{5.2}$$

where

$$\Delta(x_i, y_i) = V_{obse}(x_i, y_i) - V_{theo}(x_i, y_i).$$

If one takes into account the fact that the observed anomaly is given by the table and that the theoretical anomaly can be computed at all fixed points, /73
then it becomes clear that it is easy to compute the function $\Delta(x, y)$ at all fixed points and to write these values in tabular form.

Now we will turn to the function f (x, y). Having given a certain form to this function, it is possible to find from the conditions of the minimum of (5.2) the parameters which describe it. Thus in the very first approximation it is most convenient to approximate the local component by using a linear function with the form

$$f(x, y) = A + Bx + Cy.$$

One can almost always find a geological explanation for this function. In this case (5.2) can be written in the form

$$F = \sum_{i=1}^{n} [\Delta(x_i, y_i) - A - Bx_i - Cy_i]^2. \tag{5.3}$$

Now the task is to minimize function F (A, B, C).

2. Minimization Methods

We will examine two computer models for determining the parameters which describe a background field.

Solving the Problem Using the Fast Descent Gradient Method

It is possible to minimize function (5.3) and to determine the parameters of the local background using the fast descent method. The computation method does not differ from those used in the problems examined earlier in this work. The desired values are determined by the sequential approximations

$$\begin{aligned} A^{(k+1)} &= A^{(k)} - \lambda_k F'_A, \\ B^{(k+1)} &= B^{(k)} - \lambda_k F'_B, \\ C^{(k+1)} &= C^{(k)} - \lambda_k F'_C. \end{aligned} \tag{5.4}$$

The function F and derivatives of it depend on the geometric forms by which the geological bodies are approximated.

Solving the Problem Using the Linear Algebra Method

The problem described earlier can be formulated in the following form. The anomaly computed from the geological model hypothesis $V_{theo}(x, y)$ and the regional component of the field $V_{reg}(x, y)$ should fully correspond to the observed field, i.e.

$$V_{obse}(x, y) = V_{theo}(x, y) + V_{reg}(x, y).$$

If the regional component is approximated by the linear function A + Bx + Cy, then the last relationship can be written thus: /74

$$V_{obse}(x, y) = V_{theo}(x, y) + A + Bx + Cy.$$

For the fixed geological cross-section

$$A + Bx + Cy = V_{obse}(x, y) - V_{theo}(x, y) = \Delta(x, y).$$

We will fix n points with coordinates x_i and y_i and we will construct the system

$$\begin{aligned} &A + x_i B + y_i C = \Delta(x_i, y_i), \\ &i = 1, 2, \ldots, n. \end{aligned} \tag{5.5}$$

If n > 3, then a re-defined linear system is obtained which is written in matrix form as

$$Ka = \Delta, \tag{5.6}$$

where

$$K = \begin{bmatrix} 1 x_1 y_1 \\ 1 x_2 y_2 \\ \cdots \\ 1 x_n y_n \end{bmatrix}, \quad a = \begin{bmatrix} A \\ B \\ C \end{bmatrix}, \quad \Delta = \begin{bmatrix} \Delta(x_1, y_1) \\ \Delta(x_2, y_2) \\ \vdots \\ \Delta(x_n, y_n) \end{bmatrix} = \begin{bmatrix} \Delta_1 \\ \Delta_2 \\ \vdots \\ \Delta_n \end{bmatrix}.$$

This system can be solved using the method of the smallest squares. The method itself relieves us of the necessity of investigating the compatability of the given system. For each variation of the geological schematic and the system of assigned points, we will obtain the optimum solution to the problem.

Without citing computations, we will simply indicate that vector a is found from solving the system

$$K'Ka = K'\Delta.$$

Here K' is the transposed matrix K. As is known, this relationship always leads to a fully determined system of exactly the same number of equations as we have unknowns [45].

For our purposes the matrix for deriving P = K'K can easily be determined. It is always symmetrical:

$$P = \begin{bmatrix} 1 & 1 & \dots & 1 \\ x_1 & x_2 & \dots & x_n \\ y_1 & y_2 & \dots & y_n \end{bmatrix} \begin{bmatrix} 1 & x_1 & y_1 \\ 1 & x_2 & y_2 \\ \cdot & \cdot & \cdot \\ 1 & x_n & y_n \end{bmatrix} = \begin{bmatrix} n & \sum x_i & \sum y_i \\ \sum x_i & \sum x_i^2 & \sum x_i y_i \\ \sum y_i & \sum x_i y_i & \sum y_i^2 \end{bmatrix}.$$

Vector K'Δ is determined thus:

$$K'\Delta = \begin{bmatrix} 1 & 1 & \dots & 1 \\ x_1 & x_2 & \dots & x_n \\ y_1 & y_2 & \dots & y_n \end{bmatrix} \begin{bmatrix} \Delta_1 \\ \Delta_2 \\ \vdots \\ \Delta_n \end{bmatrix} = \begin{bmatrix} \sum \Delta_i \\ \sum x_i \Delta_i \\ \sum y_i \Delta_i \end{bmatrix}.$$

Thus this linear system of equations is to be solved: /75

$$\left.\begin{aligned} nA + \sum x_i B + \sum y_i C &= \sum \Delta_i, \\ \sum x_i A + \sum x_i^2 B + \sum x_i y_i C &= \sum x_i \Delta_i, \\ \sum y_i A + \sum x_i y_i B + \sum y_i^2 C &= \sum y_i \Delta_i. \end{aligned}\right\} \qquad (5.7)$$

If the observations are given in the one profile y = 0, then this system leads to

$$\left.\begin{aligned} nA + \sum x_i B &= \sum \Delta_i, \\ \sum x_i A + \sum x_i^2 B &= \sum x_i \Delta_i. \end{aligned}\right\} \qquad (5.8)$$

3. Determining the Regional Background of Local Symmetrical Gravitational Force Anomalies

For local symmetrical anomalies where geological bodies have a branching structure, the form of each geological object can be approximated by a sphere. If there are in all m geological bodies, then the anomaly from the perturbing masses can be written in the following way:

$$\Delta g_{\text{theo}}(x, y) = k \sum_{j=1}^{m} \frac{M_j h_j}{(x - x_{0j})^2 + (y - y_{0j})^2 + h_j^2}. \qquad (5.9)$$

It is most convenient to express linear values in kilometers. We will decide to consider excess mass in units of 10^9 T. For instance if $M_{exc} = 12 \cdot 10^{10}$ T,

then it is necessary to insert into the formula M = 120 units. In this scale the coefficient K = 6.67 and the gravitational force anomaly are expressed in milligals.

The calculation diagram can be described in the following way:

1. Initial data. In order to solve the problem, it is necessary to assign a diagram of the geological structure. Its parameters are entered into a special table where the mass of each body and the coordinates of its center of gravity are fixed.

In the anomalous field n points are selected which can completely describe all the peculiarities of the observed field. The coordinates of these points and the value of Δg are entered into another table. Thus the initial data for solving the problem are reduced into two tables.

2. For the point, the coordinates of which are assigned, the function $\Delta g_{theo}(x, y)$ is calculated according to formula (5.9). The results of the calculations are printed out.

3. The function is computed

$$\Delta_i = \Delta(x_i, y_i) = \Delta g_{obse}(x_i, y_i) - \Delta g_{theo}(x_i, y_i).$$

4. The coefficients of equation system (5.7) or (5.8) are computed.

5. The system of 3(2) linear equations are solved and the regional background is determined. /76

6. The linear portion of the observed field is isolated, and the following function is sent to printout

$$\Delta g^{*}_{obse}(x, y) = \Delta g_{obse}(x, y) - A - Bx - Cy.$$

Now it is possible to analyze the solution of the direct problem. For this purpose, the two functions printed out are compared: $\Delta g^{*}_{obse}(x, y)$ and $\Delta g_{theo}(x, y)$.

Then there follows a selection of parameters for the geological objects using the method explained in the previous chapters.

If the initial approximation and the solution of the problem differ significantly, then the determination of background parameters can be repeated.

We will illustrate the calculation method with the following example. Let a field with an anomaly in the force of gravity (Figure 20) be assigned where four local objects are distinguishable against a background of the general local field. We will approximate these objects using spheres. The parameters of the spheres are shown in Table 28.

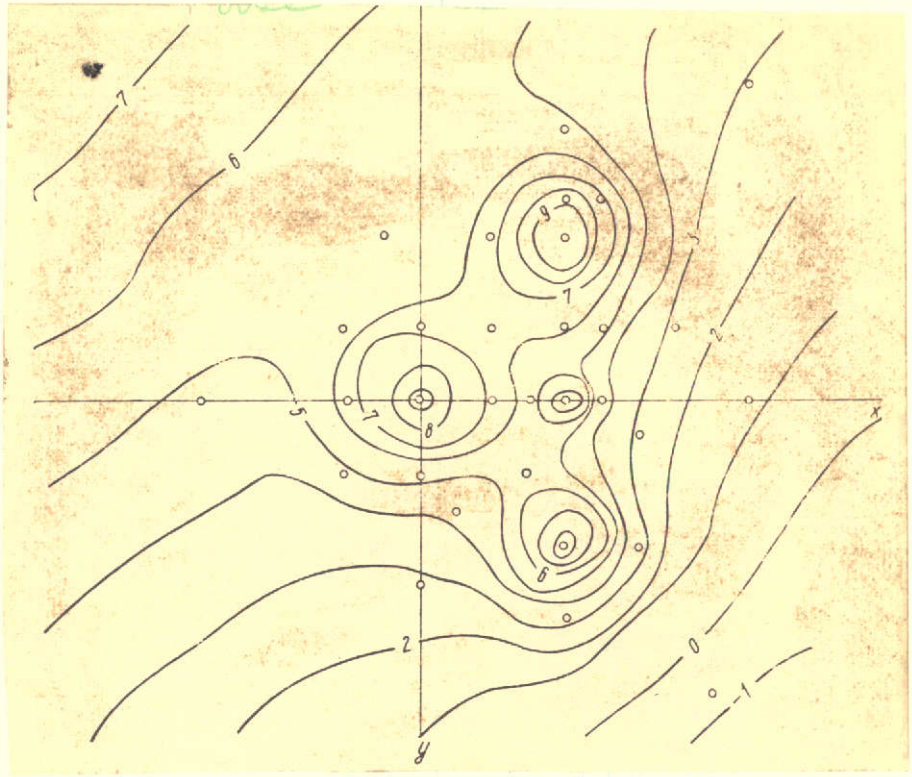

Figure 20. A Gravitational Force Complicated by Local Influences.

TABLE 28.

No. of the perturbing body	M, Units of 10^9 T	x	y	h
1	1,07	0	0	1
2	1,07	2	2	1
3	1,07	2	—2	1
4	0,135	2	0	0,5

Commas indicate decimal points.

In order to determine the background, we will select 31 points distributed in the most descriptive areas of the observed fields. We will list these points in Table 29. /77

After calculation has been completed, a function is set up for the local background (3 - 0.5 x - 0.5y) mgl. At all fixed points a calculation is made of the rest of the field:

$$\Delta g^{*}_{\text{obse}}(x, y) = \Delta g_{\text{obse}}(x, y) - [3 - 0{,}5x - 0{,}5y].$$

Only the geological heterogenities can now explain the observed anomaly.

4. Determining the Regional Background of a Gravitational Force Anomaly by Block Structure

We approximate the geological objects by selecting their straight projections which are finite in space. If m projections are given in the model, then the

gravitational force anomaly from the geological objects is approximated by formula (5.1). For two-dimensional purposes, formula (3.1) is used. The calculation diagram does not differ from the one described above.

TABLE 29.

No. of point	x	y	Δg obse	No. of point	x	y	Δg obse	No. of point	x	y	Δg obse
1	0	0	10,73	12	—1,0	—1	5,67	22	2,5	—1	5,13
2	1,5	0	5,93	13	—0,5	—2	5,29	23	2	0	7,50
3	2,5	0	4,57	14	—1,0	1	4,67	24	—1	0	6,32
4	4,5	0	1,23	15	0	2,5	2,78	25	2,5	—2,5	7,13
5	0	—1	6,69	16	0,5	1,5	4,35	26	2	—2,5	8,66
6	1	—1	6,08	17	1,5	1	5,15	27	3	2	3,30
7	3,5	—1	2,94	18	2	2	8,57	28	2	3	3,23
8	1	—2	6,64	19	3	0,5	2,83	29	0	1	5,69
9	2	—2	10,57	20	4	4	—0,67	30	1	0	6,32
10	2	—3,5	5,12	21	2	—1	6,06	31	4,5	—4	3,00
11	—3	0	4,82								

Commas indicate decimal points.

The calculation method can be illustrated by the following example. Figure 21 presents the geological model of the region and the gravitational force anomaly. Behind peak No. 20 in the rock mass, which has a density of 2.66, there is a strip of very heavy rock. The task is to divide the observed anomaly in the area from the zero point to the peak at point 10 into two components: /78

$$\Delta g_{\text{obse}}(x) = \Delta g^{*}_{\text{obse}}(x) + A + Bx.$$

In order to solve this problem, we will locate the descriptive points on a curve. Twenty of them are delineated (in our case n = 20). A list of these points is presented in Table 30.

TABLE 30.

No. of points	1	2	3	4	5	6	7	8	9	10
x	0,5	1,0	2,0	2,5	3,0	3,5	4,0	4,75	5,25	5,75
Δg	1,40	2,15	3,00	3,45	3,60	4,10	2,60	1,60	2,45	1,75
No. of points	11	12	13	14	15	16	17	18	19	20
x	6,0	6,5	7,0	7,5	8,0	8,5	9,0	9,25	9,75	10,5
Δg	2,25	2,30	2,15	1,90	1,10	1,05	1,75	1,60	1,90	1,25

Commas indicate decimal points.

The geological cross-section is represented by a selection of projections. In this case 59 projections are given in the cross-section. The parameters describing the location and dimensions of these projections are shown in Table 31.

TABLE 31.

Parameter of Perturbing body	Number of the body							
	1	2	3	4	5	6	7	8
σ	+0,05	−0,05	+0,07	−0,07	+0,05	−0,05	−0,04	+0,04
h	0,05	0,05	0,05	0,05	0,05	0,05	0,05	0,05
H	0,25	0,25	0,25	0,25	0,25	0,25	0,25	0,25
d	1,3	3,8	4,8	5,4	6,25	7,2	8,15	8,25

Parameter of Perturbing Body	Number of the body						
	9	10	11	12	13	14	15
σ	+0,07	−0,07	+0,07	−0,07	+0,22	−0,19	+0,05
h	0,05	0,05	0,05	0,05	0,05	0,05	0,25
H	0,25	0,25	0,25	0,25	0,25	0,25	0,5
d	8,75	9,05	9,45	9,95	18,7	19,45	1,25

Parameter of Perturbing Body	Number of the body							
	16	17	18	19	20	21	22	23
σ	−0,05	+0,07	−0,07	+0,05	−0,05	−0,04	+0,04	+0,07
h	0,25	0,25	0,25	0,25	0,25	0,25	0,25	0,25
H	0,5	0,5	0,5	0,5	0,5	0,5	0,5	0,5
d	3,6	4,6	5,2	6,25	7,15	8,15	8,25	9,0

Parameter of Perturbing Body	Number of the body						
	24	25	26	27	28	29	30
σ	−0,07	+0,07	−0,07	+0,07	−0,07	+0,07	−0,07
h	0,25	0,25	0,25	0,25	0,25	0,25	0,25
H	0,5	0,5	0,5	0,5	0,5	0,5	0,5
d	9,1	9,45	9,9	11,6	12,15	14,0	16,5

Commas indicate decimal points.

TABLE 31 (continued)

Parameter of Perturbing Body	Number of the body							
	31	32	33	34	35	36	37	38
σ	+0,22	−0,19	+0,05	−0,05	+0,07	−0,07	+0,05	−0,05
h	0,25	0,25	0,5	0,5	0,5	0,5	0,5	0,5
H	0,5	0,5	1,0	1,0	1,0	1,0	1,0	1,0
d	18,7	19,45	1,15	3,35	4,5	5,05	6,3	7,1

Parameter of Perturbing Body	Number of the body						
	39	40	41	42	43	44	45
σ	−0,04	+0,04	+0,07	−0,07	+0,07	−0,07	+0,03
h	0,5	0,5	0,5	0,5	0,5	0,5	0,5
H	1,0	1,0	1,0	1,0	1,0	1,0	1,0
d	8,15	8,25	9,05	9,15	9,35	9,85	19,0

Parameter of Perturbing Body	Number of the body							
	46	47	48	49	50	51	52	53
σ	+0,05	−0,05	+0,07	−0,07	−0,04	+0,04	+0,03	+0,05
h	1,0	1,0	1,0	1,0	1,0	1,0	1,0	1,75
H	1,75	1,75	1,75	1,75	1,75	1,75	1,75	3,25
d	1,05	3,15	4,25	4,85	8,15	8,25	18,75	0,75

Parameter of Perturbing body	Number of the body					
	54	55	56	57	58	59
σ	−0,05	+0,07	−0,07	−0,04	+0,04	+0,03
h	1,75	1,75	1,75	1,75	1,75	1,75
H	3,25	3,25	3,25	3,25	3,25	3,25
d	3,0	4,05	4,6	8,15	8,25	18,0

Commas indicate decimal points.

The results of the calculation are as follows: A = - 0.024 mgl, and B = 0.0665 mgl/km. Figure 21 shows the observed anomaly and the anomaly from which the linear components of the field were excluded.

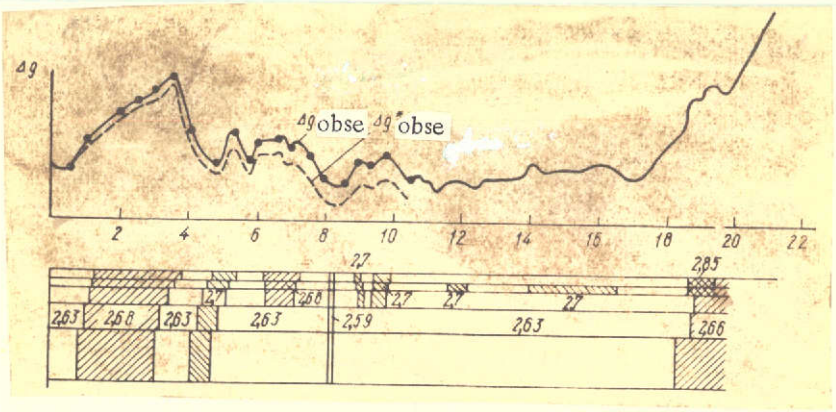

Figure 21. An Example of Excluding the Linear Component of a Gravitational Field.

CHAPTER VI

/81

DETERMINING THE PARAMETERS OF A PLANAR CROSS-SECTION

1. Posing the Problem

Earlier we examined problems in which we searched for positions of geological objects at which the difference between the observed and the theoretically calculated anomalies would be the least possible. Some parameters were considered constant. This relates primarily to planes. Let us look at Figure 22. Here an observed anomaly of gravitational force is shown. A diagram of the geological structure (cross-section along the profile) has been constructed on the basis of the totality of geological data, while taking into account the anomalous field. The direct problem has been solved for the given distribution of perturbing masses. We will compare the observed anomaly and the solution of the direct problem. Even the most cursory analysis shows that a single shift in contours cannot give us a satisfactory result. It is certain that, analogous to the example examined in the Fifth Chapter, we can obtain here a solution which obviously is far removed from the basic geological diagram. In addition, it is necessary to change the rock densities only slightly for the observed and calculated anomalies to coincide completely satisfactorily. After changing the planar parameters, it is possible to move on to selecting the contours of geological bodies. Thus arises the task of minimizing function (1.2) where all the parameters in the geological diagram except for the density have been given and are considered known.

/82

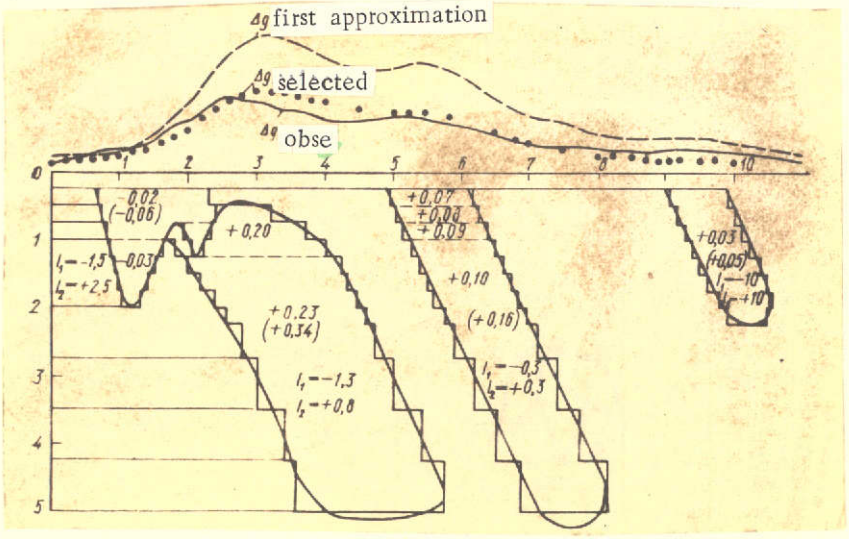

Figure 22. Example of the Selection of Planar Parameters.

In its general form, the task can be formulated this way. Let a geological diagram be constructed on the basis of data about the geological structure of the research regions, and with allowance made for the observed gravitational field. In this process the gravitational effects from it can be represented in analytic form:

$$\Delta g_{\text{theo}}(x, y) = \sum_{j=1}^{m} \sigma_j f(x, y, p_{1j}, p_{2j}, \ldots, p_{sj}). \tag{6.1}$$

All further statements will be true for any other gravitational or magnetic anomaly for which the additive property is valid. In this case the geological diagram has been approximated by m elementary bodies (for instance, projections). The parameter P_{kj} (k = 1, 2, ..., s) characterizes the location and dimensions of these bodies. In order to solve the problem, we will use the method we examined earlier. Then this functional is subject to minimization:

$$F = \sum_{i=1}^{n} [\Delta g_{\text{obse}}(x_i, y_i) - \Delta g_{\text{theo}}(x_i, y_i)]^2. \tag{6.2}$$

In order to set up this functional, n points have been fixed in the field of observed values Δg_{obse} (x, y). These are descriptive points where the field has extreme values, turning points, gradient changes, etc.

Let us turn to (6.2). If one takes into account the fact that points (x_i, y_i) are given, Δg_{theo} (x, y) is expressed by formula (6.1), and all its parameters except σ_j are given, then the functional F depends only on the densities. Representing them as components of some vector $\{\sigma_j\}$, one can write

$$F = F(\sigma_1, \sigma_2, \ldots, \sigma_m). \tag{6.2a}$$

The expression (6.2a) can be minimized according to the computation diagram examined in the first chapter. We will write only the expressions for the derivatives

$$F_{\sigma_j} = -2 \sum_{i=1}^{n} [\Delta g_{\text{obse}}(x_i, y_i) - \Delta g_{\text{theo}}(x_i, y_i)] \cdot f(x_i, y_i, p_{1j}, p_{2j}, \ldots, p_{sj}). \tag{6.3}$$

In connection with the fact that, by their nature, planar parameters for homogeneous elementary bodies are entered by means of a linear multiplier, another approach to minimization (6.2a) is possible. In this process it is necessary to somewhat change the way the problem is posed. Having fixed n points with coordinates x_i and y_i, we can compare the values of the observed /83
and calculated anomalies from the geological diagram

$$\Delta g_{\text{obse}}(x_i, y_i) = \sum_{j=1}^{m} \sigma_j f(x_i, y_i, p_{1j}, p_{2j}, \ldots, p_{sj}) = \sum_{j=1}^{m} \sigma_j f_j(x_i, y_i). \tag{6.4}$$

Expression (6.4) is a system of n linear equations with m unknown parameters σ_j. It can turn out that n is greater than m, when we would be dealing with a re-defined system of linear equations. If n is less than m, then (6.4) will be a system without supplementary definition. Both in the first and in the second cases, the system can be solved by using the method of the least squares. We will write it in matrix form

$$K\sigma = a, \tag{6.5}$$

where

$$K = \begin{bmatrix} f_1(x_1, y_1) & f_2(x_1, y_1) & \dots & f_m(x_1, y_1) \\ f_1(x_2, y_2) & f_2(x_2, y_2) & \dots & f_m(x_2, y_2) \\ \dots & \dots & \dots & \dots \\ f_1(x_n, y_n) & f_2(x_n, y_n) & \dots & f_m(x_n, y_n) \end{bmatrix},$$

$$\sigma = \begin{bmatrix} \sigma_1 \\ \sigma_2 \\ \vdots \\ \sigma_m \end{bmatrix}, \quad a = \begin{bmatrix} \Delta g_{\text{obse}}(x_1, y_i) \\ \Delta g_{\text{obse}}(x_2, y_i) \\ \vdots \\ \Delta g_{\text{obse}}(x_n, y_n) \end{bmatrix} = \begin{bmatrix} \Delta g_1 \\ \Delta g_2 \\ \vdots \\ \Delta g_n \end{bmatrix}.$$

We find vector σ from the fully determined system of linear equations

$$K'K\sigma = K'a, \tag{6.6}$$

where K' is the transposed matrix K.

As is evident from what has been said, the calculation process in its detail depends on which elements are used to approximate the geological model. The perturbing bodies are broken down into a sum of straight projections. Here two cases are distinguished, i.e., two-dimensional and three-dimensional geological models.

The Two-Dimensional Case

The geological cross-section is given by selection of straight projections, i.e., four-dimensional vectors with coordinates $\{\sigma_j, h_j, H_j, d_j\}$ (j = 1, 2, ..., m). For a gravitational force anomaly the form of the function $f(x, h_j, H_j, d_j)$ can be determined from formula (3.1). If the calculations are carried out for the V_{xz} horizontal gradient anomaly, then the form of the same function will be established from the formula (3.1a).

The Three-Dimensional Case

The geological model is given by selection of straight projections which are finite in space, i.e., six-dimensional vectors $\{\sigma_j, h_j, H_j, l_{1j}, l_{2j}, d_j\}$ (j = 1, 2, ..., m).

For a gravitational force anomaly the form of function f (x, y, h_j, H_j, l_{1j}, l_{2j}, d_j) can be determined from relationship (4.1). If the calculations are done for anomaly V_{xz}, then the same function can easily be written from formula (4.2). /84

2. Examples of Solving the Problem

We will illustrate the solution to the problem by the following example. Figure 22 shows a geological model constructed on the basis of a fairly detailed study of available geological material and an analysis of the observed field. In the region four geological objects with densities of 2.65; 3.05; 2.87; and 2.76 g/cm^3 have been distinguished. The density of the enclosing rocks is accepted as being equal to 2.71 g/cm^3. The dimensions of each body in space are determined on the basis of a map of the anomalous field. The distribution of the force of gravity was studied on the basis of profiles which were selected over the extent of each object. The configurations of the geological bodies located in the research area are represented as a whole by a sum of steps which are finite in space. In all, 84 steps have been given.

Forty-one points were used to interpret the gravitational force anomaly in the profile. The direct problem has been calculated for the given model. The selection of contours of the perturbing bodies was made according to the method described in the fourth chapter. The results of these calculations are shown in Figure 23. The outlines of the perturbing bodies changed, especially that of the rocks with a density of 2.87 g/cm^3. The horizontal thickness in the section near the surface does not agree with known data. /85

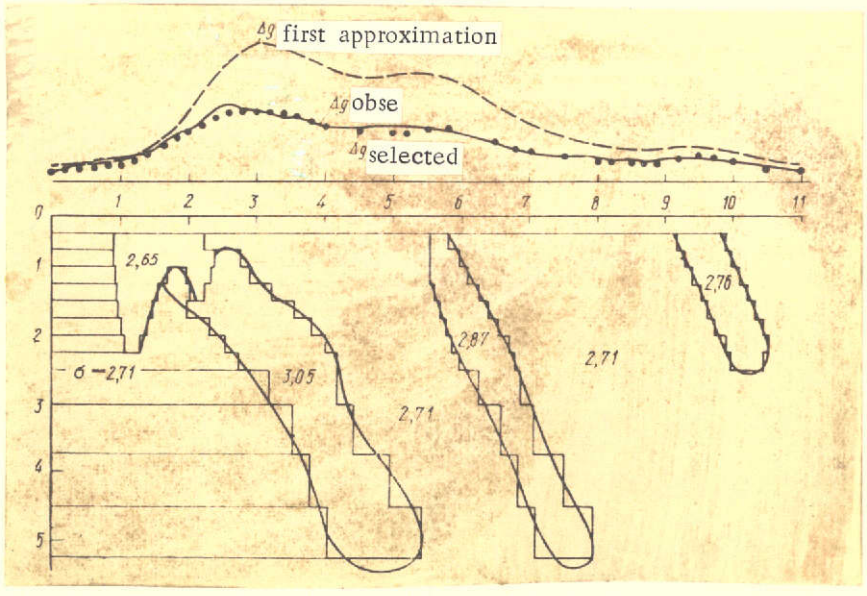

Figure 23. Example of Selecting Contours Without Changing Density Parameters.

We will compare the observed field and the result of solving the direct problem. They basically differ in amplitude, but the left and right asymtotes of the curves are relatively close. This makes it possible to propose that the basic errors in the geological model are caused by density properties.

We will select density characteristics. The new values of the excess densities are shown in Figure 22. As is evident, some of the geological objects are not homogeneous. Thus, in one of the bodies a gradual increase in density is clearly visible the more the depth increases, and in the others individual heterogenous rocks are distinguished. By itself, this material required a geological interpretation. In the same figure (Figure 22) the selected anomaly is shown. It is certain that it differed in detail from the observed anomaly. It is fully understandable that we could not obtain a good agreement between the observed and theoretical curve; after all in this case only individual densities were selected.

Now the results of the calculation will be subjected to analysis. The researcher can restructure the model somewhat, define its parametric value more precisely, and then move on to determining the configurations of the geological bodies according to the method examined earlier. Having assigned the values of the excess densities, we will again select the configuration of the geological objects. The results of the calculations are shown in Figure 24.

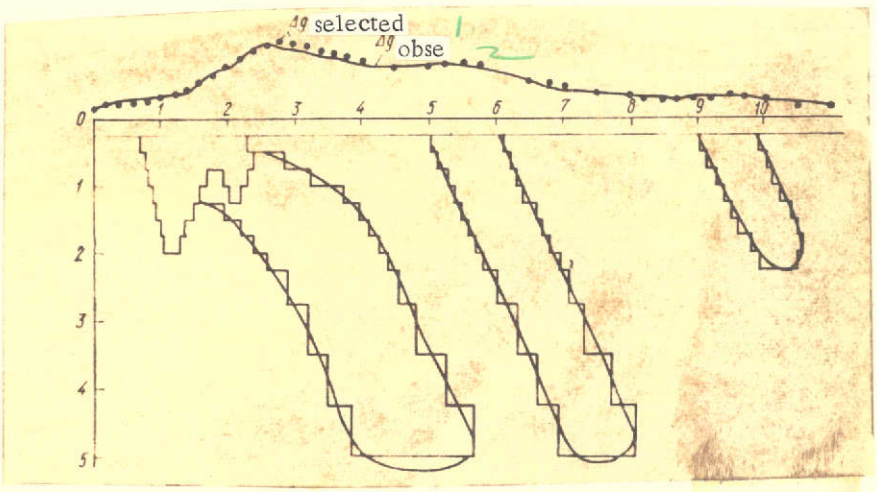

Figure 24. An Example of Selecting Contours With Allowance Made for New Density Parameter Values.

CHAPTER VII

AN AUTOMATED SYSTEM FOR INTERPRETING GRAVITATIONAL ANOMALIES (THE MINIMIZATION METHOD)

1. General Remarks

As is well-known, the inverse problems in gravimetric survey, in their most general form, are associated with incorrect problems in mathematical physics. There are two approaches to solving these problems. One of them is based on special regularizing methods [23, 43, 62-67], while the other approach consists of pre-selecting the class of the solution. All the parameters of the geological features are found in the selected class. Then they can be determined in a uniform manner [62].

Use of the functional minimization method to calculate the elements of the occurrence of geological features ensures adherence to the specific class of the pre-selected problem. This is the only way to regularize the incorrect problem.

The fast descent method used to solve inverse problems is similar, while the calculation method described in the first chapter works only for monotonic convergence.

If, when interpreting a specific anomaly, we proceed from various hypotheses about the geological structure, i.e., in each case the initial geological model is different, then the results of the minimization will naturally also be different.

It would evidently be erroneous to assume that different geological hypotheses for the same anomalous field would lead to different minima of one functional, and that one of these would be global. The fact is that in each case a different function is subject to minimization. In form, these are all the same as (1.2), but in content they depend on the constant parameters not subject to change.

We would like to emphasize that often an unsuccessful solution obtained due to a poor initial approximation will channel the interpreter's thoughts into a new area. In this case a new model of the geological structure is constructed, and one begins again to solve the problem.

2. One Possible Means of Selecting Initial Approximations

When solving the problem, it is necessary to minimize function $F = F(P_1; P_2; \ldots; P_m)$ which depends on m parameters. In order to solve the problem, it

is necessary to select the vector $\{P_j^{(o)}\}$ (j = 1; 2; ...; m). The value of this vector's parameters can be calculated in the following way. For each of the parameters, let its upper and lower limits of possible values $\{p_{jH}^{(o)}\}$ and $\{p_{jB}^{(o)}\}$ be determined. This can be done without any kind of preliminary calculations. The totalities $\{p_{jH}^{(o)}\}$ and $\{p_{jB}^{(o)}\}$ can be regarded as the coordinates of two points in m-dimensional space for the parameters. The straight line L which unites these two points should be drawn through the entire area and be diagonal to it. Therefore, it is natural to search for the points of the null approximation of this straight line. Each point on the straight line has its corresponding value F. It is necessary to select as the point of the null approximation that where $F = F_{min}$. In order to find these points, it is necessary to solve the equation $\frac{\partial F}{\partial l} = 0$ or, in its expanded form

$$\frac{\partial F}{\partial l} = \frac{\partial F}{\partial p_1}\cos\alpha_1 + \frac{\partial F}{\partial p_2}\cos\alpha_2 + \cdots + \frac{\partial F}{\partial p_m}\cos\alpha_m = 0.$$

Here $\alpha_1, \alpha_2, \ldots, \alpha_m$ are the direction cosines of straight line L which are expressed by

$$\cos\alpha_j = \frac{p_{jB}^{(0)} - p_{jH}^{(0)}}{\sqrt{\sum_{j=1}^{m}(p_{jB}^{(0)} - p_{jH}^{(0)})^2}} \quad (j = 1, 2, \ldots, m).$$

Function F along straight line L can be expressed as the function of one parameter l, and for this purpose it is sufficient to establish $p_j = p_{jH}^{(o)} + l\cos\alpha_j$. Now it is possible to find the function's minimum by using the ordinary method.

The sample method may be used to look for the roots of function $f(l) = \frac{\partial F}{\partial l} = 0$. This method, which is well known in mathematical analysis, is based on the fact that the interval (0, L) which is included between the initial point $\{p_{jH}^{(o)}\}$ and the terminal point $\{p_{jB}^{(o)}\}$, is divided into s sections (a_i, b_i) where $a_o = 0$, $b_s = L$, $a_i = b_{i-1}$.

We will find the intervals where $f(a)\cdot f(b) < 0$. We will calculate $\left(\frac{a+b}{2}\right)$. If the numerical value of $\left|f\left(\frac{a+b}{2}\right)\right|$ is sufficiently small, then $l_1 = \frac{a+b}{2}$ is the root of the function. The calculations are finished for this section. The search for the following sections continues. Otherwise, when $f(a)\, f\left(\frac{a+b}{2}\right) < 0$, we examine the interval $\left(a, \frac{a+b}{2}\right)$ and when $f(a)\, f\left(\frac{a+b}{2}\right) > 0$ we examine the interval $\left(\frac{a+b}{2}, b\right)$. It is easy to apply this method on the computer.

When all of the roots of the equation have been found, it is possible to calculate the initial values of the parameters

$$\{p_j\}_{\text{initial}} = \{p_{jH}^{(0)}\} + l_{\text{ext}} \cos \alpha_j.$$

It is obvious that there will be as many initial approximations as there are roots of function F' (l). For each root a value F (l) should be found. The most probable values are those at which F (l) has its smallest value. However, it should be regarded as worthwhile to search for a solution at all values l_{ext}. It is possible to accept as a final variation the one which best satisfies the known data on the geological structure of the region. /88

If the analytic expression of function F is sufficiently complex, then its minimum can be determined by normal tabulation. In order to check the behavior of function F or straight line L and to find the minima points, we will divide a section of the straight line into s equal intervals such that they are sufficiently small that we are confident that the changes in F will be monotonic within the limits of each section. Now it remains for us to calculate the value of function F at the sequential points on the straight line, the coordinates of which are determined thus:

$$\{p_j^{(k)}\} = \{p_j^{(k-1)}\} + \{\Delta p_j\},$$

where $\Delta p_j = \frac{p_{jB}^{(0)} - p_{jH}^{(0)}}{s}$, k is the number of the point, $\{p_j^{(0)}\} = \{p_{jH}^{(0)}\}$. The minima points are determined from the condition

$$F_{k-1} \geqslant F_k < F_{k+1}.$$

Each of these points, and there can be several of them on the same line, is sampled as an initial approximation.

3. The Basic Components of the Automated System

On the basis of what has been said, one can state that in the practice of gravimetric survey work an automated system of processing and interpreting the observed data can be constructed. This system consists of two independent parts. The first part combines the calculations for processing the observation, introducing various correction factors and reduction factors so the anomalous effect can be regarded as caused only by geological heterogeneities. Calculations of field transformation are also associated. The charts of the anomalous field and the various transformations are the final result.

The first part of the automated system has been developed and is being used by many scientific research and industrial organizations.

The second part consists of several sequential stages. It is intended to begin operation after a geological hypothesis has been constructed in the form

of sections of structural models, based on study of the anomalous fields and all information about the geological structure of the region being investigated. In this process a special role is attributed to the planar characteristics of /89
all the various types of rocks included in the model. The preliminary results of the quantative calculations can be used to create a diagram of the initial approximation. One condition is introduced: one must know how to calculate the gravitational effect from the component diagram. For this purpose, the geological structure can be approximated by selecting cylindrical, spherical, or other bodies. In a complex geological situation the perturbing bodies can be approximated by selection of contacts (gravitational steps). For three-dimensional bodies the elements of the geological system can be a projection finite in space. All the components of the automated systems are shown in the block diagram. The initial data are two groups of information. The first includes information about the observed fields, and the second contains information about geological structure (the hypothesis is the first approximation).

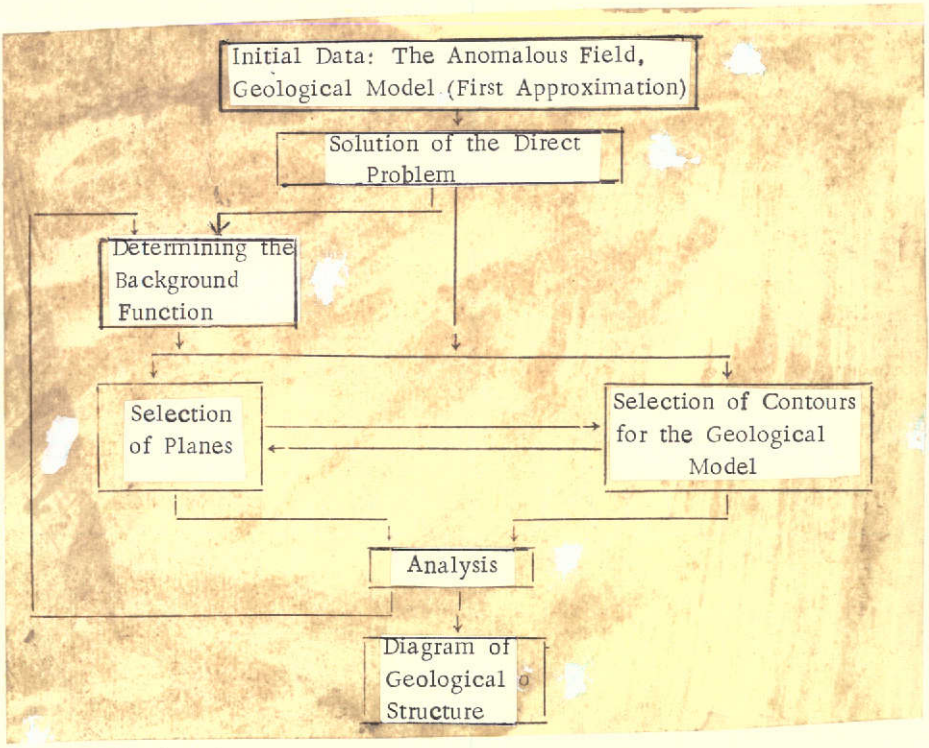

Block Diagram of an Automated System for Interpreting Gravitational Anomalies (The Minimization Method).

The following functional is subject to minimization

$$F = \sum_{i=1}^{n} [V_{\text{obse}}(x_i, y_i) - V_{\text{theo}}(x_i, y_i) - f(x_i, y_i)]^2. \qquad (7.1)$$

At the very beginning V_{theo} (x, y) is calculated, i.e., the direct problem is /90
solved. This intermediate result has an independent value. Comparing the

observed and the calculated fields, the interpreter can introduce into the initial model additions and changes in case there are very large errors. This must be done in such a way that the succeeding stages are directed at automatically solving the problems which can be formulated this way: change the geological model in such a way that the observed and theoretically calculated anomalies coincide as well as possible. It is completely natural that, if there are insufficient data in the geological model, then it is impossible to obtain an effective solution to this problem. We will clarify this with an example. Figure 25 shows a gravitational force anomaly and the geological cross-section of the initial approximation. The investigator considers that the negative gravitational effect is caused by a large block of rock with an excess density of 0.03 g/cm^3. The geological cross-section is approximated by several projections. Comparing the observed and the theoretical curve, we see that a geological body of an increased density has been omitted in the model. It should be introduced, and then one should more precisely define the initial approximation. This same figure shows the result of the automatic selection (the fourth stage of the system) without further definition of the primary model. It is evident from the configurations of the object that there was an attempt to introduce heavy masses within the body. It is impossible to draw the contours with confidence in this case, since the necessary information is lacking.

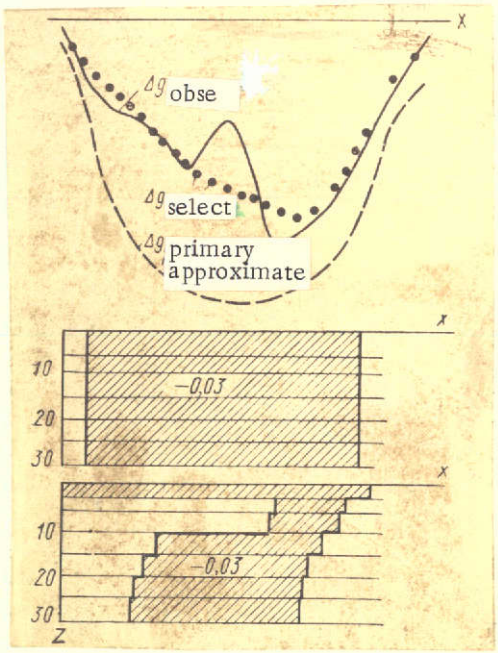

Figure 25. An Example of Selecting the Contours of a Perturbing Body Without Introducing Data About a Heavy Gravitational Body Located Within the Massif.

In the second stage of the automated system, the local components of the field are determined (if this is required). In formula (7.1) all values except the parameters of the background function $f(x_i, y_i)$ have been assigned. It is almost always possible to approximate the local background by using a linear function with the form $A + Bx + Cy$. If there are geological premises, then the form of function $f(x, y)$ can be made more complex. No matter what function we use to approximate the local effect, it is always necessary to thoroughly analyze the calculation results and to give it a geological explanation. In the opposite case some function can be selected as the background function, but its nature will be completely different. Let us examine this using an example. /91

We will assume that no contact has been introduced between two blocks of rock, i.e., a gravitational step has been omitted. Its effect is included in the observed field, but not in the theoretical function. This means that some function which complements this omission will be determined. As a result of the analysis, the interpreter should not make this mistake.

Now the local component is excluded from the observed function. The intrepreter is required to solve the problem of the next step in the calculation. If the differences between the observed and the theoretical anomalies are basically amplitudinal, and if the planar parameters in the geological model have approximated values, then naturally the third stage should be the selection of the planes. The fourth stage will be the selection of the geological model's contours. If the interpreter has decided that the basic differences between the observed field and the calculated field can be explained by an incorrect configuration in the geological model, then the third stage is the selection of contours. Then follows the selection of the planes (if this stage is required).

Finally, the interpreter should analyze all the computation stages. Some stages can be repeated, and their sequence can be changed. If the geological model has undergone significant changes, then it can become necessary to recalculate the background function; after all it was determined for a particular geological structure. Then the calculations can be repeated, i.e., one can do more literations. After each stage the divergence between the iterations is determined, and the interpreter decides whether to continue the calculations.

4. The Results of Sampling the Effectiveness of the Automated System for Interpreting Gravitational Observations When Solving Geological Problems*

The minimization method has been used with success to calculate the block structure of deep sections and surface areas of the Earth's crust, thus defining more precisely the structural peculiarities of the outline of the crystalline bedrock concealed under a thick covering of sedimentary formations. This method also makes it possible to study more in detail the deep differentiated intrusive massifs, and the quantitative characteristics of the formations with their complex sedimentary structure, these formations being characteristic of the geosynclinical and flexible parts of the Earth's core, for map making in difficult regions, and for solving other geological problems.

In the following sections we will cite several examples of determining the quantitative characteristics of geological structures.

Studying the Structural Forms of the Outline of the Crystalline Bedrock /92

The territory on the western incline of the Ukrainian shelf was studied. Structurally, the region is characterized by a two-layer structure. The lower layer is represented by a multifolded complex of Precambrian crystalline rock, among which granitodes of the granodiorite type predominate. The upper layer is characterized by a horizontal or very gently sloping occurrence of sedimentary formations of loess (average density 2.12 g/cm^3) and volcanogenic sedimentary rocks of the Volhynian Series (2.8 g/cm^3). The characteristic features of the gravitational force field which corresponds to the given territory is the presence of unique zone or belt nearly latitudinal in direction and consisting of a

*This section was written in collaboration with V. A. Rzhamitfyniy.

series of relatively isometric positive anomalies of varying intensity. This zone does not appear in a magnetic field. The results of interpreting the data of the resistivity surveying indicate variations in the surface of the crystalline foundation.

Figure 26 shows the geological cross-section of one of the areas in the anomalous zone. The crystalline rocks were investigated to a depth of 30 to 65 meters by drill-holes bored into the center of the anomaly. In the marginal zone the resistivity surveying establishes this type of rock at a depth of 300 - 350 meters. The presence of a strong gravitational force anomaly and a significant fixed value for the density gradient at the boundary between the crystalline and the sedimentary rock makes it possible to determine the parameters of the perturbing feature. In the given case these are the outlines of a projection of the crystalline foundation. The density characteristic of the rock making up the projection were determined by approximation, as was also the average density value of the rocks opened by the drill-holes (2.82 g/cm^3). The approximation model was constructed by using all geological and geophysical data and was presented in the form of a geological cross-section in which the rocks' main characteristic was their density. The body which caused the anomaly was considered to be a three-dimensional object. The isometric form of the anomaly in the map served as the basis for this premise. The direct problem is solved from the model of the first approximation. The anomalous effect obtained in this process was compared with the observed gravitational force anomaly. There exists a considerable disagreement between the anomalies both at their maximum points as well as in the sloping regions. However, the disagreement is very regular, i.e., at every point the calculated anomaly remains below the observed anomaly, i.e., is small in absolute value. This type of discrepancy may be caused by the following factors: either the density of the rocks which make up the projection has decreased or the depth of its occurrence has not been correctly determined. Since the distance to the surface of the foundation was determined on the basis of drilling data and the results of resistivity surveying, it is possible to change the parameters of the projection only within the given depth limits, from 30 to 350 meters. Since the greatest disparity between the /93
calculated and observed anomalies occurred in the zone of the maximum, and since the average value of the rocks' excess densities in the foundation has been determined in approximation, it became necessary to begin solving the inverse problem with automatic selection of the excess densities. As a result of the solution, the excess density of the crystalline rock was found to be 0.74 g/cm^3 as opposed to the 0.70 g/cm^3 adopted in the first approximation model. In this process an insignificant differentiation of the density parameters within the limits of $\pm$ 0.01 g/cm^3 was established on the basis of depth. This can be explained by the lithological peculiarities of the rocks in this region.

From Figure 26 it is evident that the selection of density parameters yielded a satisfactory agreement between the observed and calculated anomalies in the zone of the maximum. The next stage of the automated system makes it possible to solve the problem concerning the configuration of the geological feature. This amounted to automated distribution of the elementary projections /94
within the limits of the assigned depths at the selected density values. As a

result of the selection, almost complete agreement was attained between the gravitational force anomaly calculated from the cross-section selected and the observed anomaly.

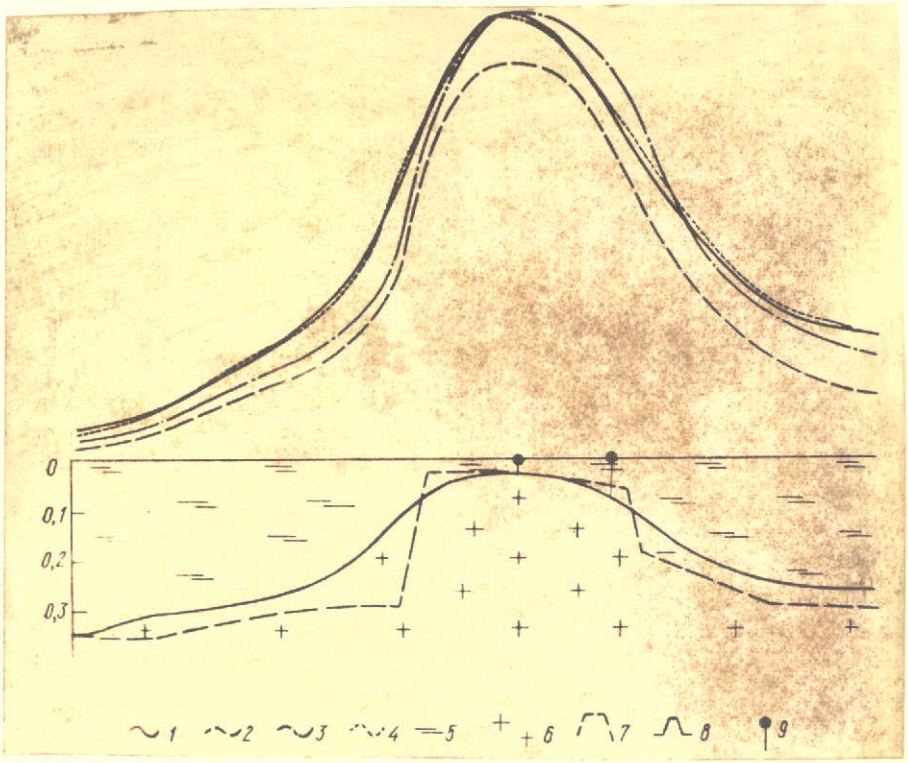

Figure 26. An Example of Selecting Density Parameters and Contours for the Topography of the Crystalline Foundation: 1) Observed Gravitational Force Anomaly; 2) Anomaly Calculated From the First Approximation Model; 3) Anomaly Calculated From Model With Selected Densities; 4) Calculated Anomaly After Selection of Contacts; 5) Sedimentary Deposits; 6) Crystalline Rocks of Projection; 7) Relief of Projection in First Approximation Model; 8) Relief Selected by Computer; 9) Drill Holes.

Among the geological results obtained by use of the minimization method, mention should be made of the differentiated density boundary in the sloping portion of the projection and the gentler slopes themselves in contrast to the sharp, abrupt scarps shown in the first approximation model. The results obtained can be used in future investigations into the nature of the foundation relief.

Figure 27 shows an example of a more complex case of determination of parameters which give a quantitative estimate of the projection of a crystalline foundation. Dense basalt mantles of the Volhynian series which occur in the

form of a stratum with a thickness of approximately 70 meters at a depth of around 70 meters also take part in forming the observed gravitational anomaly. The development boundary between these two formations is clearly fixed in a magnetic field. /95

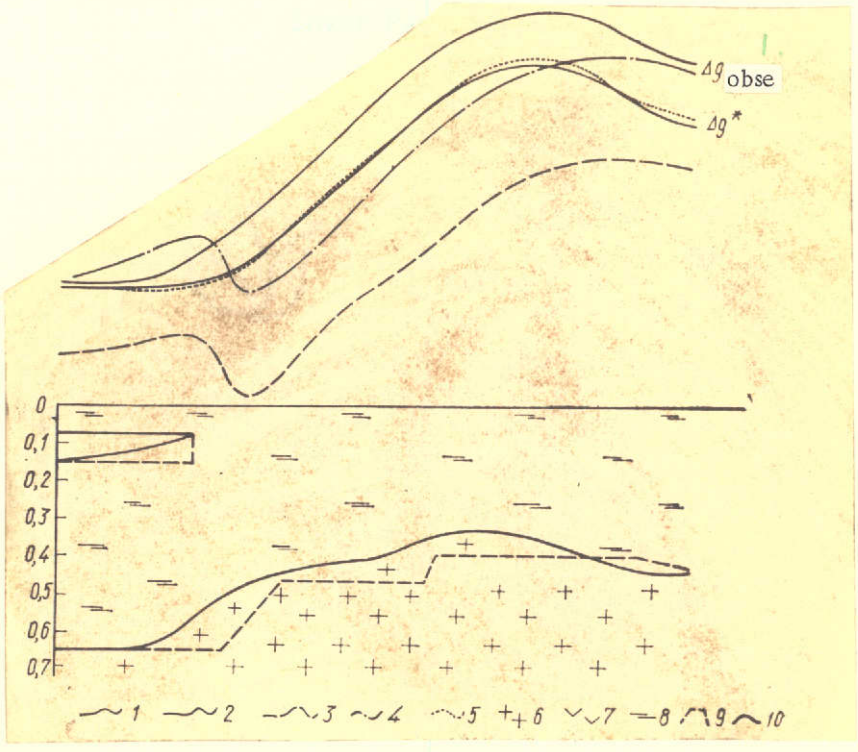

Figure 27. Example of Exclusion of Linear Components of the Regional Background and Selection of Relief Outlines of a Crystalline Foundation: 1) Observed Gravitational Force Anomaly; 2) Observed Anomaly With Allowance Made for the Local Background; 3) Amomaly Calculated From the First Approximation Model; 4) Anomaly Calculated From the Second Approximation Model With Allowance Made for the Local Background; 5) Anomaly Calculated From the Selected Diagram; 6) Crystalline Rock of the Formation; 7) Basalts; 8) Sedimentary Deposits; 9) Outline of Projection in the First Approximation Model; 10) Outline Selected by Computer.

As in the first case, all information about the structure of the region has been used to construct the first approximation model. In solution of the direct problem a considerable divergence was noted between the calculated and the observed anomaly, a divergence reaching 1 mgl in the left part, 4 mgl in the central part, and 3 mgl in the right part of the cross-section. The

difference of 2 mgl may be ascribed to incorrect selection of the level. A 2 mgl difference between the extreme right and left parts of the anomalies being compared (where the effect is felt least of all) can be explained as the influence of a large anomalous mass located far beyond the limits of the given cross-section. This most likely is the effect of an abrupt general movement in the surface of the foundation from right to left. This effect can be included in the general local background, which in the given area can be approximated by the linear function A + Bx. In this process the anomalies being compared are automatically combined at one level. The divergence between them in the central or maximum part can perhaps be explained by insufficient elevation of the central part above the general level of the foundation, or perhaps by the density differential of the rocks which make up the projection in the sketch. Since we had no confirmation of the second premise, it remained possible to reduced the occurrence depth of the highest part of the uplift. This correction was reflected in the second approximation model. The bend in the calculated anomaly was caused by a lack of mass of increased density in the aperture between the basalt mantle and the left slope of the projection. This discrepancy in the anomalous field can be eliminated by increasing the excess mass by moving the projection within the assigned depth limits.

The direct problem is again solved from the augmented geological model. This is done in order to estimate the effects of the corrections been made in the first model. General agreement is noted between the calculated and the observed anomaly. After the parameters of the local background had been determined, the anomalies agreed quite well in configuration (and, what is most important, they agreed in the maximum part); this is evidence of the fact that the occurrence of the anomalous features taken into account were determined correctly. The configurations of the perturbing features were then determined. The results of the selections are shown in Figure 27.

Let us examine one more example. Figure 28 clearly demonstrates the capability of an automated system in interpreting a more complex gravitational force anomaly. Since there was no material available on the geological features which caused the observed anomalies, then, by anology with areas which had been subjected to more extensive study, and which were similar to the territory under investigation, the following concept of the geological structure was evolved. The anomaly is the aggregate effect of a thick tectonic zone made up of cataclastic rocks and causing a broad minimum, as well as of a projection of foundation rock causing a less broad maximum. The anomaly was primarily complicated by the very intense background caused by the general sharp subsidence of the foundation. Figure 28 shows the anomaly already free of the linear component, which was allowed for automatically as in the previous example. /96

A highly simplified model of the geological medium which served as the first approximation model for quantitative calculations was constructed with allowance made for the following circumstances. The depth of the foundation surface, according to resistivity surveying data, is 600 meters. The cataclastic rocks within the limits of the tectonic zones are on the average 0.1 g/cm^3 lighter than the massive rocks, and the massive rocks themselves of the foundation

0.7 g/cm^3 denser than the sedimentary formations. It is evident from Figure 28 that the anomaly calculated from the first approximation model differs considerably in absolute value from the observed anomaly, although it copies it in its general outlines. The solution of the inverse problem by automatic selection of contact points not only has made it possible to achieve good agreement between the anomaly calculated from the selected model and the observed anomaly, but has also made it possible to draw certain geological conclusions. /97 Although the premise which served as the basis for creating the model of the geological structure has not been confirmed by actual geological material, it nevertheless gives us reason to state that the given complex gravitational force field anomaly consisting of a broad minimum and a relatively narrow maximum may most likely be caused by a thick tectonic zone which tends toward large values for the field of gravity. The maximum in this case may be caused by block uplift over the destruction zone or along one of the feather joints. The expansion of the tectonic zone in the upper part of the cross-section may be ascribed to the presence of a thick linear crust deriving from weathering of cataclastic rocks.

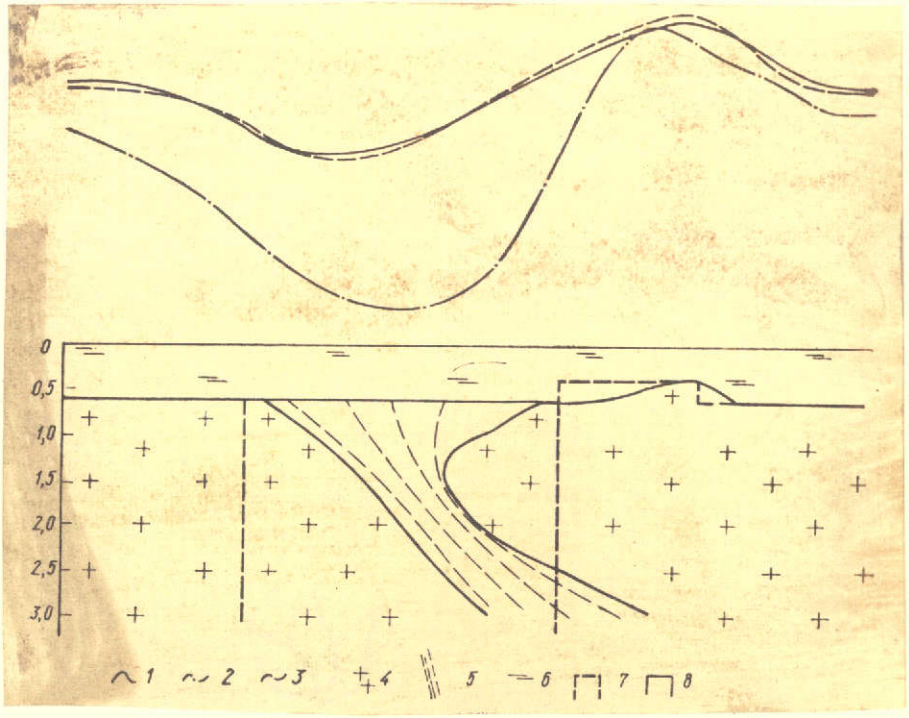

Figure 28. Example of Selection of a Geological Cross-Section in Interpretation of a Gravitational Force Anomaly: 1) Observed Anomaly; 2) Anomaly Calculated From First Approximation Geological Model; 3) Anomaly Calculated From Selected Model; 4) Crystalline Rocks; 5) Zone of the Catclasis; 6) Sedimentary Deposits; 7) Outline of Geological First Approximation Model; 8) Outline of Geological Model Selected by Computer.

Possibilities of Studying Folded Structures

A region was studied within the limits of a territory which was characterized structurally by a two-layer structure. Metamorphic rocks of the gneissic series, as well as granitoids, have taken part in the formation of the lower multifolded layer. The upper layer is represented by cenozoic sedimentary deposits lying horizontally on the waterworn precambrian surface. The basic structural units which characterize the precambrian formation in the territory being investigated are the dome-shaped branchyanticlines. Their cores are made up of biotitic porphyroblastic granites (with a density of 2.63-2.67 g/cm^3). In the other gravitational force field anomalies they are manifested in the form of relative broad gently sloping minima. The dome-shaped structures mentioned are flanked by amphibolous biotitic medium-grained migmatites (2.71-2.72 g/cm^3). The development areas of the latter are characterized by quite intensive (up to 3.0 mgl) maxima in the gravitational force field. Sometimes tectonic contacts are noted between the above-mentioned various types of rock. Of the tectonic dislocations of a local nature, the sublatitudinal ones are considered to be the most recent. They control the movements of the dike complex, i.e., diabases (2.8 g/cm^3). Biotitic gneisses (2.66 g/cm^3) play a significant role in the geological structure of the territory. Intense erosion of the cataclastic rocks has caused the rugged topography of the surface of the crystalline base. In this process significant depressions are traced which are filled by light Cenozoic carboniferous deposits as well as areas where the weather-worn crust has developed to a great depth. These depressions are clearly reflected in the gravitational force field in the form of broad minima.

The presence of a differentiated gravitational force field within the limits of the territory the geological picture of which is characterized by the development of different types of rock differing quite sharply in density characteristics (the average density was determined on the basis of samples from natural outcrops and from the core samples of drill-holes) have allowed us /98
to attempt to analyze the abyssal structure by using quantitative interpretation. A first approximation geological cross-section was constructed for this purpose. In order to create this cross-section, all available factual geological material and the results of qualitative interpretation of geophysical observations were used. The depth of occurrence of the proposed structures was chosen tentatively with allowance made for relative comparison of individual areas of the gravitational force field anomaly along the profile. The entire geological model was converted to a density cross-section. It served as the first link characterizing the correctness of the hypothesis regarding the structural interrelationships among the petrographic types of rock distinguished. With this purpose in mind, the gravitational force anomaly was calculated from the cross-section of the first approximation and was compared with the observed anomaly. The results of this comparison are shown in Figure 29 and indicate that the geological hypothesis may be accepted as a basis. However, certain additions to the first approximation model are still required. Without such correction, it is impossible even in the most tentative approximation to solve the problem of the structural interrelationships of the rocks. In particular, the insufficient amplitude of

the maximum portions of the calculated anomaly indicates that the depth of the main structures made up of dense amphibolous biotitic migmatites is obviously small and should perhaps be increased considerably, possibly even multiplied manifold. This premise has made it possible to increase the depth of the structures to 1.5 - 2 kilometers, i.e., almost fourfold in comparison to the initial cross-section.

The presence of narrow local maxima within the limits of the broad minima which correspond to the depressions and wide cataclastic zones often accompanied by dikes of diabases has made it possible to assume the presence of thin dike-like bodies of dense rocks. Even with a small thickness (on the order of 100 - 200 meters), these bodies could be reflected in the gravitational force field, since they are of considerable size and should be detected in the form of relief projections within the limits of the depressions as younger and denser formations. In addition, as research has shown, the dike formations within the limits of the region are usually characterized by a branchlike arrangement of several thin bodies, and this makes it easier to detect them in a gravimetric survey.

Thus, in the revised cross-section several thin dike bodies are distinguished which are similar to the one reflected in the cross-section of the first approximation.

The presence of two relatively intense local minima within the limits of the maximum which formed by the structure of the left half of the cross-section has made it possible to increase the development depth of the body of cataclastic biotitic gneisses reflected in the cross-section of the first approximation, and has also made it possible to assume the presence of a body of the same rock, but of smaller dimensions, in the zone of the minimum near the left edge of the cross-section.

Within the limits of the tectonic contacts, which are characterized by /99
zones of cataclasis, the form of their minima and their intensity have indicated a somewhat lesser thickness of the largest zone and at the same time a great depth of development of the cataclastic rock. The intense gradient in the extreme right part of the cross-section indicates a steeper occurrence of tectonic contact and a corresponding increase in the depth of the migmatite structure at this end of the cross-section.

The depth of occurrence of the foundation is very small (10 - 60 meters), while the difference between the crystalline and the sedimentary rocks reaches 0.92 g/cm^3. Even insignificant variations in the topography of the foundation are sharply reflected in the gravitational force field. Therefore, determining refinement of the parameters of the depressions was a very important task. /100
Solving this problem was made easier by the fact that in a number of cases the rock mass had been drilled through. The corresponding data were taken into account on introduction of additions and revisions into the initial model. Because of the small thickness of the sedimentary deposits, the topography of the crystalline foundation is shown on a scale which exceeds by a factor of 10 the vertical scale of the crystalline rock structures. These and other revisions

are reflected in the second approximation model (Figure 29). In order to estimate the effect of the correction factors introduced, the direct problem was again solved on the basis of the geological second approximation model. Comparison of the observed and calculated anomalies revealed relatively good agreement between their configurations, especially in the extreme portions of the force of gravity curve. This indicates that the correction factors were proper.

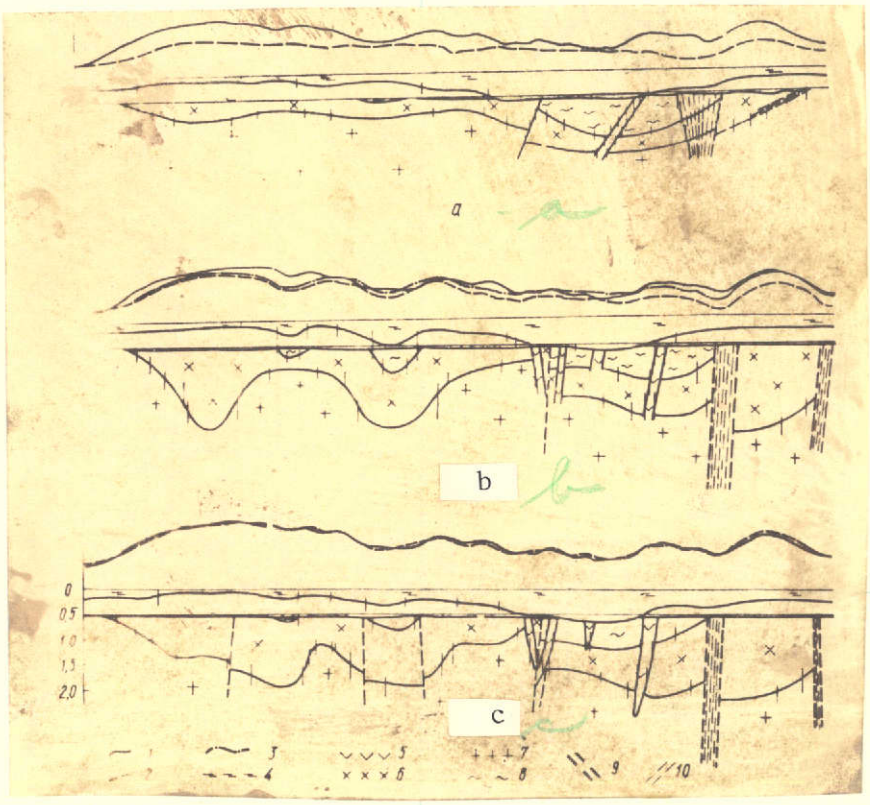

Figure 29. Geological First Approximation Model (a), Geological Model Modified After Solution of Direct Problem (b), and Geological Model Selected by Computer (c): 1) Observed Gravitational Force Anomaly; 2) Anomaly Calculated From Density Cross-Section; 3) Anomaly From the Calculated Cross-Section With Allowance Made for the Locak Background; 4) Cenozoic Deposits; 5) Gabbro-Diabases; 6) Amphibolous Biotitic Migmitates; 7) Biotitic Granites; 8) Biotitic Gneisses; 9) Cataclasites; 10) Tectonic Contacts.

Along with the agreement mentioned above between the configurations of the anomalies being compared, a divergence is noted in their absolute value, one which increases gradually from left to right along the relief. In the extreme right portion this divergence reaches 1 mgl. It is impossible to explain this by the geological peculiarities of the rock, since the same granites with a

density of 2.63 g/cm^3 are detected both in the left and the right portions of the cross-section. Therefore, this divergence can only be explained by the influence of anomalous features which are either located far beyond the limits of the area or which occur at a greater depth. This effect can be calculated in the form of linear function A + Bx, which is the local background for a given territory. When making quantitative calculations, it is absolutely necessary to make allowance for the effects of the local background. After allowance has been made for the local background, the calculated anomaly assumed another form and exhibited much better agreement with the observed anomaly.

The last stage of the construction was solution of the inverse problem. The elementary projections characterizing contacts between rocks of different densities were arranged in a pattern permitting the best possible approximation of the anomaly calculated from the selected cross-section to the observed anomaly. The results of solution of the inverse problem are shown in Figure 29. As we see, within the limits of the possible measurement error, the agreement between the anomalies is sufficiently good. However, it can be found immediately that in some cases a discrepancy is caused by insufficiency of the geological information taken into account in setting up the geological cross-section of the first and second approximations. This applies principally to the minor details of the cross-section. The large features are characterized quite clearly.

Even with insignificant initial information about the geological structure and with few details about the anomaly as concerns its profile, the system has made it possible to obtain good results for all the questions examined.

Geological Mapping of Complex Regions /101

We will examine a small area within the limits of the Central Bug River Valley. A large amount of factual geological and geophysical material was collected. The initial data for the selection were the observed gravitational force anomaly and the primary geological cross-section containing the density characteristics of all the various types of rocks. The calculation was carried out by use of a system of parallel profiles intersecting the basic geological structures of the region, and also by using small profiles within the limits of the individual structures. This distribution of profiles makes it possible to correlate spatially both the larger structures and the individual extended bodies. In the area under study there are geological features the configurations of which have been fairly well studied by geological and geophysical methods. In this case the dimensions of the bodies were assigned in advance and could not change during subsequent calculations. Individual areas of the Tarnovatskiy syncline which has been drilled in detail can serve as an example. The syncline is filled with rocks of the metabasite and ultrabasite complex, and these rocks differ sharply in their physical properties from the relatively monotonic mass of mignatites. The latter are more common in the region in question and serve as a kind of intrusive mass for all the other rock complexes. After the direct problem had been solved on the basis of the initial geological cross-section, the various items of supplemental information and corrections were introduced into the model. The amount of work required by this stage depends completely on the reliability of the initial geological model.

Figure 30 shows a diagram of the geological structure of one of the areas in the region being investigated. The Tarnovatskiy syncline is clearly to be distinguished. In the northern parts it is a shallow (150-200 meters) fold with a very gently sloping of the limbs. To the south one observes subsidence of the fold bend to a depth of 600 meters and more, while the width of the structure simultaneously decreases. This causes gradual increase in the steepness of the fold limbs until inverted rock bedding is formed in the eastern limb. The structure is made up of dense (σ = 3.04 g/cm^3) rocks of the metabasite complex, but to the south strata of amphiolous gneisses (density 2.9 g/cm^3) are included in its structure. Small bodies of serpentinites (density 2.46 g/cm^3) are clearly fixed. They cause local minima in the zones of the gravitational force maxima. These maxima are caused by the dense rocks of the productive stratum. On analyzing the gravitational force field, we found a basis for assuming the presence of several small serpentinite bodies in the shallow synclinal folds to the west of the Tarnovatskiy syncline.

It has been established that the bodies of the serpentinites and the serpentinous ultrabasites coincide in space with the metabasite massifs and normally comprise small concordant massifs of slight thickness. Relatively large areas of individual bodies on the map within the limits of the Tarnovatskiy, Kapitanovskiy, and Derenyukhinskiy [Translator's Note: as Transliterated] synclines are caused by the very gentle slope of the rock strata within the limits of these structures. /102

Thus it has been possible to distinguish within the plan and to observe to significant depth a considerable number of large and small folded structures, as well as a large number of individual extended bodies which take part in the formation of the folds.

Small geological bodies are distinguished in the region in question. They are made up of very dense and highly magnetic rocks of the skarn type which, judging from the results of geological studies, are confined to the contact zones between rocks of the metabasite and hyperbasite complexes and the granites. In rare cases the thickness of these bodies reaches 100 meters over a considerable extent. Their formation should probably be associated with the intensive introduction of free magnetite into the active contact zone.

Even in the areas where the gravitational force anomaly is little differentiated above anticlinal structures, it is possible to determine the spatial position of individual bodies of dense rock which are included in the structural formation. The geological charts and diagrams known up to the present have shown large massifs of charnockites in the nuclear portions of these structures, the presence of which explains the high background (up to 1000 γ) and the mosaic character of the magnetic field. There are no charmockites in our massif construction, and the nature of the magnetic field is explained by the complicated structure of these regions, within the limits of which considerable saturation is noted by small bodies of dense, intensively magnetic rock such as amphibolites, pyroxenes, amphibolous and biotitic gneisses, charnockites, and pink magnetoactive fine-grained granites. The high magnetic intensity of the rocks

mentioned is caused primarily by their considerable (from 1 to 3%) content of free finely dispersed magnetite. This mineral is observed in microsections. The rocks which make up the small bodies within the limits of the anticlines are characterized primarily by the presence of free magnetite. These same rocks in synclinal structures are manifested as practially non-magnetic ones.

It is probable that the singling out of free magnetite is caused by the higher level of granitization of the rocks of the lower structural level. Xenoliths of these rocks have a periclinal closure on relatively sharp (60-70°) drop from the center. This has served as the basis for distinguishing these structures as anticlines or dome-shaped elevations. In our constructions they represent formations in the lower structural stage in the form of hard blocks, to which the development of linear folding by the rock in the upper structural level is subject.

In order to map the rocks correctly, one must know the tectonic structure of the region under investigation. The fracture tectonics, in causing the block-like structure of the region, create a unique regional background for the small structures in the uppermost layer of the Earth's crust, and these small structures determine the intensive differentiation of the observed gravitational force field. The exclusion of or allowance for this background makes it possible /104 to carry out quantitative interpretation of anomalies properly both for individual profiles and for the overall map. In the region under investigation, the border of the large blocks, which differ insignificantly in density, are clearly to be seen. These tectonic contacts of the fault type are traced to a considerable degree in extent and in depth.

The structural tectonic map of the region is predetermined by the presence of two systems of tectonic distortion, a northwestern and a northeastern one, of which the first exerts a more significant influence on the formation of the small-block nature of the region's precambrian formations. In this process a scalariform elevation (of the horst type) is noted in the central part of the rigid blocks. It is possible that these elevations cause the formation of the gently sloping folds made up of rocks of the gneissic mass. It should be noted that not only are the folding of the rocks in the upper structural levels subordinate to the contours of the rigid blocks; the tectonic distortions also exhibit a tendency to bend around the central portions of these blocks.

It is quite typical that the elevated blocks consist of lighter rocks. These block movements have affected chiefly the structure of the intrusive rock mass, which is represented by monotonic migmatites with numerous xenoliths of denser rocks. Therefore, it is possible to draw the conclusion that with depth the density of the rock of the intrusive rock mass decreases to a certain limit. This pattern can be explained by the higher degree of granitization, and accordingly by the decrease in the number of xenoliths in the dense rock. It is probably this that explains the considerable variations in the density of the migmatites (2.51 - 2.67 g/cm^3).

The examples cited above show the effectiveness of using the minimization method when solving problems in structural geology in various situations and under various conditions of information coverage. It is natural that the more

the area is studied from the geological viewpoint, and the more reliable is the first approximation model, the more effective will be the use of an automated system. However, even with the most scanty geological information, the system makes it possible from the quantatitive point of view to estimate the reliability of any assumption and to select the optimum geological model from among many optional versions. This latter factor can serve as a starting point for bringing geological investigations up to date.

Conclusion

/105

In this work several questions relation to application of the minimization method to interpret gravitational anomalies have been examined. A fairly complete automated system of interpretation has been obtained: estimation of the initial version of the hypothetical geological model, selection of the background function, refinement of the density parameters, and refinement of the configurations of geological features. Over a period of several years this method has been tested with a variety of examples. Good results have always been obtained. It may be noted that on occasion, when the geological first approximation model was very incomplete, results were obtained which contradicted the geological premises. An analysis of this solution has always enabled the interpreter to restructure his hypothetical model properly and to overcome any contradictions which have occurred.

The same method can be used to create an automated system for interpreting magnetic anomalies [50]. Of course, the methods described can be used most effectively in cases in which the boundaries of the perturbing bodies form steep contacts.

Lastly, the system described can be considered as a subsystem of a more general system which would include other calculation methods.

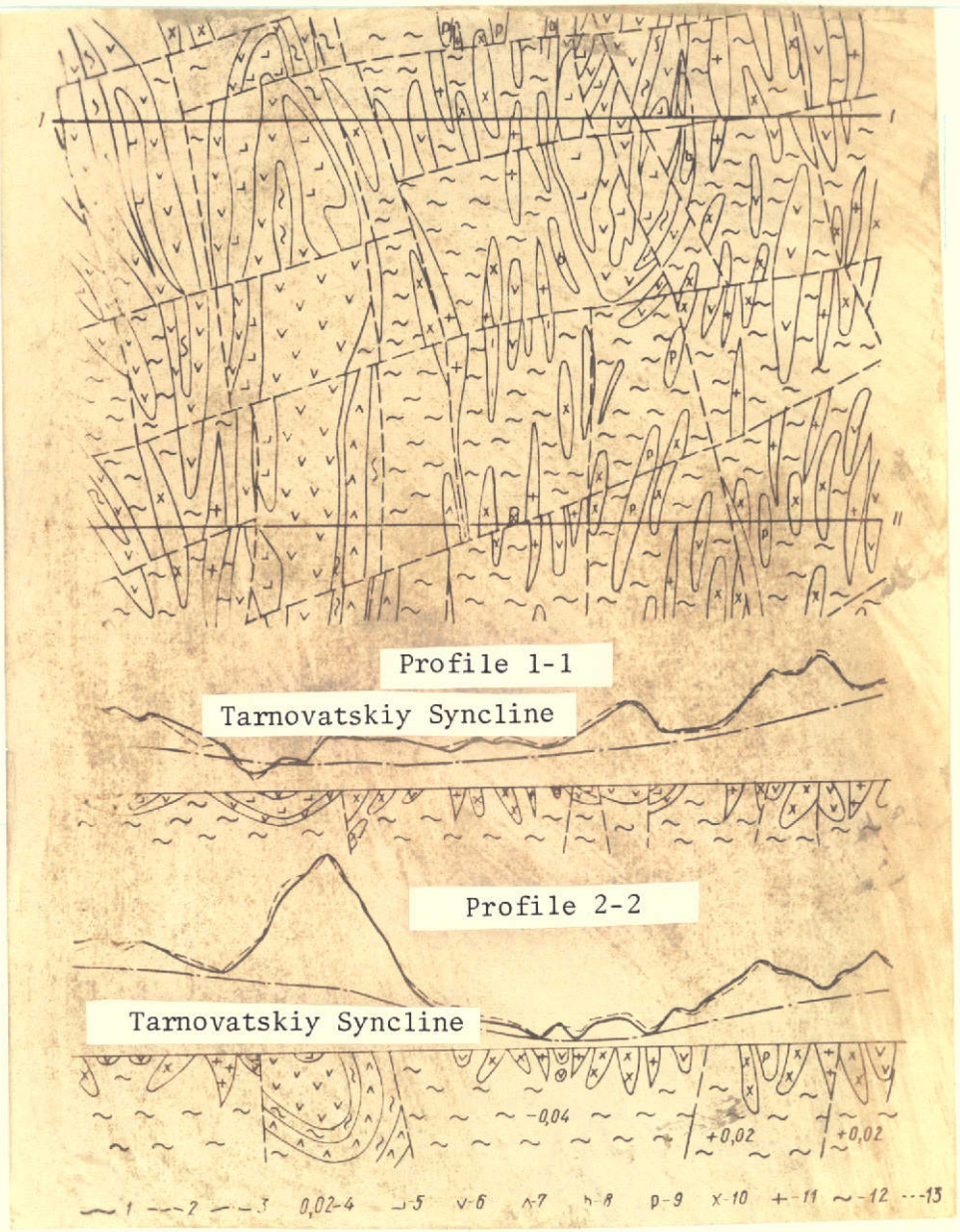

Figure 30. Geological Model and Cross-Sections of One of the Areas in the Central Bug River Valley: 1) Observed Gravitational Force Anomaly, 2) Anomaly Calculated From Selected Cross-Section, 3) Anomaly Due to Fracture Tectonics, 4) Excess Density Value, 5) Serpentinites, 6) Amphibolites, 7) Amphibolous Gneisses, 8) Biotitic Gneisses, 9) Pyroxenite Gneisses, 10) Charnockites, 11) Granites, 12) Migmatites, 13) Tectonic Distortions.

REFERENCES

1. Alekseyev, A. S. and M. M. Lavrent'yev, In the book: *Matematicheskiye Problemy Geofiziki* [Mathematical Problems of Geophysics], No. 1, Siberian Branch, Academy of Sciences USSR Press, Novosibirsk, 1969.
2. Aleksidze, M. A., *Reduktsiya Sily Tyazhesti* [Reduction of the Force of Gravity], "Metsniyereba" Press, Tbilisi, 1965.
3. Andreyev, B. A. and I. G. Klushin, *Geologicheskoye Istolkovaniye Gravitatsionnykh Anomaliy* [Geological Interpretation of Gravitational Anomalies], Gostoptekhizdat, Leningrad, 1962.
4. Aronov, V. I., In the book: *Geofiz. Razvedka* [Geophysical Prospecting], Issue 6, "Nedra" Press, Moscow, 1961.
5. Aronov, V. I. and I. B. Konoval'tsev, *Izvestiya Vuvoz, Geologiya i Razvedka*, No. 10, 1963.
6. Balavadze, B. K., *Gravitatsionnoye Pole i Stroyeniye Zemnoy Kory v Gruzii* [The Gravitational Field and the Structure of the Earth's Crust in Georgia], Georgian SSR Publishing House, Tbilisi, 1957.
7. Bas, R. G., et al., *Geofiz. SB. AN USSR* [Geophysical Collection of the AN USSR], Issue 38, 1970.
8. Berezhnaya, L. T. and M. A. Telepin, In the book: *Prikladnaya Geofizika* [Applied Geophysics], Issue 46, "Nedra" Press, Moscow, 1965.
9. Berezhnaya, L. T. and M. A. Telepin, In the book: *Razvedochnaya Geofizika* [Survey Geophysics], Issue 16, "Nedra" Press, Moscow, 1966.
10. Berezin, I. S. and M. P. Zhidkov, *Metody Vychisleniy* [Calculation Methods], Vol. 1-2, "Fitmatgiz" Press, Moscow, 1959.
11. Bondarenko, B. V. and D. N. Kravchuk, *DAN BSSR*, Vol. IV, No. 12, 1960.
12. Bondarenko, B. V., *Trudy In-ta Geol. Nauk* [Transactions of the Institute of Geological Sciences], AN BSSR, Issue 3, 1961.
13. Budak, B. M. and F. P. Vasil'yev, *Priblizhennyye Metody Resheniya Zadach Optimal'nogo Upravleniya* [Approximation Methods for Solving the Problems of the Optimum Equation], No. 11, Moscow State University Press, 1969.
14. Bulakh, Ye. G., *Integral'nye Sootnosheniya Dlya Interpretatsii Gravitatsionnykh Anomaliy* [Integral Relationship for Interpreting Gravitational Anomalies], "Naukova Dumka" Press, Kiev, 1965.
15. Bulakh, Ye. G. and M. N. Markova, *Metodicheskoye Rukovodstvo i Sbornik Programm Dlya Resheniya Obratnykh Zadach Gravirazvedki na ETsVM Minsk-22* [Methodological Direction and Summary of Programs for Solving Inverse Problems of Gravitational Prospecting on the Minsk-22 Computer], "Naukova Dumka" Press, Kiev, 1971.
16. Bulakh, Ye. G., et al., *Metodicheskoye Rukovodstvo i Sbornik Programm Dlya Resheniya Pryamykh Zadach Gravirazvedki Na EVM Minsk-22* [Methodological Control and Correction of Programs for Solving the Direct Problem of Gravitational Prospecting on the Minsk-22 Computer], "Naukova Dumka" Press, Kiev, 1971.
17. Veselov, K. Ye. and M. U. Sagitov, *Gravimetricheskaya Razvedka* [Gravimetric Surveying], "Nedra" Press, Moscow, 1968.

18. Volodarskiy, R. S., et al., *Primeneniye Elektronno-schetnykh Mashin Dlya Interpretatsii Gravitatsionnykh i Magnitnykh Poley* [The Use of Computers to Interpret Gravitational and Magnetic Fields], Gostoptekhizdat, Moscow, 1962.
19. Voladarskiy, R. F. and T. I. Landa, *Geologicheskaya Interpretatsiya Gravitatsionnykh i Magnitnykh Poley s Pomoshch'yu EVM* [The Geological Interpretation of Gravitational and Magnetic Fields Using Computers], "Nedra" Press, Moscow, 1970.
20. Gol'tsman, F. M., *Statisticheskiye Modeli Interpretatsii* [Statistical Interpretation Models], "Nauka" Press, Moscow, 1971.
21. Zhuravlev, I. A., *DAN USSR*, Series B, No. 10, 1970.
22. Zaguskin, V. L., *Spravochnik Po Chislennym Metodam Resheniya Uravneniy* [Guide to the Numerical Method of Solving Equations], "Fitmatgiz" Press, Moscow, 1960.
23. Zukhovitskiy, S. I. and L. I. Avdeyeva, *Lineynoye i Vypukloye Programmirovaniye* [Linear and Convex Programming], "Nauka" Press, Moscow, 1967.
24. Ivanov, V. K., *Mat. sb.*, Vol. 61, No. 2, 1963.
25. Ivanov, V. V., *DAN SSR*, Vol. 143, No. 4, 1962.
26. Igumnov, S. A. and A. M. Glyuzman, *Izvestiya Vuvoz, Geologiya i Razvedka*, No. 9, 1962. /107
27. Il'in, V. A. and E. G. Poznyak, *Osnovy Matematicheskogo Analiza* [The Bases of Mathematical Analysis], "Nauka" Press, No. 1, Moscow, 1971.
28. Kadyrov, I. N., I. V. Bocharov and L. L. Lyakhov, *Izvestiya Vuvoz, Geologiya i Razvedka*, No. 11, 1966.
29. Kagan, B. N., in the book: *Primeneniye Vychislitel'noy Tekhniki Dlya Avtomatizatsii Proizvodstva* [The Use of Computer Technology to Automate Production], "Mashgiz" Press, Moscow, 1971.
30. Kalinina, T. V. and F. M. Gol'tsman, in the book: *Prikladnaya Geofizika* [Applied Geophysics], "Nedra" Press, No. 28, Moscow, 1960.
31. Kantorovich, L. V., *Sib. Mat. Zhrn.*, Vol. 3, No. 5, 1962.
32. Karatayev, G. N., et al., *Trudy IGiG SOAN SSSR* [Papers of the Institute of Geology and Geography, Siberian Branch, Academy of Sciences USSR], No. 21, 1963.
33. Karatayev, G. N., *Korrelyatsionnaya Skhema Geologicheskoy Interpretatsii Gravitatsionnykh i Magnitnykh Anomaliy* [A Correlation Diagram for the Geological Interpretation of Gravitational and Magnetic Anomalies], "Nauka" Press, Novosibirsk, 1966.
34. Kartvelishvili, K. M., *Izv. AN SSSR, Seriya Geofiz.*, No. 8, 1964.
35. Konstantinov, G. N., *Geol. i Geofiz.* [Geology and Geophysics, No. 8, 1968.
36. Korneychuk, A. A., O. K. Litvinenko and Yu. M. Kryzhanovskiy, *Byull. NTI VIEMS*, No. 1, Page 54, 1965.
37. Kravtsov, G. G., S. V. Shalayev and V. A. Dyadyura, in the book: *Voprosy Razved Geofie* [Questions of Geophysical Surveying], No. 3, "Nedra" Press, Moscow, 1968.
38. Kudrya, A. V., V. O. Sergeev and Yu. A. Chernyshov, in the book: *Mat. Problemy Geofiziki* [Mathematical Problems of Geophysics], No. 1, Novosibirsk, 1969.
39. Klushin, I. G. and Yu. I. Nikol'skiy, in the book: *Prikladnaya Geofizika* [Applied Geophysics], "Nedra" Press, No. 22, Moscow, 1959.

40. Koval', L. A., *Izv. AN Kaz SSR, Seriya Geol.*, No. 5 (50), 1962.
41. Kolmogorova, P. P., *Geol. i Geofiz.*, No. 4, 1962.
42. Kuz'min, Yu. I., "Several Questions of the Method of Interpreting a Gravitational Field While Studying the Geological Structure of Kazakhstan", *Synopsis of Candidate's Thesis*, 1969.
43. Lavrent'ev, M. M., *O Nekotorykh Nekorrektnykh Zadachakh Matematicheskoy Fiziki* [Several Incorrect Problems of Mathematical Physics], Siberian Branch, Academy of Sciences USSR, Novosibirsk, 1962.
44. Lavrent'ev, M. M. and V. G. Vasil'ev, *Sib. Mat. Zhurn.*, Vol. 7, No. 3, 1966.
45. Lantsosh, K., *Prakticheskiye Metody Prikladnogo Analiza* [Practical Methods of Applied Analysis], "Fitmatgiz" Press, Moscow, 1961.
46. Litvinenko, O. K., in the book: *Prikladnaya Geofizika* [Applied Geophysics], "Nedra" Press, No. 25, Moscow, 1960.
47. Litvinenko, O. K., In the book: *Razved. i Promysl. Geofizika* [Surveying Industrial Geophysics], "Nedra" Press, No. 37, Moscow, 1960.
48. Litvinenko, O. K. and V. A. Makarov, in the book: *Prikladnaya Geofizika* [Applied Geophysics], "Nedra" Press, No. 33, Moscow, 1962.
49. Litvinenko, O. K., et al., *Primeneniye Elektronnykh Tsifrovykh Vychislitel'nykh Mashin v Gravirazvedke* [The Use of Computers in Gravitational Prospecting], ONTI - VIEMS, No. 46, Moscow, 1970.
50. Loginov, V. E., "Methods for Interpreting Magnetic Anomalies on Computers Using the Collection Method", *Synopsis of Candidate's Thesis*, Kiev, 1970.
51. Lomtadze, V. V., *Geol. i Geofiz.*, No. 8, 1966.
52. Lomtadze, V. V., in the book: *Voprosy Razved. Geofiz.* [Questions of Surveying Geophysics], "Nedra" Press, No. 6, Moscow, 1967.
53. Lomtadze, V. V., in the book: *Voprosy Razved. Geofiz.* [Questions of Surveying Geophysics], "Nedra" Press, No. 8, Moscow, 1968.
54. Luk'yanova, N. N., *Geol. i Geofiz.*, No. 4, 1962.
55. Malovichko, A. K., *Metody Analitich. Prodolzheniya Anomaliy Sily Tyazhesti i ikh Primeneniya k Zadacham Gravirazvedki* [Method of Analytical Continuation of Gravitational Force Anomalies and Their Use for the Problems of Gravitational Prospecting], Gostoptekhizdat, Moscow, 1956.
56. Malovichko, A. V., *Osnovnoy Kurs Gravirazvedki*. Perm University Press, No. 1, 1966; No. 2, 1968.
56a. Nepomnyashchikh, A. A., in the book: *Geologiya, Gornoye Delo, Metallurgiya* [Geology, Mining, and Metalurgy], Metallurgizat, No. 13, Moscow, 1956.
57. Nikitskiy, V. E., *Byull. NTI MG ON SSSR*, No. 5-6, Pages 39-40, 1962.
58. Savenko, S. S., in the book: *Primeneniye Mat. Metodov i Vychisl. Tekhniki v Gornom Dele.* [Use of Mathematical Methods and Computer Technology in Mining], "Nedra" Press, Moscow, 1965.
59. Strakhov, V. M., *Izv. AN SSSR, Seriya Geofiz.*, Pages I-III, No. 3-4, 1962. /108
60. Strakhov, V. M., *Izv. AN SSSR, Seriya Geofiz.*, No. 1, 1961.
61. Strakhov, V. M., *Izv. AN SSSR, Seriya Geofiz.*, No. 4, 1964.
62. Tikhonov, A. N., *DAN SSSR*, Vol. 39, No. 5, 1943.
63. Tikhonov, A. N., *DAN SSSR*, Vol. 151, No. 3, 1963.
64. Tikhonov, A. N., *DAN SSSR*, Vol. 153, No. 1, 1963.
65. Tikhonov, A. N. and V. B. Glasko, *Vych. Mat. i Mat. Fizika*, Vol. 5, No. 3, 1965.
66. Tikhonov, A. N., in the book: *Vychislitel'nyye Metody i Programmirovanie* [Computer Methods and Programming], No. 8, MGU Press, 1967.

67. Tikhonov, A. N., V. B. Glasko and O. K. Litvinenko, *Izv. AN SSSR. Fizika Zemli*, No. 12, 1968.
68. Tyapkin, K. S. and G. Ya. Golizdra, *Kratkiy Obzor Sovremennykh Metodov Oslableniya Regional'nogo Fona Gravitatsionnogo i Magnitnogo Poley* [A Short Summary of Modern Methods for Weakening the Local Background of Gravitational and Magnetic Fields], ONTI Gosgeolkoma SSSR, Moscow, 1963.
69. Uspenskiy, D. G., In the book: *Voprosy Razvedochnoy Geofiziki* [Questions of Surveying Geophysics], "Nedra" Press, Moscow, 1964.
70. Uspenskiy, D. G., *Gravirazvedka* [Gravitational Prospecting], "Nedra" Press, Moscow, 1968.
71. Fedynskiy, V. V., *Trudy IV Mezhdunarodn. Neftyanogo Kongressa* [Works of the IV International Petroleum Congress], 2, 1956.
72. Fedynskiy, V. V., *Razvedochnaya Geofizika* [Surveying Geophysics], "Nedra" Press, Moscow, 1964.
73. Khammer, Z., *Trudy IV Mezhdunarodn. Neftyanogo Kongressa* [Works of the IV International Petroleum Congress], 2, 1956.
74. Shalayev, S. V., *DAN SSSR*, Vol. 117, No. 3, 1957.
75. Shalayev, S. V., In the book: *Prikladnaya Geofizika* [Applied Geophysics], "Nedra" Press, No. 31, Moscow, 1961.
76. Shalayev, S. V., in the book: *Prikladnaya Geofizika* [Applied Geophysics], "Nedra" Press, No. 33, Moscow, 1962.
77. Shalayev, S. V., *Zap. Leningradsk. Gorn. In-ta*, Vol. 46, No. 2, 1963.
78. Shalayev, S. V., *Zap. Leningradsk. Gorn. In-ta*, Vol. 50, No. 2, 1966.
79. Shreyder, Yu. A., In the book: *Voprosy Teorii Matematicheskikh Mashin* [Questions of Computer Theory], "Fizmatgiz Press, No. 1, Moscow, 1958.
80. Yun'kov, A. A. and Ye. G. Bulakh, "Papers of the Institute of Geological Sciences", *Seriya Geofiz* [Geophysics Theories], AN USSR, Edition 2, 1958.
81. Yun'kov, A. A., In the book: *Geofizicheskaya Razvedka* [Geophysical Surveying], Gostoptekhizdat, No. 3, Moscow, 1961.
82. Yun'kov, A. A., M. L. Afanas'ev and N. A. Fedorova, *Interpretatsiya Anomaliy* V_{Δ}, V_{zz} *i Z Nad Kontaktami i Sbrosami* [Interpretation of the Anomalies V_{Δ}, V_{zz} and Z Over Contacts and Faults], Gosgeoltekhizdat, Moscow, 1961.
83. Yun'kov, A. A., M. L. Afanas'yev and N. A. Fedorova, *Interpretatsiya Anomaliy* V_{xz} *i N Nad Kontaktami i Sbrosami* [Interpretation of the Anomalies V_{xz} and H Over Contacts and Faults], Gosgeoltekhizdat, Moscow, 1961.
84. Yun'kov, A. A., *Interpretatsiya Magnitnykh i Gravitatsionnykh Anomaliy Nad Kupoloobraznymi Strukturami* [Interpreting Magnetic and Gravitational Anomalies Over Dome-Shaped Structures], Gosgeoltekhizdat, Moscow, 1962.
85. Baranov, V., *Rev. Inst. franc. petrole*, Vol. 17, No. 4, 1962.
86. Bott, M. H. P., *Geophys. prospecting*, Vol. 7, No. 1, 1957.
87. Bott, M. H. P., *Geophys. J. R. Astron. Soc.*, Vol. 3, No. 1, 1960.
88. Bott, M. H. P., *Geophys. prospecting*, Vol. 11, No. 3, 1963.
89. Bott, M. H. P., *Geophys. J. R. Astron. Soc.*, Vol. 13, 1967.
90. Corbato, C. E., *Geophys.*, Vol. 30, No. 2, 1965.
91. Cordel, L. and R. Henderson, *Geophys*, Vol. 33, No. 4, 1968.

92. Danes, Z. F., *Geophys.*, Vol. 25, No. 6, 1960.
93. Dyrelins, D. and A. Vogel, *Improvement of convergency in iterative gravity interpretation*, University of Uppsala, Report No. 5, 1971.
94. Fajklewicz, Z., *Przeglad geologiczny*, Vol. 8, No. 9, 1960.
95. Hammer, S., *Geophys.*, Vol. 28, No. 3, 1963.
96. Hall, D. H., *Trans. Am. geophys. Un.*, Vol. 39, 1958.
97. Healy, J. H. and F. Press, *Geophys.*, Vol. 29, No. 3, 1964.
98. Jung, K., *Schwerkraftverfahren in der angewandten Geophysik* [Gravitational Procedures in Applied Geophysics], Leipzig, 1961.
99. Kane, M. F., *Geophys.*, Vol. 27, No. 4, 1962.
100. Mottlova, L., *Geofysikalni sbornik*, No. 178, 1963.
101. Morgan, N. and F. Grant, *Geophys. prospecting*, Vol. 11, No. 1, 1963.
102. Nedyalkov, I., *Godishn. Vissh. Tekhnich. Uchebni Zaved* [Annual: Higher Technology Educational Institutions], "Fizmatgiz" Press, Vol. 6, 2nd collection, 1969. /109
103. Pick, M., *Geophys. sbornik*, No. 126-145, 1960.
104. Pick, M., *Geofys. sbornik*, No. 177, 1963.
105. LaPorte, M., *Geophys. prospecting*, Vol. 10, No. 3, 1962.
106. Rosen, I. B., *J. Soc. Ind. and Appl. Mat.*, Vol. 8, No. 1, 1960.
107. Roy, A., *Geophys.*, Vol. 26, No. 5, 1961.
108. Roy, A., *Geophys.*, Vol. 27, 1962.
109. Sharma, P. V., *Pure and Appl. Geophys.*, Vol. 65, No. 3, 1966.
110. Sharpel, A. and P. W. Fullerton, *Geophys.*, Vol. 17, No. 4, 1952.
111. Stojan, E., *Canadian Oil and Gas industries*, Vol. 15, No. 5, 1962.
112. Talwani, M., J. Worzel and M. Landisman, *J. Geophys. Res.*, Vol. 64, 1959.
113. Talwani, M. and M. Ewing, *Geophys.*, Vol. 25, No. 1, 1960.
114. Tanner, J. G., *Geophys. J. R. astr. Soc.*, Vol. 13, 1967.
115. Vogel, A., *Geophys. prospecting*, Vol. 11, No. 1, 1963.
116. Zidarov, D., *Izv. Na Geofizich. In-t*, Vol. 8, Bulgarian Academy of Sciences, 1966.
117. Zidarov, D. and Z. Zhelev, *Geophys. prospecting*, Vol. 18, No. 1, 1970.
118. Zidarov, D., *O Reshenii Nekotorykh Obratnykh Zadach Potentsial'nykh Poley i Ego Primeneniya k Voprosam Geofiziki* [The Solution of Several Inverse Problems of Potential Fields and the Application of the Solution to the Problems of Geophysics], Bulgarian Academy of Sciences Press, Sofia, 1968.

Translated for the National Aeronautics and Space Administration under contract No. NASW-2485 by Techtran Corporation, P. O. Box 729, Glen Burnie, Maryland, 21061, translator: Thomas W. Appich, Jr.